

**EVALUATION OF  
TRANSCRIPTIONAL CYCLIN  
DEPENDENT KINASE INHIBITORS  
AS POTENTIAL CANCER  
THERAPEUTICS**

**XIANGRUI LIU, BSc. MSc.**

**Thesis submitted to the University of Nottingham  
for the degree of Doctor of Philosophy**

**January 2012**

# Table of Contents

	Page
Table of Contents.....	I
Abstract.....	VII
Acknowledgments .....	IX
List of Abbreviations .....	X
List of Figures.....	XIII
List of Tables.....	XVI
Chapter One: Introduction .....	1
1.1 Cancer.....	1
1.1.1 Hallmarks of cancer.....	2
1.1.1.1 Sustaining proliferative signalling.....	2
1.1.1.2 Evading Growth Suppressors .....	3
1.1.1.3 Resisting Cell death .....	4
1.1.1.4 Enabling replicative immortality .....	4
1.1.1.5 Inducing Angiogenesis .....	5
1.1.1.6 Activating invasion and metastasis.....	6
1.1.1.7 Other hallmarks of cancer.....	6
1.1.2 RB protein and cell cycle control .....	7
1.1.2.1 The mammalian cell cycle.....	7

1.1.2.2 Cyclins and cyclin-dependent kinases .....	8
1.1.2.3 RB pathway in cell cycle regulation .....	9
1.1.2.4 Cell cycle deregulation in human tumours .....	13
1.1.3 p53: Policeman of the oncogenes .....	13
1.1.3.1 p53 mutations and cancer .....	14
1.1.3.2 p53 activation.....	15
1.1.3.3 Policeman of oncogenes .....	18
1.1.4 Apoptotic and non-apoptotic death in tumour cells.....	19
1.1.4.1 Different types of cell death .....	19
1.1.4.2 Bcl-2 family proteins and apoptosis .....	23
1.1.4.3 Caspase family and cell death.....	26
1.2 Preclinical cancer drug discovery.....	27
1.2.1 Target identification and validation.....	28
1.2.2 Lead identification and optimisation .....	31
1.2.3 Target confirmation in tumour cells .....	33
1.3 Targeting cyclin dependent kinases for cancer therapy.....	34
1.3.1 Kinases.....	34
1.3.2 Cyclin dependent kinases (CDKs).....	35
1.3.2.1 Cell cycle regulation CDKs.....	37
1.3.2.2 Transcriptional regulation CDKs.....	39
1.3.3 Cyclin Dependent Kinase 9 .....	41
1.3.3.1 CDK9 and cancer.....	42

1.3.3.2 CDK inhibitors in clinic trials.....	43
1.3.3.3 Discovery of novel CDK9 inhibitors.....	47
1.4 Aims and objectives.....	49
<b>Chapter Two: Materials and Methods .....</b>	<b>51</b>
2.1 Materials .....	51
2.2 Methods .....	55
2.2.1 Cell culture.....	55
2.2.2 Compound solutions .....	56
2.2.3 MTT cell viability assay .....	57
2.2.4 Caspase activation assay.....	58
2.2.4.1 Caspase-3 assay .....	58
2.2.4.2 Caspase 3/7 activity assay .....	59
2.2.5 p53 stabilization assay .....	59
2.2.6 Mitotic index assay .....	60
2.2.7 Kinase assay.....	60
2.2.8 Cell cycle analysis .....	61
2.2.9 Annexin V/PI staining assay.....	61
2.2.10 Western blot analysis .....	62
2.2.10.1 Preparation of cell lysate .....	62
2.2.10.2 Protein assay .....	62
2.2.10.3 SDS PAGE .....	62
2.2.10.4 Immunoblotting .....	63

2.2.10.5 Enhanced chemiluminescence (ECL) reaction.....	64
2.2.10.6 Membrane stripping.....	64
2.2.11 $\gamma$ -H2AX foci .....	64
2.2.12 Comet assay .....	65
2.2.13 Reverse Transcription polymerase chain reaction (RT-PCR).....	66
2.2.13.1 RNA preparation and quantification.....	66
2.2.13.2 Reverse transcription and PCR.....	66
2.2.14 Microarray .....	67
<b>Chapter Three: Screening and classification of an inhibitor compound library</b>	<b>69</b>
3.1 Introduction.....	69
3.2 Results and Discussion .....	70
3.2.1 Cell viability .....	70
3.2.2 Activation of caspase-3 .....	72
3.2.3 Induction of p53 protein .....	77
3.2.4 Summary.....	81
3.2.3 Cell cycle effects.....	83
3.3 Conclusion.....	86
<b>Chapter Four: Cellular mechanism of action of a novel CDK9 inhibitor CDKI-</b>	<b>71</b>
4.1 Structure and kinase activity.....	88
4.2 Growth inhibition effect .....	89
4.3 Induction of apoptosis.....	93

4.4 Cell cycle effect .....	100
4.5 Inhibition of cellular RNAPII CTD phosphorylation.....	103
4.6 Effect on gene transcription.....	104
4.7 Down-regulation of anti-apoptotic protein Mcl-1 and up-regulation of p53 .....	108
4.8 Flavopiridol induces DNA double-strand breaks .....	112
4.9 Cellular model of action of CDKI-71 and flavopiridol .....	117
4.10 Conclusion .....	120
<b>Chapter Five: In vitro anti-tumour mechanism of a novel cyclin-dependent kinase inhibitor CDKI-83 .....</b>	<b>121</b>
5.1 Introduction.....	121
5.2 CDKI-83 is a potent inhibitor of CDK9 and CDK1 .....	122
5.3 CDKI-83 is a potent anti-proliferative agent and an effective apoptotic inducer .....	124
5.4 CDKI-83 induces cell arrest in G2 phase .....	126
5.5 Cellular CDK1 inhibition of CDKI-83 .....	128
5.6 CDKI-83 reduces both mRNA and protein level of Mcl-1 by targeting CDK9.....	129
5.7 Conclusion .....	132
<b>Chapter Six .....</b>	<b>133</b>
<b>General discussion and conclusion .....</b>	<b>133</b>
<b>References.....</b>	<b>136</b>

Appendix..... 154

## Abstract

Cancer cells depend heavily on sustained expression of anti-apoptotic proteins. Targeting transcription to suppress these anti-apoptotic proteins seems a promising strategy for anti-cancer therapy. Cyclin-dependant kinase 9 (CDK9) regulates transcription elongation by phosphorylating Ser2 on the C-terminal domain of RNA polymerase II, while CDK7 phosphorylates Ser5 during transcription initiation. A screening cascade comprised of an MTT assay, a caspase-3 activation assay, a p53 stabilization assay and a mitotic index assay was developed to classify compounds and identify lead transcriptional CDK inhibitors from a novel class of 2,4,5-trisubstituted pyrimidines. Compounds S3-41 and CDKI-71 are the most potent CDK9 inhibitors identified by the screening cascade. They showed potent anti-proliferative activity in the MTT assay and induce both caspase-3 activity and p53 protein level at the GI<sub>50</sub> concentration. In addition, no significant effect on mitotic index was observed.

The detailed mechanism of action of CDKI-71 was further investigated and compared with the clinical compound, flavopiridol. Like flavopiridol, CDKI-71 displayed potent cytotoxicity and caspase-dependent apoptosis that were closely associated with the inhibition of RNAPII phosphorylation at Ser2. This indicated effective targeting of cyclinT-CDK9 and the downstream inhibition of anti-apoptotic proteins such as Mcl-1 in cells. Similar to flavopiridol, CDKI-71 down-regulated a large range of genes, including Mcl-1 and Bcl-2. No correlation between apoptosis and inhibition of cell cycle CDKs 1 and 2 was observed. Non-transformed lung fibroblast cell lines showed resistance to

CDKI-71 treatment. In contrast, flavopiridol showed little selectivity between cancer and normal cells. Flavopiridol also induced genotoxic stress through the induction of DNA double-strand breakage. These results suggest that CDKI-71 has a great potential to be developed as an anti-cancer agent.

Another study focused on *in vitro* anti-tumour mechanism of CDKI-83, a dual inhibitor of CDK9 and CDK1, was performed in A2780 ovarian cancer cells. CDKI-71 presented potent anti-proliferation activity and induced apoptosis in A2780 cells. By inhibiting cellular CDK1 and CDK9 activities, CDKI-83 arrested cells in G2 phase and reduced anti-apoptotic proteins at both mRNA and protein levels, respectively. This study suggests that the combination of CDK9 and CDK1 inhibition results in effective induction of apoptosis in cancer cells.

# Acknowledgments

I would like to express my sincerest gratitude to a number of amazing scientists and friends who made this thesis possible. First of all, I am heartily thankful to my supervisor Dr Shudong Wang who offered invaluable assistance, support and guidance in all the time of research and writing of this thesis. I sincerely thank Drs L. Dekker, C. de Moor, T. Bradshaw and Professor P. Fischer for their useful advices for this project. I am grateful to Dr F. Lam for his help in experimental work.

Further thanks go to Dr T. Self for the technical support in the use of ImageXpress<sup>MICRO</sup><sup>TM</sup> automated fluorescent microscope; Dr A. Barthelet-Barateig for microarray slides preparation and helps on microarray data analysis.

I am appreciative of the chemists in Dr Wang's group for providing compounds, especially Mr S. Shi who synthesized the potent CDK9 inhibitors. I thank everyone in Laboratory C62, Centre for Biomolecular Sciences, for their help and entertainment for the past three years.

Finally, my greatest thanks go to my parents and Sujing for supporting me throughout my PhD studies.

# List of Abbreviations

APAF-1	Apoptotic protease activating factor - 1
ARF	ADP-ribosylation factor
ATP	Adenosine triphosphate
BAG	Bcl-2-associated athanogene
BAK	Bcl-2 antagonist killer
Bax	Bcl-2-associated X
Bcl-2	B-cell CLL/Lymphoma 2
Cdc	Cell division cycle
CDK	Cyclin-dependent kinase
cDNA	Complementary DNA
Chk	Cell cycle checkpoint kinase
CLL	Chronic lymphocytic leukaemia
CO <sub>2</sub>	Carbon dioxide
CTD	C-terminal domain
DISC	Death-inducing signalling complex
DMSO	Dimethyl sulfoxide
DNA	Deoxyribonucleic acid
DRB	5,6-dichloro-1-β-d-ribofuranosylbenzimidazole
DSIF	DRB sensitivity inducing factor
ECL	Enzymatic chemiluminescence
EGFR	Epidermal growth factor receptor
FACS	Fluorescence activated cell sorting
FasL	Fas ligand
FBS	Foetal bovine serum
FITC	Fluorescein isothiocyanate
G1	Gap phase I
G2	Gap phase II
GI <sub>50</sub>	Half growth inhibitory concentration
HCl	Hydrogen chloride/Hydrochloric acid
HTS	High-throughput screening
IC <sub>50</sub>	Half maximal inhibitory concentration

Mcl-1	Myeloid cell leukaemia-1
MEM	Minimum essential medium eagle
MeOH	Methanol
MOMP	Mitochondrial outer membrane permeabilization
MPF	Maturation promoting factor
mRNA	Messenger ribonucleic acid
MS	Mass spectrometry
MTD	Maximum tolerated dose
MTT	3-(4,5-Dimethylthiazol-2-yl)-2,5 diphenyltetrazolium bromide
NaOH	Sodium hydroxide
NCI	National Cancer Institute
NMR	Nuclear magnetic resonance
NSCLC	Non-small cell lung cancer
PARP	Poly (ADP-ribose) polymerase
PBS	Phosphate Buffered Saline
PCR	Polymerase chain reaction
PI	Propidium iodide
Plk	Polo like kinase
P-TEFb	Positive transcription factor b
R point	Restriction point
RB	Retinoblastoma
RNA	Ribonucleic acid
RNAi	RNA interference
RNAP	RNA polymerase
RT-PCR	Reverse transcription polymerase chain reaction
SA- $\beta$ -gal	Senescence-associated $\beta$ -galactosidase
SAR	Structure activity relationship
Ser	Serine
siRNA	Small interference RNA
TBS	Tris Buffered Saline
THF	Tetrahydrofuran
Thr	Threonine
TNF	Tumour necrosis factor

<b>TNFR-1</b>	<b>Tumour necrosis factor receptor 1</b>
<b>UV</b>	<b>Ultraviolet</b>
<b>VEGF</b>	<b>Vascular endothelial growth factor</b>
<b>XIAP</b>	<b>X-linked inhibitor of apoptosis</b>

# List of Figures

Figure 1.1 The six hallmarks of cancer .....	2
Figure 1.2 The mammalian cell cycle.....	7
Figure 1.3 Cyclins and CDKs in the cell cycle regulation .....	8
Figure 1.4 The RB pathway and G1/S phases regulation.....	10
Figure 1.5 Pocket proteins .....	12
Figure 1.6 Different expression of pocket proteins throughout the cell cycle..	12
Figure 1.7 p53 structure and location of tumour-associated mutations.....	14
Figure 1.8 Effects of p53 mutation on survival. ....	15
Figure 1.9 Refined model for p53 activation.....	17
Figure 1.10 Impact of p53 on cellular fate upon DNA damage or oncogenic signalling.....	19
Figure 1. 11 The Bcl-2 protein family.....	24
Figure 1.12 Intrinsic apoptotic pathway .....	25
Figure 1.13 Relationship between caspase dependency and cell death.....	27
Figure 1.14 The preclinical cancer drug discovery cascade.....	28
Figure 1.15 Cancer specific targets. ....	29
Figure 1.16 The specific complexes and functions of 10 human CDKs which have been identified.....	36
Figure 1.17 The transcription process regulated by CDKs.....	39
Figure 1.18 Targeting transcription as a potential cancer therapy.....	40
Figure 1.19 Gene and sequence of human CDK9 isoforms.. ....	42
Figure 1.20 Apoptosis induced by CDK9 inhibition.....	43

Figure 1.21 The crystal structure of the CDK9 (green) /cyclin T1 (brown) complex.....	48
Figure 1.22 Similar binding modes of 2,4,5-trisubstituted pyrimidine and ATP to ATP binding pocket of CDK2.....	49
Figure 3.2 GI <sub>50</sub> values of 46 compounds in HCT-116 cells (MTT assay). .....	71
Figure 3. 3 Induction of Caspase-3 activities in HCT-116 cells.....	75
Figure 3.4 p53 protein levels in HCT-116 cells after treatments.. .....	80
Figure 3.5 Cell cycle status detected by mitotic index.. .....	85
Figure 4.1 Growth inhibition curves of CDKI-71 for different treatment time points.. .....	92
Figure 4.2 Images of cell death after CDKI-71 treatment. ....	94
Figure 4. 3 Induction of caspase 3/7 activity in cancer cell lines HCT-116 and A2780, and fibroblast MRC-5 after treatment with CDKI-71 (A) or flavopiridol (B) for 24 hours.....	95
Figure 4.4 Induction of caspase-dependent apoptosis in HCT-116 cells. ....	97
Figure 4. 5 Induction of caspase-dependent apoptosis in A2780 cells.....	99
Figure 4.6 Induction of caspase-dependent apoptosis in MRC-5 cells.. .....	100
Figure 4.7 Cell cycle effects of CDKI-71 or flavopiridol.. .....	102
Figure 4.8 Inhibition of RNAPII CTD phosphorylation and other cell cycle CDKs by Western blot analysis. ....	104
Figure 4.9 Gene expression patterns of A2780 cells treated with CDKI-71 or flavopiridol.. .....	108

Figure 4.10 Effects on anti-apoptotic proteins and the p53 pathway by Western blot analysis in A2780 cells.....	109
Figure 4.11 Effects on anti-apoptotic proteins and the p53 pathway by Western blot analysis in MRC-5 cells..	111
Figure 4.12 Induction of $\gamma$ -H2AX by flavopiridol.....	114
Figure 4.13 Comet assay (single-cell gel electrophoresis) on MRC-5 cells treated with DMSO vehicle, CDKI-71 or flavopiridol.....	116
Figure 4.14 Cellular distribution model for CDKI-71 and flavopiridol.....	118
Figure 4.15 Cellular model of action of CDKI-71 and flavopiridol.....	119
Figure 5.1 Structure and in vitro kinase activity of CDKI-83. ....	123
Figure 5.2 Growth inhibition curves of CDKI-83 for different treatment time points. ....	124
Figure 5.3 Induction of caspase-3 activity in A2780 cells after treatment with CDKI-83 for 24 or 48 hours. ....	125
Figure 5.4 Detection of apoptosis by flow cytometry analysis after Annexin V-PI double staining..	126
Figure 5.5 Cell cycle effects in A2780 cells.....	127
Figure 5.6 Effect on Mitotic index in A2780 cells. A2780 cells were treated with CDKI-83 for 7 hours and the percentages of cells in mitotic were measured.....	128
Figure 5.7 Effect on the phosphorylation status of CDK1 substrate PP1 $\alpha$ at Thr <sup>320</sup> .....	129
Figure 5.8 Inhibition of CDK9 and reduction of survival factors in A2780 cells. ....	130

## List of Tables

Table 1.1 Characteristics of different types of cell death .....	20
Table 1.2 Screening strategies .....	31
Table 1. 3 Small-molecule CDK inhibitors in clinical trials .....	44
Table 3.1 Summary of MTT, caspase-3 activity and p53 stabilization assays.	82
Table 3.2 Inhibition of CDKs by in vitro kinase assay.....	86
Table 4. 1 Chemical structures and summary of CDK inhibitory activity. ....	88
Table 4.2 Average GI <sub>50</sub> values (nmol/L) for CDKI-71/flavopiridol-mediated growth inhibition in a panel of human cell lines. ....	90
Table 4.3 Tail length and Tail intensity after CDKI-71 or flavopiridol treatment in the comet assay.....	116

# Chapter One: Introduction

## 1.1 Cancer

Cancer is a class of diseases characterized by uncontrolled cell growth of abnormal cells which invade and destroy other tissues. Every year, more than 1.3 million people in the US and UK are diagnosed with cancer, leading to 165,000 deaths per year (David and Zimmerman, 2010). According to an official report (Babb, 2000), cancer has become the major cause of death in England and Wales.

Remarkable progress has been seen in cancer research and treatment in the past three decades. However, cancer continues to be a worldwide killer. The causes of cancer can be divided into two groups: those with internal factors (such as inherited mutations, hormones, and immune conditions) and those with environmental factors (such as diet, tobacco, infractions). Although dynamic changes are involved in cancer and all cancers are due to multiple mutations (Hahn and Weinberg, 2002; Loeb and Loeb, 2000), most mutations are a result of interaction with the environment and only 5–10 % of all cancers are due to an inherited gene defect (Anand et al., 2008; Lichtenstein et al., 2000).

### 1.1.1 Hallmarks of cancer

Douglas Hanahan and Robert A. Weinberg have proposed six hallmarks of cancer which are shared in common by most, if not all, types of human tumours (Hanahan and Weinberg, 2000): sustaining proliferative signalling, evading growth suppressors, resisting cell death, enabling replicative immortality, inducing angiogenesis and metastasis (Figure 1.1). These capabilities provide a solid foundation for understanding the biology of cancer and are described in turn below.

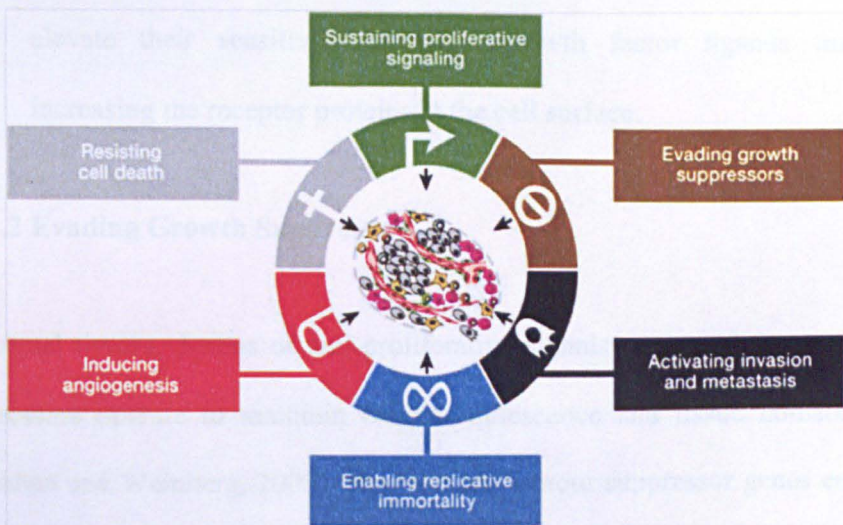


Figure 1.1 The six hallmarks of cancer (Hanahan and Weinberg, 2011).

#### 1.1.1.1 Sustaining proliferative signalling

Before moving from a quiescent state into a cell growth-and-division cycle, normal tissues require growth-promoting signals whose production and release are carefully controlled. In contrast, cancer cells can sustain proliferative

signalling and become masters of their own destinies (Hanahan and Weinberg, 2011).

Cancer cells deregulate mitogenic signalling in several ways (Cheng et al., 2008; Hanahan and Weinberg, 2011): they can;

- generate their own proliferative factor ligands;
- send stimulating signals to induce expression of growth factors from normal cells nearby;
- elevate their sensitivity to some growth factor ligands through increasing the receptor proteins at the cell surface.

#### **1.1.1.2 Evading Growth Suppressors**

In normal tissues, dozens of anti-proliferative signals generated from tumour suppressors operate to maintain cellular quiescence and tissue homeostasis (Hanahan and Weinberg, 2000). Two famous tumour suppressor genes encode the retinoblastoma (RB) and p53 proteins which are central to the regulation of proliferation, senescence or apoptosis (Hanahan and Weinberg, 2011).

The RB protein is a critical gatekeeper of the cell cycle, deciding whether or not a cell can proceed through its growth-and division cycle (Burkhart and Sage, 2008; Deshpande et al., 2005; Hanahan and Weinberg, 2011; Lapenna and Giordano, 2009). RB pathway receives growth-inhibitory signals, mainly from outside of the cell, while p53 is activated by intracellular operating systems. In response to stresses, such as DNA damage, oxidative stress (Han

et al., 2008), and deregulated oncogene expression, p53 can activate DNA repair proteins, arrest the cell cycle and trigger apoptosis.

The genes encoding RB and p53 tumour suppressor proteins are functionally inactivated in a broad range of cancers. Loss of p53 tumour suppressor function occurs in approximately 50% cancers (Vogelstein et al., 2000). The detailed mechanisms of the two suppressors will be described later.

#### **1.1.1.3 Resisting Cell death**

Tumour cells can evade apoptosis in several ways. The BCL-2 family proteins which contain counterbalancing pro- and anti- apoptotic members constitute a critical control point in apoptosis regulation (Adams and Cory, 2007; Danial, 2007). The multiple apoptosis-avoiding mechanisms found in tumour cells include: up-regulation of anti-apoptotic proteins (Bcl-2, Mcl-1); down-regulation of pro-apoptotic factors (Bax, Bim, Puma), increasing expression of survival signals and evading the extrinsic ligand-induced pathway (Hanahan and Weinberg, 2011). In contrast to apoptosis, which is a barrier to cancer development, recent research shows necrosis has tumour-promoting potential (Grivennikov et al., 2010).

#### **1.1.1.4 Enabling replicative immortality**

In contrast to normal cells, which only pass through a limited number of cell cycles, cancer cells have limitless replicative potential giving rise to tumours (Hanahan and Weinberg, 2011). It has been indicated that telomeres, which protect the ends of chromosomes, play a key role in the unlimited proliferation

(Blasco, 2005). Telomeres are composed of repetitive DNA sequences and protect the end of the chromosome from deterioration or from fusion with neighbouring chromosomes (Talks, 2008). Non-immortalized cells gradually lose telomeric sequences as a result of incomplete replication (Counter et al., 1992). Eventually the shortened telomeres lose the capacity to protect the ends of chromosomal DNAs after which cells reach the limit of their replicative capacity and progress into senescence.

Cancer cells have to overcome the telomere shortening to maintain unlimited proliferation and the majority (85% - 90%) of malignant cells succeed in doing so by up-regulating expression of telomerase, which adds repetitive nucleotide sequences to the ends of telomeric DNA (Bryan and Cech, 1999).

#### **1.1.1.5 Inducing Angiogenesis**

The growth of new blood vessels (the process of angiogenesis) is essential for growing tumour tissues to obtain essential nutrients and oxygen. Multiple lines of evidence have indicated that counteracting factors with induction or inhibition effects regulate the process of angiogenesis (Baeriswyl and Christofori, 2009; Bergers and Benjamin, 2003). As the most important and well-known angiogenesis inducer, the vascular endothelial growth factor (VEGF) can be up-regulated by oncogene signals during an early stage of the development of invasive cancers.

#### **1.1.1.6 Activating invasion and metastasis**

During the development of most human cancers, some pioneer cells from primary tumour masses acquire the ability to penetrate the walls of lymphatic and/or blood vessels, circulate through the bloodstream to other tissues, re-penetrate through the vessel or walls, continue to multiply, and eventually form another tumour. The capability for invasion and metastasis are the cause of approximately 90% of human cancer deaths (Sporn, 1996). E-cadherin, a key cell-to-cell adhesion molecule is the best characterized antagonist of invasion and metastasis. Down-regulation and inactivation of E-cadherin are frequently detected in human carcinomas (Cavallaro and Christofori, 2004; Hanahan and Weinberg, 2011)

#### **1.1.1.7 Other hallmarks of cancer**

Conceptual progress in cancer research in the last decade has resulted in two emerging hallmarks: deregulating cellular energetics and avoiding immune destruction. The first involves the capability to regenerate cellular metabolism to support tumour growth more effectively and the second describes the ability of cancer cells to avoid immunological destruction by T/B lymphocytes, macrophages or natural killer cells. In addition, genome instability and tumour-promoting inflammation facilitate the acquisition of both core and emerging hallmarks and thus are labelled as enabling characteristics. (Hanahan and Weinberg, 2011)

## 1.1.2 RB protein and cell cycle control

As mentioned previously, cancer cells have to evade growth suppressors to enable their unlimited proliferation. RB protein (pRb) is a well known tumour suppressor and a critical cell cycle gatekeeper. Mutation of the RB gene is common in many types of cancer. This section will describe the mammalian cell cycle and the RB pathway.

### 1.1.2.1 The mammalian cell cycle

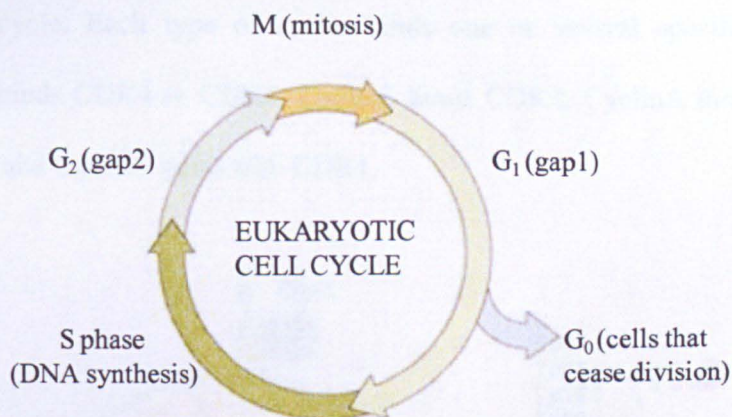


**Figure 1.2** The mammalian cell cycle.

There are four phases in the mammalian cell cycle (**Figure 1.2**): S-phase, during which DNA is replicated; M-phase, in which the chromosomes are separated into two new nuclei in the process of mitosis. These two phases are separated by two “Gap” phases, G<sub>1</sub> and G<sub>2</sub>. Cells prepare for the entering into S phase in G<sub>1</sub> phase and for upcoming events of M phase in G<sub>2</sub>. G<sub>0</sub> denotes the quiescent state of the cells which withdraw from the active cell cycle. Critical

decisions are made by cells in  $G_1$  phase on whether to commence a new proliferation cycle or proceed from mitosis into a resting state,  $G_0$ .

### 1.1.2.2 Cyclins and cyclin-dependent kinases

During the cell cycle, different Cyclins accumulate and activate cyclin dependent kinases (CDKs) at specific times to control the progression of cells. Cyclins are so named because their concentrations cycle up and down during the cell cycle. They activate CDKs by forming cyclin-CDK complexes which send out signals to responder molecules to push forward the growth-and-division cycle. Each type of cyclin binds one or several specific CDKs: CyclinD binds CDK4 or CDK6, CyclinE binds CDK2, CyclinA binds CDK1 or CDK2 and CyclinB pairs with CDK1.

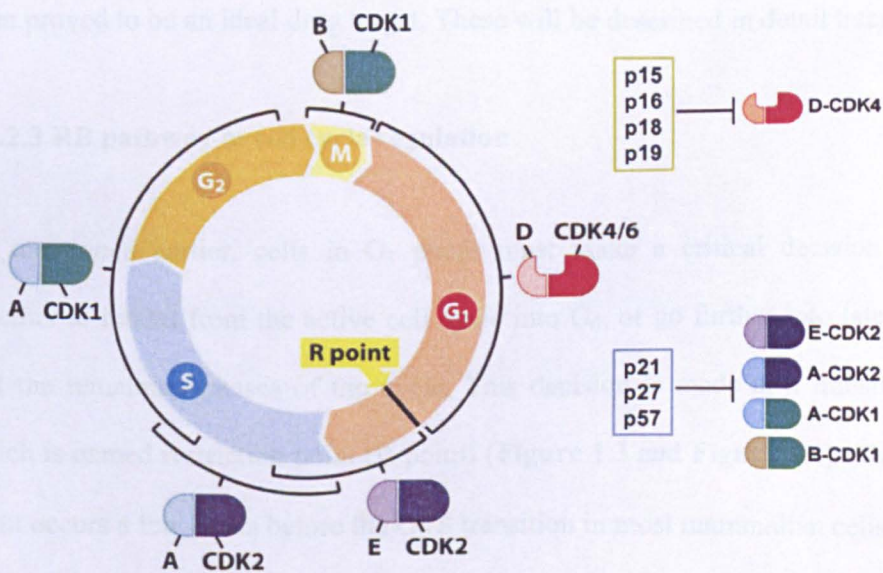


Figure 1.3 Cyclins and CDKs in the cell cycle regulation (Adapted from Weinberg, 2007).

In mammalian cells, distinct Cyclin-CDK complexes take part in regulating specific cell cycle transitions: CyclinD-CDK4/6 for sustaining G<sub>1</sub>, CyclinE-CDK2 for entering into S phase, CyclinA-CDK2 for S phase progression, and CyclinA/B-CDK1 for G<sub>2</sub>/M progression and transition (**Figure 1.2**). Some general CDK inhibitors, which specifically inhibit certain Cyclin/CDK complexes, are also activated and inactivated at appropriate times during the cell cycle. INK4 family proteins (p15, p16, p18 and p19) inhibit CDK4 and CDK6 by interfering with their association with D-type cyclins, while Cip/Kip family members (p21, p27 and p57) regulate the activities of Cyclin A/B/E-CDK complexes (Sherr and Roberts, 1999) (**Figure 1.3**). In the past two decades, extensive research on novel small molecular CDK inhibitors from pharmaceutical companies and academics has led to many clinical candidates for cancer treatments. CDKs, especially transcription regulator CDK9, have been proved to be an ideal drug target. These will be described in detail later.

#### **1.1.2.3 RB pathway in cell cycle regulation**

As mentioned earlier, cells in G<sub>1</sub> phase must make a critical decision on whether to retreat from the active cell cycle into G<sub>0</sub>, or go further into late G<sub>1</sub> and the remaining phases of the cycle. This decision is made at a transition which is named restriction point (R point) (**Figure 1.3** and **Figure 1.4**). The R point occurs a few hours before the G<sub>1</sub>/S transition in most mammalian cells.

RB, which was the first cloned tumour suppressor gene, was found to regulate the R-point transition and RB mutation was observed in many tumour types (Classon and Harlow, 2002).

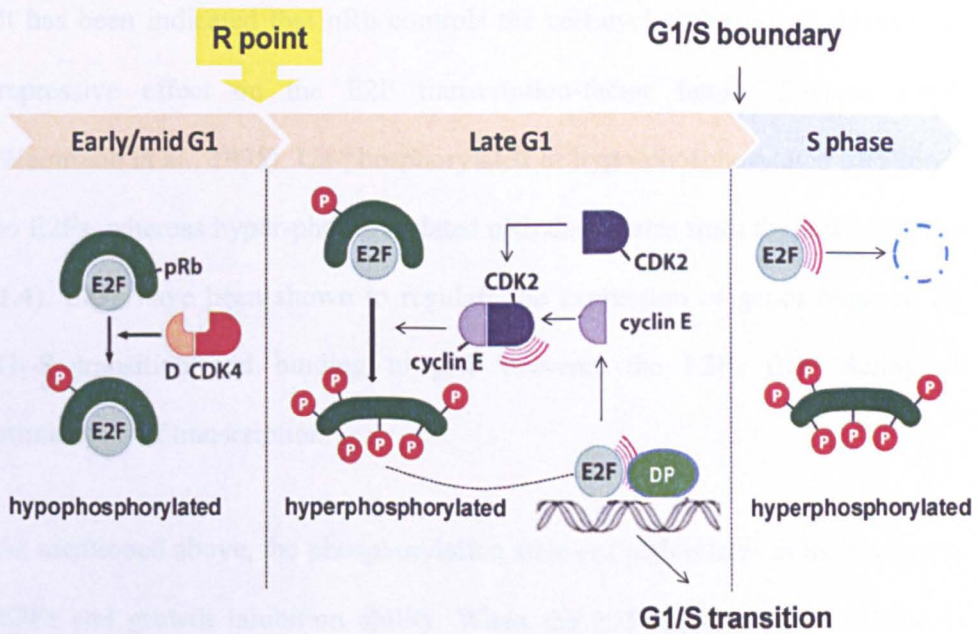


Figure 1.4 The RB pathway and G1/S phases regulation (Adapted from Weinberg, 2007).

The retinoblastoma protein (pRb) is phosphorylated and dephosphorylated during specific phases of the cell cycle (Buchkovich et al., 1989) and its growth inhibition ability depends on the phosphorylation status. Considerable evidence indicates non- or hypo- phosphorylated pRb inhibits cell growth through early to mid-G<sub>1</sub> phase until it becomes hyper-phosphorylated when it loses its growth inhibition ability and permits cells to pass through the R point into late G<sub>1</sub> and the other remaining phases of the cell cycle (Goodrich et al., 1991; Weinberg, 1995). Other evidence supports RB's role as a cell-proliferation regulator in G<sub>1</sub> phase: RB over-expression arrested cells in G<sub>1</sub> phase (Huang et al., 1988) while RB deficiency accelerates G<sub>1</sub> transition (Herrera et al., 1996).

It has been indicated that pRb controls the cell cycle progression through its repressive effect on the E2F transcription-factor family (Dyson, 1998; Weintraub et al., 1995). Un-phosphorylated or hypo-phosphorylated pRb binds to E2Fs, whereas hyper-phosphorylated pRb dissociates from the E2Fs (**Figure 1.4**). E2Fs have been shown to regulate the expression of genes required for G<sub>1</sub>-S transition and binding to pRb prevents the E2Fs from acting as stimulators of transcription.

As mentioned above, the phosphorylation status of pRb relates to its binding to E2Fs and growth inhibition ability. When the E2F-mediated transcription is negatively regulated by pRb, cyclin-CDK complexes regulate the phosphorylation of pRb (**Figure 1.4**). In early/mid G<sub>1</sub>, cyclinD-CDK4/6 complex first hypo-phosphorylates pRb, which is further phosphorylated at the R point by cyclinE-CDK2 complex, leading to its hyper-phosphorylation. In addition, the activity of cyclin-CDK4/6 complexes is regulated by INK4 (p15, p16, p18 and p19) and Cip/Kip (p21, p27 and p57) family CDK inhibitors (Malumbres and Barbacid, 2009; Sherr and Roberts, 1999).

Two other pRb related proteins, p107 and p130 are also involved in G<sub>1</sub> regulation and repress E2F-mediated gene transcription. These three proteins are called pocket proteins because their main sequence similarity resides in a “pocket” domain (regions A and B, separated by a spacer) (**Figure 1.5**) which is required for their interaction with E2Fs and many other factors (Classon and Harlow, 2002)

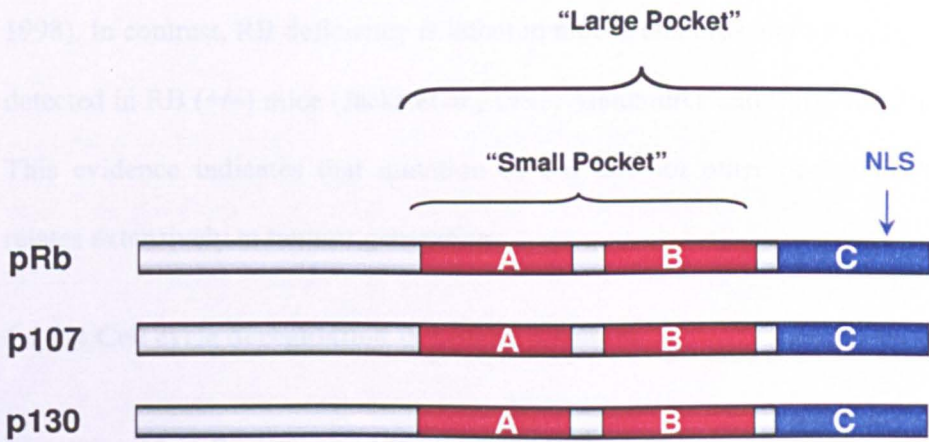


Figure 1.5 Pocket proteins (Cozar-Castellano et al., 2006).

Although the pocket proteins have similar structure and functions, they are expressed at different times during the cell cycle (Figure 1.6). p130 associates with E2Fs primarily in G<sub>0</sub> and p107 is involved in controlling advance through late G<sub>1</sub> and S phase. However, pRb is expressed at a constant level (Classon and Harlow, 2002).

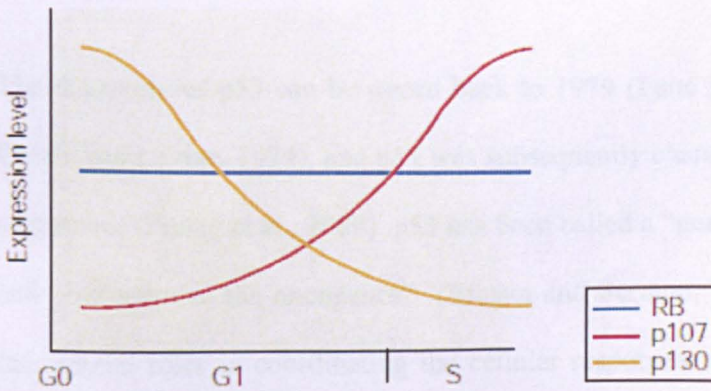


Figure 1.6 Different expression of pocket proteins throughout the cell cycle (Classon and Harlow, 2002).

Deletion of p107 or p130 has no significant effects on tumour susceptibility and mouse embryos without p107 or p130 grow normally (Mulligan and Jacks,

1998). In contrast, RB deficiency is lethal in mouse embryos and tumours were detected in RB (+/-) mice (Jacks et al., 1992; Malumbres and Barbacid, 2001). This evidence indicates that mutation of RB but not other pocket proteins relates extensively to tumour generation.

#### **1.1.2.4 Cell cycle deregulation in human tumours**

Mutation of cell cycle regulators occurs frequently in human cancers. Molecular analysis has shown the pRb pathway is frequently deregulated in most types of human tumours. Lots of abnormalities lead to dysfunctional pRb, such as inactivation of RB gene, methylation of RB gene promoter and sequestration of pRb by the HPV E7 viral oncoprotein. Other alterations in cell cycle regulation involve up-regulation of cyclins, over-expression of CDKs, and decrease of general CDK inhibitors (Malumbres and Barbacid, 2001).

#### **1.1.3 p53: Policeman of the oncogenes**

The discovery of p53 can be traced back to 1979 (Lane and Crawford, 1979; Linzer and Levine, 1979), and p53 was subsequently characterized as a tumour suppressor (Finlay et al., 1989). p53 has been called a “guardian of the genome and policeman of the oncogenes” (Efeyan and Serrano, 2007) because of its two central roles in coordinating the cellular responses to DNA damage and oncogenic signalling. Because DNA damage is widely present in cancer, more attention has been paid to oncogenic signalling induced p53.

### 1.1.3.1 p53 mutations and cancer

Regarded as “the guardian of the genome”, p53 regulates the expression of a wide variety of genes involved in apoptosis, growth arrest and inhibition of cell cycle progression. Intensive research on p53 over the last three decades has revealed the crucial role of p53 pathway in cancer prevention and mutations in TP53 (the gene encoding p53 tumour suppressor) are found in about half of all human cancers (Toledo and Wahl, 2006). Most of the tumour-associated mutations in TP53 are point mutations (93.6%) which lead to single amino-acid substitutions, while 95% of the mutations are found in the sequence-specific DNA binding region (Figure 1.7) (Vousden and Lu, 2002). Importantly, 28% of the mutations occur at only six residues (R175, G245, R248, R249, R273 and R282).

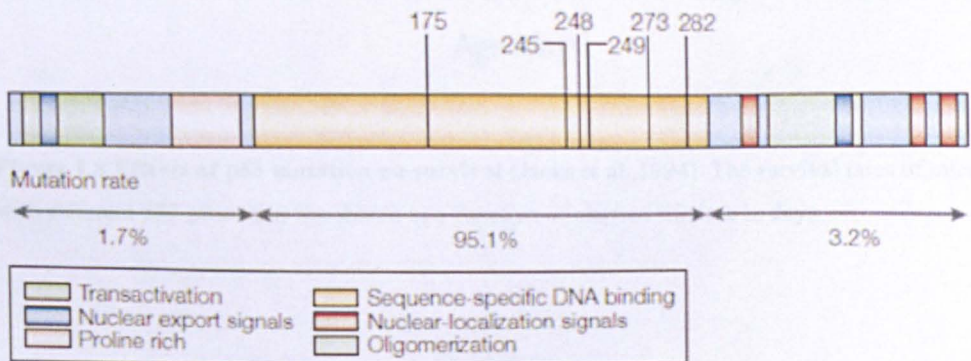


**Figure 1.7 p53 structure and location of tumour-associated mutations** (Vousden and Lu, 2002). The numbers above the figure indicate the amino acid residue number.

Animal studies on mice carrying germ-line p53 mutations indicate that p53 is not necessary for normal mouse development but that it is a tumour suppressor

gene (Jacks et al., 1994). While all mice lacking both germ-line copies of the p53 show normal embryo development, significantly increased mortality and a short life span were observed in p53<sup>-/-</sup> mice, which died mainly from sarcomas and lymphomas (**Figure 1.8**). In addition, mice with p53<sup>+/-</sup> heterozygotes began to develop tumours at about 250 days of age.

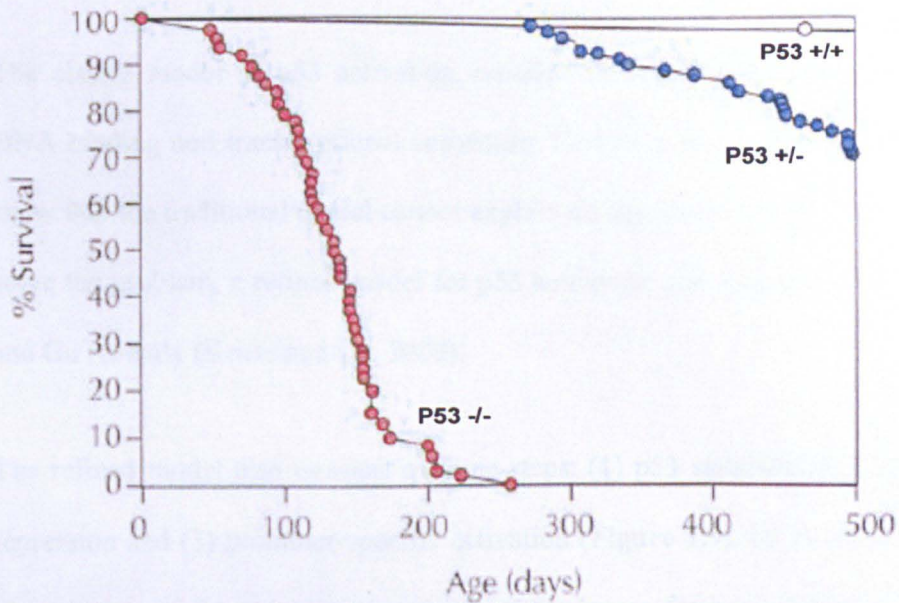


**Figure 1.8** Effects of p53 mutation on survival (Jacks et al., 1994). The survival rates of mice with different p53 genotypes are shown as a function of elapsed lifetime in days.

### 1.1.3.2 p53 activation

p53 protein is maintained at low levels and low activity by Mouse Double Minute-2 (MDM2) mediated degradation. MDM2 is an important negative regulator of the p53 tumour suppressor by ubiquitinating N-terminal transactivation domain of p53 (Marine and Lozano, 2010; Piette et al., 1997). MDM2 also binds to the transactivation domain of p53, preventing interaction

with the transcriptional machinery. Stabilization of p53 can be induced by a variety of cell-physiologic stresses, such as lack of nucleotides, UV and ionizing radiation, hypoxia, blockage of transcription and oncogenic signalling (Weinberg, 2007). MDM2 is phosphorylated at multiple sites in cells. Following stresses, phosphorylation of Mdm2 leads to changes in protein function and stabilization of p53.

The classic model of p53 activation contains three steps: p53 stabilization, DNA binding and transcriptional activation. However, *in vivo* genetic studies show that the traditional model cannot explain all aspects of p53 activation. To solve the problem, a refined model for p53 activation was suggested by Kruse and Gu recently (Kruse and Gu, 2009).

The refined model also consists of three steps: (1) p53 stabilization, (2) anti-repression and (3) promoter-specific activation (**Figure 1.9**). In this model the second step, anti-repression, in which p53 releases from repression factors MDM2 and MDMX is the key step in the physiological activation of p53 (Kruse and Gu, 2009).

MDM2 and MDMX (also known as MDM4) are structurally related proteins, both of which are required to restrain p53 in a non-redundant manner (Marine et al., 2006). The p53 repression function of MDM2 and MDMX are clearly indicated by *in vivo* studies carried out in mice. Mice lacking either MDM2 (Montes de Oca Luna et al., 1995) or MDMX (Parant et al., 2001) cannot survive but the lethality is rescued by inactivation of p53.

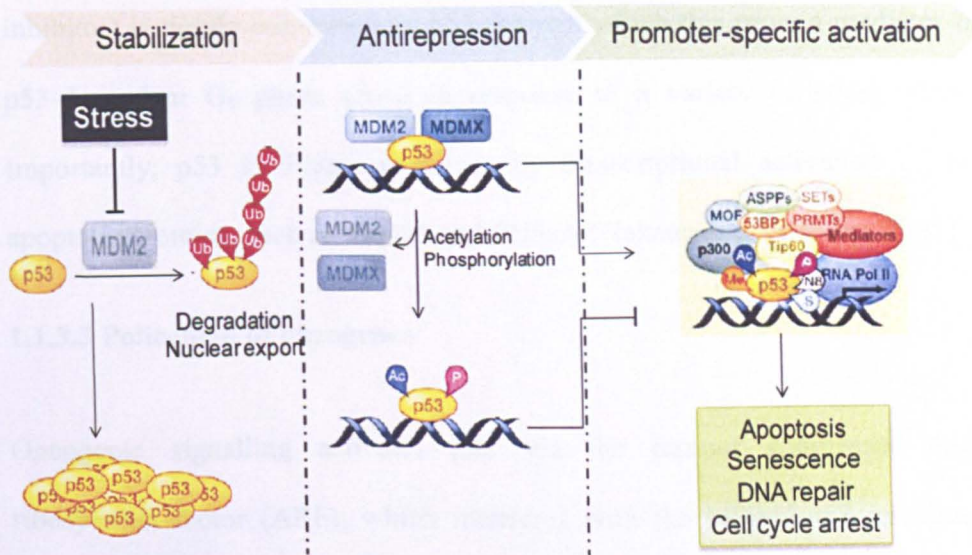


**Figure 1.9 Refined model for p53 activation** (adapted from Kruse and Gu, 2009). Promoter-specific p53 activation in vivo includes three key steps: (1) p53 stabilization, (2) anti-repression and (3) promoter-specific activation. Ac, acetylation; P, phosphorylation; Me, methylation; N8, neddylation; S, sumoylation.

Despite its sequence homology with MDM2, MDMX does not modulate p53 levels but instead inhibits p53-induced transcription (Marine et al., 2006). In addition, recent studies in mutant mice indicate that repression of p53 is the major role of MDMX (Iwakuma and Lozano, 2007). Transcription of p53 targets can be repressed by both MDM2 and MDMX at p53 promoter regions by many different mechanisms, whereas acetylation or phosphorylation of p53 at specific lysine residues facilitates the release of p53 from the repression mediated by MDM2 and MDMX (Kruse and Gu, 2009).

After release from its repression status, p53 interacts with many cofactors which facilitate special p53 targets for DNA repair, cell cycle regulation, apoptosis, senescence, autophagy and metabolism (**Figure 1.9**) (Kruse and Gu, 2009). For example, the expression of p21 (a potent cyclin-dependent kinase

inhibitor) is tightly controlled by p53 through which this protein mediates the p53-dependent G<sub>1</sub> phase arrest in response to a variety of stress stimuli. Importantly, p53 facilitates apoptosis by transcriptional activation of pro-apoptotic proteins, such as NOXA and PUMA (Nakano and Vousden, 2001).

### **1.1.3.3 Policeman of oncogenes**

Oncogenic signalling activates p53 via the tumour suppressor ADP-ribosylation factor (ARF), which interferes with the MDM2/p53 interaction and leads to p53 activation (Palmero et al., 1998; Stott et al., 1998). In addition, oncogenic signalling cannot activate p53 in the absence of ARF in mice (Efeyan et al., 2006). Recent studies also indicate that ARF-dependent activation of p53 rather than DNA damage response of p53 is critical to cancer protection, (Efeyan and Serrano, 2007). In response to DNA damage, apoptosis occurred rapidly in cells with p53, whereas cells without p53 also undergo cell death by mitotic catastrophe. In contrast, only cells with p53 are eliminated through apoptosis or senescence under oncogenic signalling (**Figure 1.10**).

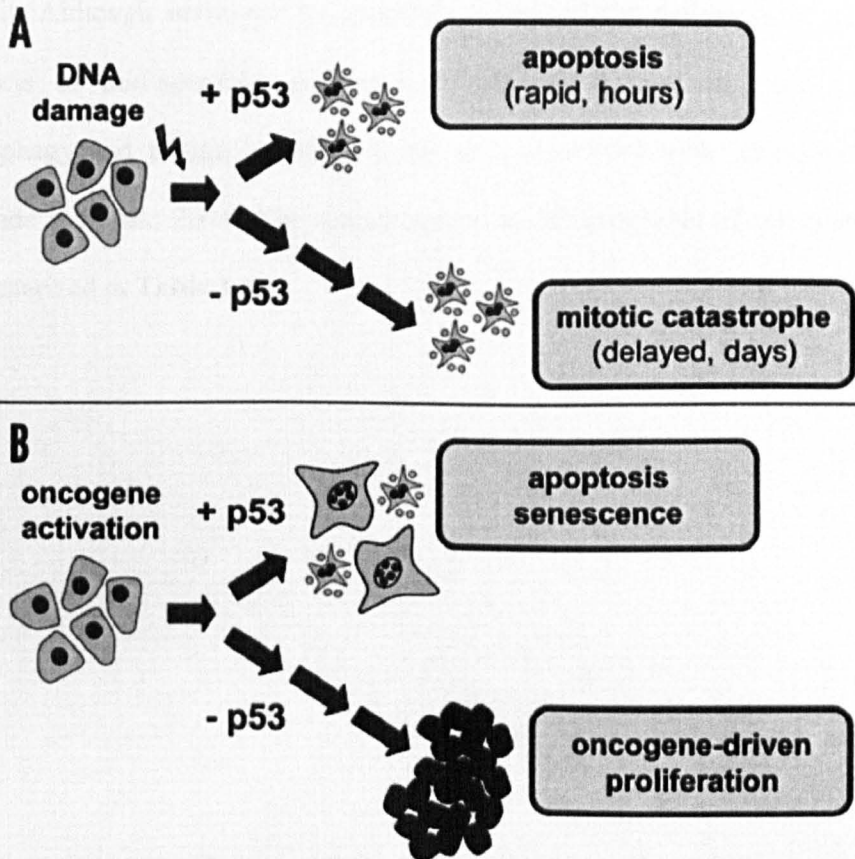


**Figure 1.10 Impact of p53 on cellular fate upon DNA damage or oncogenic signalling** (Efeyan and Serrano, 2007). In response to DNA damage, apoptosis occurred rapidly in cells with p53, whereas cells without p53 also undergo cell death by mitotic catastrophe (A). Under oncogenic signalling, cells with p53 are eliminated through apoptosis or senescence; whereas cells lacking p53 continue to proliferate (B).

One of the major responses to p53 activation is the induction of apoptosis. The role of p53 in apoptosis will be described in the following section.

### 1.1.4 Apoptotic and non-apoptotic death in tumour cells

#### 1.1.4.1 Different types of cell death

Apoptosis is the process of programmed cell death and the most common and best defined type of cell death. The Bcl-2 family proteins constitute critical controllers of apoptosis and the apoptotic pathways will be introduced later in

detail. Although resistance to apoptosis is one of the hallmarks of cancer, defects in non-apoptotic pathways, which include necrosis, senescence, autophagy and mitotic catastrophe are also associated with tumourigenesis (Okada and Mak, 2004). The characteristics of different types of cell death are summarized in **Table 1.1**.

**Table 1.1 Characteristics of different types of cell death** (adapted from Okada and Mak, 2004).

Type of cell death	Morphological changes			Biochemical features
	Nucleus	membrane	Cytoplasm	
<b>Apoptosis</b>	Chromatin condensation; nuclear fragmentation; DNA laddering.	Blebbing	Fragmentation (formation of apoptotic bodies)	Caspase-dependent
<b>Autophagy</b>	Partial chromatin condensation; no DNA laddering	Blebbing	Increased number of autophagic vesicles	Caspase-independent; increased lysosomal activity

<b>Mitotic catastrophe</b>	Multiple micronuclei; nuclear fragmentation	–	–	Caspase-independent (at early stage); abnormal CDK1/cyclinB activation
<b>Necrosis</b>	Clumping and random degradation of nuclear DNA	Swelling; rupture	Increased vacuolation of organelle degeneration mitochondrial swelling	–
<b>Senescence</b>	Senescence-associated heterochromatic foci	–	Flattening and increased granularity	SA-β-gal activity

Senescence is the phenomenon by which cells lose the ability to divide when the telomeres are not long enough to protect their chromosomes. Some morphological changes, such as flattened cytoplasm and increased granularity can be observed in senescent cells (Okada and Mak, 2004). Induction of senescence-associated β-galactosidase (SA-β-gal) activity was reported to be a biomarker of senescence and can be used to identify senescence (Dimri et al., 1995). Senescence also occurs under tumourigenic stresses and contributes to tumour suppression (Campisi, 2001). The senescence programme usually requires the function of p53 and the RB pathway as well as CDK inhibitors, such as p21 and p16 (Sage et al., 2003; Stein et al., 1999).

In contrast to naturally occurring apoptosis, necrosis is an unregulated process of traumatic cell destruction with special morphological features (**Table 1.1**), such as organelle degradation, membrane swelling and rupture (Okada and Mak, 2004). During apoptotic cell death, a dying cell turns into an almost-invisible corpse which is consumed immediately by its neighbours. Conversely, necrotic cells have bloated bodies, releasing their components into the local tissue environment (Hanahan and Weinberg, 2011).

Autophagy is a form of non-apoptotic and non-necrotic cell death involving the degradation of a cell's own components within lysosomes. It helps to maintain the balance between synthesis, degradation and recycling of cell components. Although autophagy was first described in the 1960s, its detailed processes and mechanisms are still unclear (Stromhaug and Klionsky, 2001). The distinct morphology is summarized in **Table 1.1**, which involves an increased number of autophagic vesicles and cell blebbing.

The M phase of the cell cycle can be divided into two processes: mitosis and cytokinesis. During mitosis, sister chromatids are aligned and then separate into two daughter cells with the cytoplasm being partitioned into those cells during cytokinesis. Mitotic catastrophe is a cell death modality that is caused by aberrant mitosis (Kepp et al., 2011). Multinucleate and uncondensed chromosomes are typical morphological characters which are different from apoptosis, necrosis and autophagy (Okada and Mak, 2004).

#### **1.1.4.2 Bcl-2 family proteins and apoptosis**

The programmed cell death (apoptosis) of unwanted or damaged cells is essential to maintain normal development through two programmes (extrinsic and intrinsic) which finally activate the cysteinyl aspartate – specific protease (Caspase) family, leading to cell cleavage and death (Danial, 2007). The extrinsic pathway operates downstream of death receptors, such as the tumour necrosis factor (TNF) and Fas receptor family, resulting in the formation of the death-inducing signalling complex (DISC), which in turn activates caspase-8. In the intrinsic pathway, caspase activation is under the regulation of the apoptosome, which is composed of apoptotic protease – activating factor-1 (APAF-1), caspase-9 and cytochrome c.

The Bcl-2 family can be divided functionally into anti-apoptotic proteins (Bcl-2, Bcl-X<sub>L</sub>, Bcl-w, Mcl-1 and A1) and pro-apoptotic proteins (BAK, BAX BIM, BID, PUMA, NOXA, BAD, HRK, BMF, BIK)(Lessene et al., 2008) (**Figure 1.11**). Based on the sequence and structural features, the family comprises multidomain proteins and BH3-only proteins. Multidomain proteins share four Bcl-2 homology (BH) domains while BH3-only pro-apoptotic proteins show sequence homology only within a single  $\alpha$  helical segment, the BH3 domain (Lessene et al., 2008).

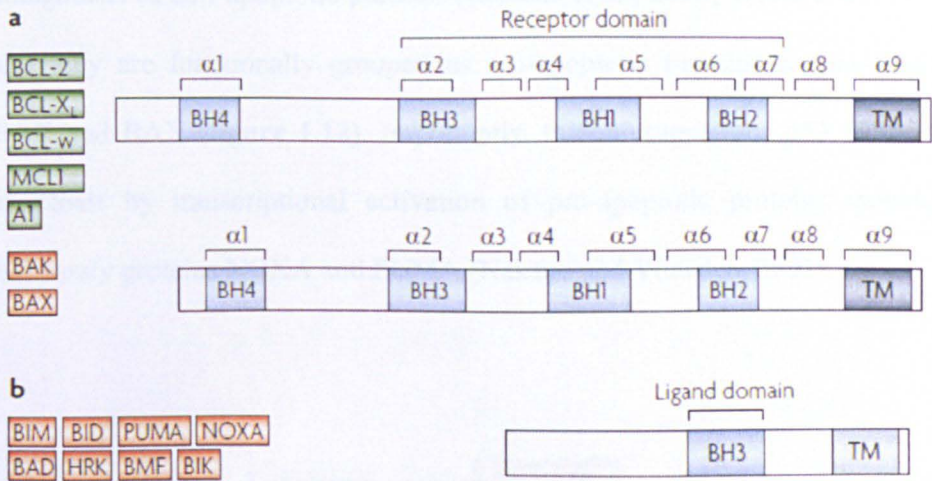


**Figure 1. 11 The Bcl-2 protein family** (Lessene et al., 2008). This family can be divided functionally into anti-apoptotic proteins (green boxes) and pro-apoptotic proteins (red boxes). Based on the sequence and structure features, the family comprises multidomain proteins (a) and BH3-only proteins (b).

Interactions between pro-survival and pro-apoptotic proteins control the switch of cell death through governing mitochondrial outer membrane permeabilization (MOMP) and release of cytochrome c into the cytoplasm. Pro-apoptotic proteins BAK and BAX are essential for apoptosis through forming pores capable of releasing cytochrome c in the mitochondrial outer membrane (MOM) (Danial and Korsmeyer, 2004). Once cytochrome c is released, it binds to the apoptotic protease – activating factor-1 (APAF-1) to facilitate the formation of apoptosome, which is in charge of caspase activation. There are several models concerning the pro- or anti- apoptotic effects of the Bcl-2 family. In one theory, anti-apoptotic proteins, such as Bcl-2 and Bcl-X<sub>L</sub>, bind to the BH3 domain of pro-apoptotic proteins BAK or BAX and inhibit their activity. As sensors of cellular stress, BH3-only proteins are the natural

antagonists of anti-apoptotic proteins (Lessene et al., 2008; Willis et al., 2007) and they are functionally grouped as pro-apoptotic proteins for facilitating BAK and BAX (figure 1.12). Importantly, tumour suppressor p53 facilitates apoptosis by transcriptional activation of pro-apoptotic proteins including BH3-only proteins NOXA and PUMA (Nakano and Vousden, 2001).

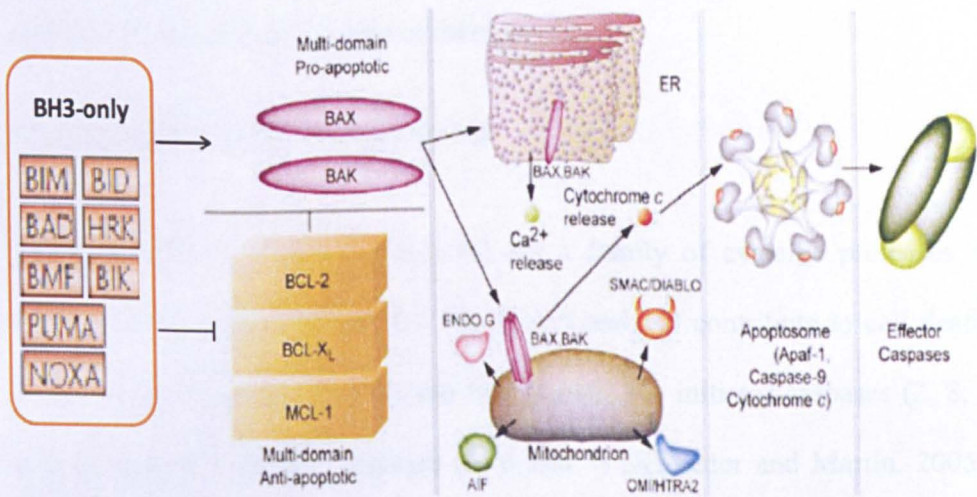


**Figure 1.12 Intrinsic apoptotic pathway** (adapted from Danial and Korsmeyer, 2004). See text for details.

In addition to their roles in the mitochondria, Bcl-2 family members BAK and BAX induce  $Ca^{2+}$  release from the Endoplasmic Reticulum, which is involved in regulating the threshold of apoptosis (Danial, 2007; Rong and Distelhorst, 2008).

As one of the most important anti-apoptotic proteins, Mcl-1 plays two main roles in the cellular apoptosis machinery (Akgul, 2009). Firstly, Mcl-1 may function as an anti-apoptotic factor by sequestering Bak on the outer mitochondrial membrane (OMM) to inhibit Bak oligomerization and

cytochrome c release from mitochondria. Secondly, Mcl-1 could display its pro-survival functions by heterodimerizing with activator BH3-only proteins, such as tBid, PUMA and Bim. Importantly, Mcl-1 has a short half-life and is a highly regulated protein. It's rapidly down-regulated during apoptosis while its expression is induced by survival and differentiation signals. Moreover, specific knockdown of Mcl-1 expression by RNA interference resulted in induction of apoptosis in cancer cell lines (Polier et al., 2011), indicating Mcl-1 could be an ideal target for cancer therapy.

#### **1.1.4.3 Caspase family and cell death**

Caspases (cysteine-aspartic proteases) are a family of cysteine proteases of which at least seven (caspase 2, 3, 6, 7, 8, 9 and 10) contribute to cell death. These caspases can be divided into two groups: the initiator caspases (2, 8, 9 and 10) and the effector caspases (3, 6 and 7) (Kroemer and Martin, 2005). Effector caspases further cleave other protein substrates and trigger the apoptotic process.

Although caspase activation has frequently been viewed as a sign of apoptosis, caspase inhibition is not always enough to stop cell death and often leads to morphology changes (Chipuk and Green, 2005). The relationships between cell death and caspase activation have been classified into 3 groups: cell death through caspase activation, cell death with caspase activation and cell death without caspase activation (**Figure 1.13**) (Kroemer and Martin, 2005). As shown in **Figure 1.13**, death with caspase activation and death without caspase activation are classified as caspase-independent death.

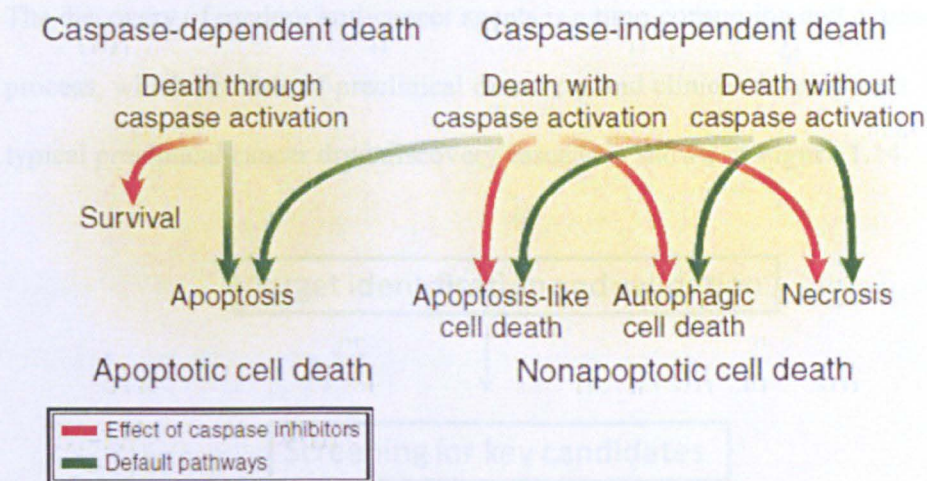


**Figure 1.13 Relationship between caspase dependency and cell death** (Kroemer and Martin, 2005).

## 1.2 Preclinical cancer drug discovery

The majority of anti-cancer drugs on the market were discovered either by chance, for example alkylating anti-neoplastic agents or by screening programmes, such as paclitaxel. However, selectivity is a main issue for these agents. For example, genotoxic drugs which are widely used in chemotherapy for cancer treatment induce general DNA damage in cancer cells but are also highly toxic to normal tissues. Therefore, new and better anti-cancer agents are urgently needed for cancer treatment. Recent research into the fundamental biochemical characteristics of tumour cells has provided a rational approach to the drug design process and the combination of rational drug design and modern screening techniques is being used to identify compounds against specific cancer-related targets (Thurston, 2006).

The discovery of modern anti-cancer agents is a time-consuming and expensive process, which consists of preclinical discovery and clinical development. The typical preclinical cancer drug discovery cascade is shown in **Figure 1.14**.

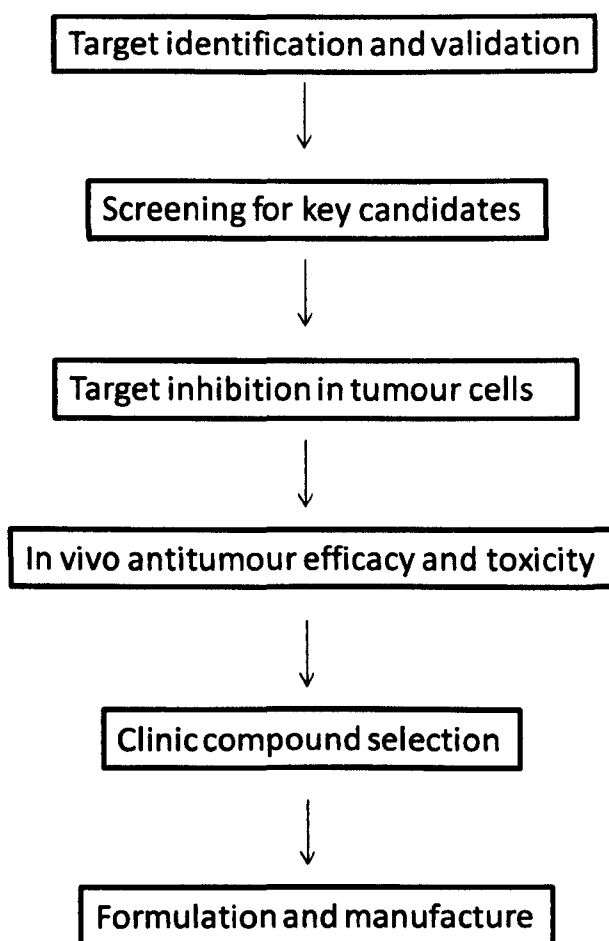


**Figure 1.14** The preclinical cancer drug discovery cascade (adapted from Neidle, 2008)

### **1.2.1 Target identification and validation**

The first step of developing a new drug is target identification and validation (figure 1.14). A good target for cancer should be effective and safe. The best approach to develop anti-cancer drugs is targeting the hallmarks of cancer, as

illustrated in **Figure 1.15**. Drugs that inhibit one of the 6 classic hallmarks (**Figure 1.1**) as well as the enabling characteristics and emerging hallmarks of cancer have been in clinical trials or approved for clinical use (Weinberg, 2007). As highlighted in **Figure 1.15**, inhibition of cell cycle CDKs (the master regulators of the cell cycle) may conquer the proliferative disorder of cancer, and transcriptional CDK9 inhibitors may induce apoptosis in tumour cells by down-regulation of anti-apoptotic proteins, such as Mcl-1 and Bcl-2 (section 1.3.3).

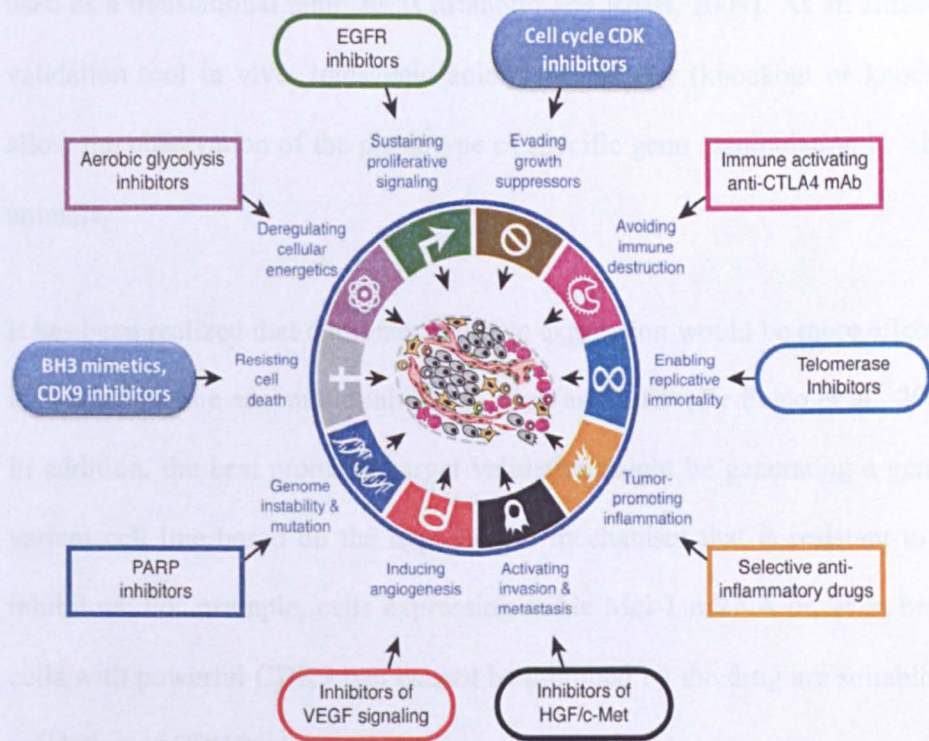


**Figure 1.15 Cancer specific targets** (Adapted from Weinberg, 2007). The drugs listed are only illustrative examples. Many other drug candidates with different molecular targets are under development for most of these hallmarks.

Once an ideal target is chosen, it needs to be fully validated. Validation techniques include knockdown or knockout of target protein expression using *in vitro* methods (antisense RNA and small interfering RNA – siRNA, etc.) and animal models (transgenic animals, etc.) (Hughes et al., 2011). Antisense RNA is single-stranded RNA which is complementary to a messenger RNA (mRNA). By using antisense technology, the synthesis of a target protein can be blocked through translational inhibition of mRNA when binding to the antisense oligonucleotide (Henning SW, 2002). Recently, siRNA (a class of short double-stranded RNA molecules) has been widely used for target validation. The siRNAs induce cleavage of their target mRNA and prevent it from being used as a translational template (Castanotto and Rossi, 2009). As an attractive validation tool *in vivo*, transgenic animal technology (knockout or knockin) allow the observation of the phenotype of specific gene manipulation in whole animals.

It has been realized that dominant negative expression would be more effective in blocking some enzymatic inhibitors, such as CDK9 (De Falco et al., 2000). In addition, the best proof for target validation might be generating a genetic variant cell line based on the hypothetical mechanism that is resistant to the inhibitors. For example, cells expressing stable Mcl-1 mRNA or, even better, cells with powerful CDK9 that cannot be inhibited by the drug are suitable for validation of CDK9 inhibitors.

## 1.2.2 Lead identification and optimisation

After target identification and validation, the next step in the drug discovery process is to identify 'hit' molecules by means of screening assays. There are many screening methods, reviewed by JP Hughes etc. (Hughes et al., 2011), including: high throughput, focused screen, fragment screen, structural aided drug design, virtual screen, physiological screen and NMR screen (**Table 1.2**). In high throughput screening (HTS), an entire compound library is screened against the drug target in 384 -, 1536 -, or 3456 - well plates. More than 100,000 compounds can be screened in one day on a routine basis. For compounds with similar structures to molecules for which the target has been identified, focused or knowledge-based screening is a cheaper and effective method. In Chapter 3, the development of a cell-based focused screening cascade is described which is able to classify compounds and identify effective transcription CDK (CDK7 and especially CDK9) inhibitors from analogues of reported compounds. Other screening methods shown in **Table 1.2** are also widely used in both industry and academia. Additionally, in order to predict the *in vivo* absorption, distribution, metabolism and elimination (ADME) of lead compounds, high-throughput *in vitro* assays were performed for the physicochemical determination of aqueous solubility, lipophilicity (LogP), pKa and membrane permeability (Neidle, 2008).

**Table 1.2 Screening strategies** (adapted from Hughes et al., 2011).

Screen	Description	Comments
<b>High throughput</b>	Large numbers of compounds analysed in an assay generally designed to run in plates of 384	Large compound collections often run by big pharma but smaller compound banks can also be run in either pharma or

	wells and above	academia which can help reduce costs. Companies also now trying to provide coverage across a wide chemical space using computer assisted analysis to reduce the number of compounds screened.
<b>Focused screen</b>	Compounds previously identified as hitting specific classes of targets (e.g. kinases) and compounds with similar structures	Can provide a cheaper avenue to finding a hit molecule but completely novel structures may not be discovered and there may be difficulties obtaining a patent position in a well-covered IP area
<b>Fragment screen</b>	Soak small compounds into crystals to obtain compounds with low mM activity which can then be used as building blocks for larger molecules	Can join selected fragments together to fit into the chemical space to increase potency. Requires the availability of a crystal structure
<b>Structural aided drug design</b>	Use of crystal structures to help design molecules	Often used as an adjunct to other screening strategies within big pharma. Usually a compound is docked into the crystal and this used to help predict where modifications could be made to provide increased potency or selectivity
<b>Virtual screen</b>	Docking models: interrogation of a virtual compound library with the X-ray structure of the protein or, if have a known ligand, as a base to develop further compounds.	Can provide the starting structures for a focused screen without the need to use expensive large library screens. Can also be used to look for novel patent space around existing compound structures
<b>Physiological screen</b>	A tissue-based approach for determination of the effects of a drug at the tissue rather than the cellular or subcellular level, for example, muscle contractility	Bespoke screens of lower throughput. Aim to more closely mimic the complexity of tissue rather than just looking at single readouts. May appeal to academic experts in disease area to screen smaller number of compounds to give a more disease relevant readout
<b>NMR screen</b>	Screen small compounds (fragments) by soaking into protein targets of known crystal or NMR structure to look for hits with low mM activity which can then be used as building blocks for larger molecules	Use of NMR as a structure determining tool

### **1.2.3 Target confirmation in tumour cells**

After the screening programme, lead compounds are then evaluated using *in vitro* tumour cell lines. By testing against a panel of different tumour cell lines, the selective cytotoxicity of a compound toward a particular tumour type may be determined (Thurston, 2006). The US National Cancer Institute (NCI) developed 60 human tumour cell lines which are derived from 9 tumour types in late 1980s and used them for drug discovery (Shoemaker, 2006). Until now, more than 30,000 compounds have been tested. It has been demonstrated that compounds with a similar cell growth inhibition mechanism usually show similar patterns of activity against the NCI 60 cell lines (Paull et al., 1989). Based on this finding, the NCI 60-cell-line panel also provides an algorithm called COMPARE which has been successfully used to predict the mechanisms of new compounds (Zaharevitz et al., 2002).

Detailed mechanism studies are also performed in tumour cell lines to confirm the targets of lead compounds. For example, in order to identify new CDK9 inhibitors, the phosphorylation status of Ser 2 site of RNA polymerase II (CDK9 phosphorylation site) and reduction of anti-apoptotic protein Mcl-1 can be tested by western blots (Liu et al., 2011b)

## **1.3 Targeting cyclin dependent kinases for cancer therapy**

### **1.3.1 Kinases**

Kinases are enzymes that transfer phosphate groups from molecules with high energy (ATP, etc.) to specific substrates in a process known as phosphorylation. The largest groups of kinases are protein kinases, which regulate cell function by modifying the activities of functional proteins. They regulate activity, location and stability of many proteins through the addition of a phosphate group (Jans and Hubner, 1996).

Among the 518 human protein kinases identified, 478 have similar catalytic domains which are related in sequence. Based on sequence similarity and biochemical function, the 478 protein kinases are classified into 7 major groups. Based on different phosphorylation site, protein kinases can also be divided into 2 categories which contain kinases which phosphorylate proteins on tyrosine residues (the tyrosine kinases, TK group) or kinases which phosphorylate primarily on serine and threonine residues (the other six groups). More than 100 kinases in the sub-families of the human protein kinase tree have not been characterized yet. However, the relationship shown on the tree can be used to predict their substrates and biological functions.

Kinases have become one of the most intensively studied drug targets and more than 30 distinct kinase targets have been developed to the level of Phase I clinical trials (Zhang et al., 2009). As mentioned earlier, cancer cells can evade

cell growth suppressors and apoptosis. Therefore, cyclin-dependent kinases (CDKs), which are critical regulators of cell cycle progression and RNA transcription, are ideal targets for cancer treatment.

### **1.3.2 Cyclin dependent kinases (CDKs)**

CDKs, one of the most extensively studied kinase groups in the family of serine/threonine (Ser/Thr) protein kinases, phosphorylate serine and threonine amino acid residues in specific sequences of numerous proteins, particularly those involved in mitosis and cell cycle division when associated with their cyclin complexes. Cdc2 (CDK1) was first discovered to regulate the cell cycle in yeast. To date, 13 CDKs and 25 proteins with homologous cyclin boxes have been found in the human genome and the function of 10 the human CDKs and their associated complexes have been identified (**Figure 1.16**) (Knockaert et al., 2002).

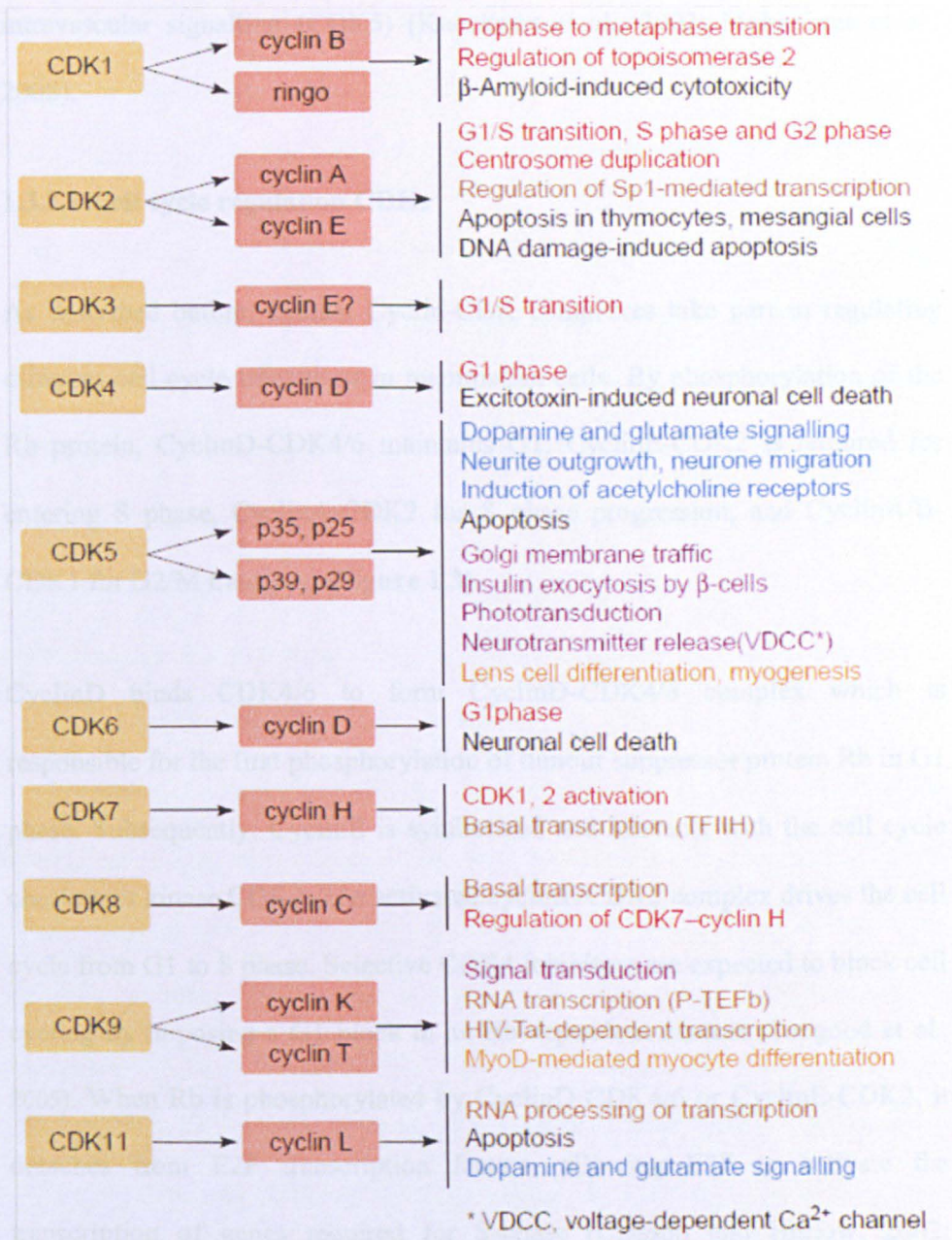


**Figure 1.16** The specific complexes and functions of 10 human CDKs which have been identified (Knockaert et al., 2002).

Most CDKs are activated by association with cyclins, forming CDK complexes. These heterodimeric complexes can phosphorylate various substrates involved in transcriptional regulation (CDK7, CDK8, CDK9, and CDK11), and cell-cycle progression (CDK1, CDK2, CDK4, CDK6, and CDK7), as well as

intravascular signalling (CDK5) (Knockaert et al., 2002; Malumbres et al., 2008).

### **1.3.2.1 Cell cycle regulation CDKs**

As described before, distinct Cyclin-CDK complexes take part in regulating different cell cycle transitions in mammalian cells. By phosphorylation of the Rb protein, CyclinD-CDK4/6 maintains G1, CyclinE-CDK2 is required for entering S phase, CyclinA-CDK2 for S phase progression, and CyclinA/B-CDK1 for G2/M transition (**Figure 1.3**).

CyclinD binds CDK4/6 to form CyclinD-CDK4/6 complex which is responsible for the first phosphorylation of tumour suppressor protein Rb in G1 phase. Subsequently, CyclinE is synthesized and interacts with the cell cycle checkpoint kinase CDK2. The activated cyclinE/CDK2 complex drives the cell cycle from G1 to S phase. Selective CDK4 inhibitors are expected to block cell cycling by imposing a G1 block in an Rb-dependent manner (Toogood et al., 2005). When Rb is phosphorylated by CyclinD-CDK4/6 or CyclinE-CDK2, it detaches from E2F transcription factors, allowing E2F to activate the transcription of genes required for S-phase (Classon and Harlow, 2002; Ezhevsky et al., 2001). One of the genes transcribed by E2F is CyclinE itself, causing a positive feedback cycle as CyclinE accumulates.

Cyclin B is made in G2 and M-phases (Coverley et al., 2002). It combines with CDK1 to form the major mitotic kinase MPF (M-phase Promoting Factor), which is a heterodimeric protein that stimulates the mitotic and meiotic cell cycles. Degradation of Cyclin-B, followed by MPF inactivation, is required for

exit from mitosis. Previous work suggests that Cdk2 may facilitate accumulation of cyclin B and contribute to G2/M progression (Lukas et al., 1999). Inhibition of CDK2 also results in G2 phase arrest (Hu et al., 2001).

Cell cycle CDK inhibitors have been developed as potential new cancer drugs based on the premise that they should counteract the unchecked proliferation of transformed cells by modulating the functions of CDKs in the regulation of the cell cycle. In recent years, the conventional understanding of how CDKs function and their role in the cell cycle has been challenged. The observation that cancer cell lines and some embryonic fibroblasts lacking CDK2 proliferate normally, and that knockout mice are viable (Barriere et al., 2007; Berthet et al., 2003), suggest CDK2 performs non-essential roles and that other CDK paralogues substitute in cell cycle control. In addition, the redundancy of CDK4 and 6 was also suggested by null mammalian cells that enter the cell cycle, and S phase, normally (Malumbres et al., 2004). It has been demonstrated that mouse embryos deficient in all interphase CDKs develop to mid-gestation as CDK1 can form complexes with all cyclins and consequently phosphorylates pRb, thus activating E2F mediated transcription of proliferation factors (Santamaria et al., 2007). Elimination of CDKs 2, 3, 4 and 6 in these investigations shows that expression levels of CDK1, and the cell cycle cyclins, appears to be unchanged, that catalytic activity of CDK1 is sufficient for cell cycle progression and that CDK1 can execute all necessary events for cell division. Moreover, specific CDK1 depletion in some cancer cells results in accumulation of cells with G2/M DNA content, but causes only minimal cell death, and CDK2/cyclin B is readily detected in cells deleted for CDK1 to facilitate G2/M progression (Cai et al., 2006b). Taken together, these studies

suggest that specifically targeting individual cell cycle CDKs may not be an optimal therapeutic strategy.

### 1.3.2.2 Transcriptional regulation CDKs

RNA polymerase (RNAP) makes a copy of a gene from the DNA to mRNA during a process called transcription. RNAP II, which is a 550 KDa complex of 12 subunits, is the most studied type of RNAP in eukaryotic cells.

In contrast to CDKs involved in cell cycle transitions, cyclinH-CDK7 and cyclinT-CDK9 complexes regulate RNAPII transcription. The carboxy-terminal domain of human RNA polymerase II typically consists of 52 repeats of the sequence Tyr-Ser-Pro-Thr-Ser-Pro-Ser. CDK7 first phosphorylates the Ser-5 residues of the CTD in the heptapeptide repeats Y1S2P3T4S5P6S7 as part of transcription initiation. The positive transcription elongation factor b (P-TEFb), which is composed of cyclinT-CDK9, phosphorylates the Ser-2 in the heptapeptide repeats and facilitates transcriptional elongation (**Figure 1.17**).

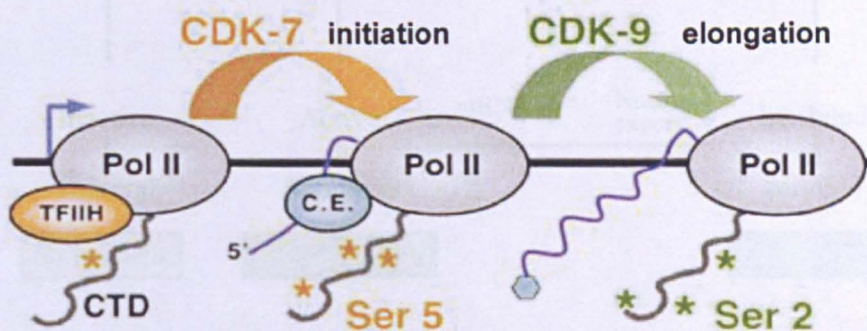


**Figure 1.17 The transcription process regulated by CDKs.** CDK7/cyclin H first phosphorylates RNAP II CTD at Ser 5, which allows the dissociation of TFIIH from RNAP II and promotes the initiation of RNAP II. This phosphorylation is also necessary for recruitment of the Capping enzyme (C.E.) which binds to RNAP II to generate a 5'cap for mRNAs.

Phosphorylation of CTD Ser 2 by CDK9 facilitates transcription elongation. (Adapted from Walker, 2006).

Transcriptional inhibitors can be used for selective cancer therapy (**Figure 1.18**). Usually, normal cells have relatively low sensitivity to apoptotic stimuli and oncogenic transformed cells show increased sensitivity to apoptotic signals. However, this apoptotic sensitivity is counteracted by the induction of anti-apoptotic proteins, whose transcription procedures are tightly dependent on the activity of RNAPII. Inhibition of RNAPII transcription activity would result in a reduction of the anti-apoptosis proteins, which finally leads to apoptosis of tumour cells. In contrast, normal cells should not be affected by decreased levels of anti-apoptosis proteins (Koumenis and Giaccia, 1997).

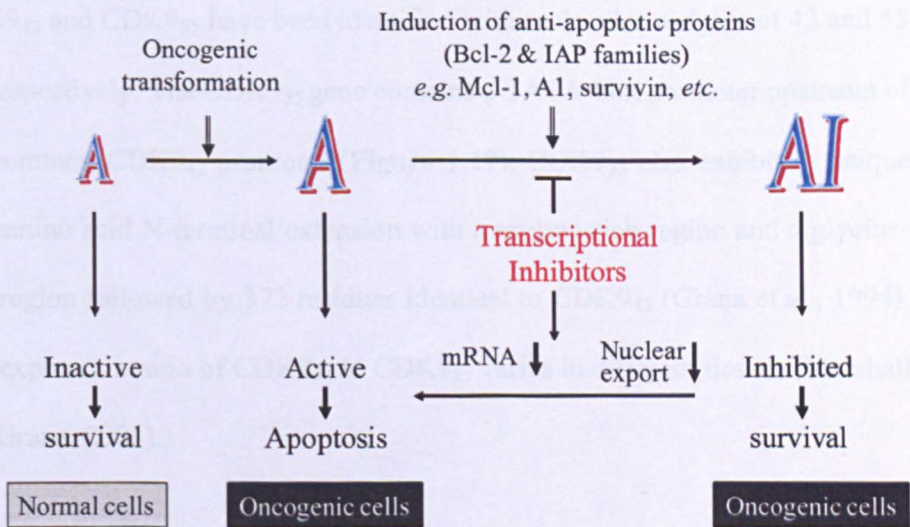


**Figure 1.18 Targeting transcription as a potential cancer therapy** (adapted from Koumenis and Giaccia, 1997). Oncogenic transformation usually enhances the sensitivity of cells to apoptotic signals (A). However, anti-apoptotic proteins expressed in cancer cells inhibit the function of apoptotic signals (AI) and enable cancer cell survival. Transcriptional inhibitors recover the sensitivity of cancer cells to apoptosis by reducing anti-apoptotic proteins and increasing p53 tumour suppressor.

As described before in section 1.1.3, p53 induces apoptosis or other effects as a transcription regulator and the transcription inhibition by CDK9 is supposed to counteract the function of p53. Paradoxically, pharmacological inhibition of mRNA synthesis by P-TEFB leads to global inhibition of mRNA synthesis but activation of the p53 pathway through p53 accumulation and expression of specific p53 target genes (Gomes et al., 2006).

### **1.3.3 Cyclin Dependent Kinase 9**

CDK9 is unique in apparently lacking cell-cycle-related roles (Wang and Fischer, 2008). It was originally named PITALRE and identified in a human cDNA library screen in 1994 (Grana et al., 1994). The region of CDK9 shares 33 - 47 % amino acid identity with other CDKs. Two isoforms of CDK9, CDK9<sub>42</sub> and CDK9<sub>55</sub> have been identified with molecular weights of 42 and 55 kD respectively. The CDK9<sub>55</sub> gene contains a TATA-box promoter upstream of the common CDK9<sub>42</sub> promoter (**Figure 1.19**). CDK9<sub>55</sub> also exhibits a unique 117 amino acid N-terminal extension with a proline-rich region and a glycine-rich region followed by 372 residues identical to CDK9<sub>42</sub> (Grana et al., 1994). The expression ratio of CDK9<sub>42</sub> to CDK9<sub>55</sub> varies in different tissues (Marshall and Grana, 2006).

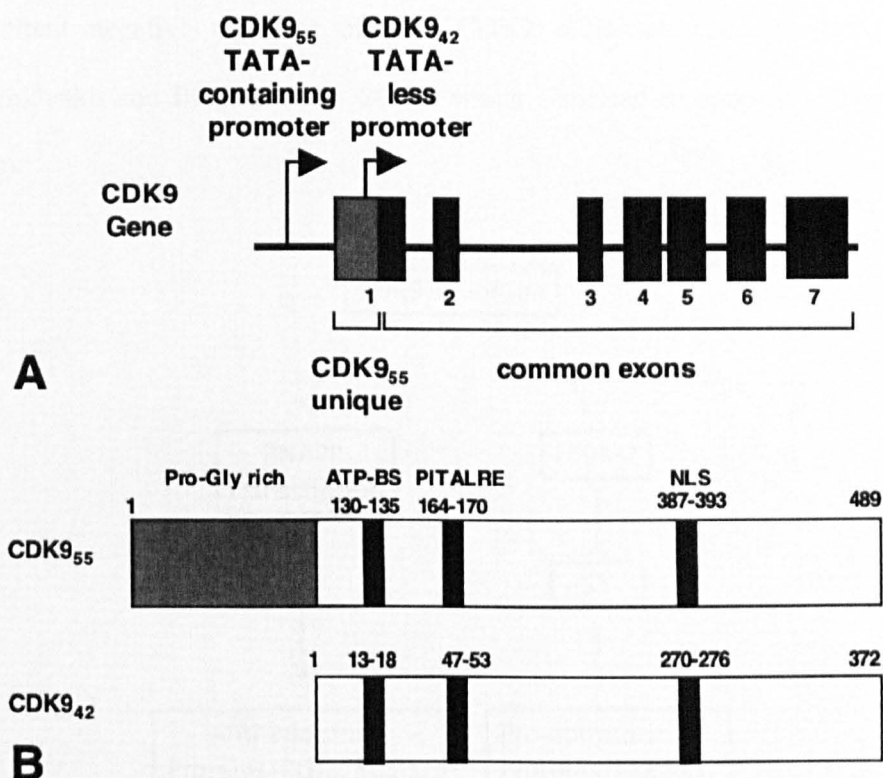


**Figure 1.19 Gene and sequence of human CDK9 isoforms** (Marshall and Grana, 2006). (A) CDK9<sub>42</sub> has a TATA-less promoter and CDK9<sub>55</sub> contains an upstream TATA-containing promoter. (B) CDK9<sub>42</sub> consists of 372 amino acids, whereas CDK9<sub>55</sub> exhibits a unique 117 amino acid N-terminal domain (Pro-Gly rich) followed by 372 residues identical to CDK9<sub>42</sub>. Both CDK9 isoforms contain the ATP-binding site (ATP-BS), the PSTAIRE-like motif PITALRE, and the putative nuclear localization signal (NLS).

### 1.3.3.1 CDK9 and cancer

As described earlier, resisting cell death is a general hallmark of cancer. Cancer cells are “addicted” to transcription because they need continuous production of anti-apoptotic proteins such as Bcl-2 and Mcl-1 (Wang and Fischer, 2008). Therefore, a therapeutic window for the use of transcriptional CDK inhibitors, especially CDK9, could be predicted. Targeting CDK9 regulated transcription can recover the sensitivity of cancer cells to apoptosis by reducing anti-apoptotic proteins (**Figure 1.20**). Through down-regulation of MDM2, an

important negative regulator of p53, CDK9 inhibition can stabilize p53 (Demidenko and Blagosklonny, 2004), which also lead to apoptosis (Figure 1.20).

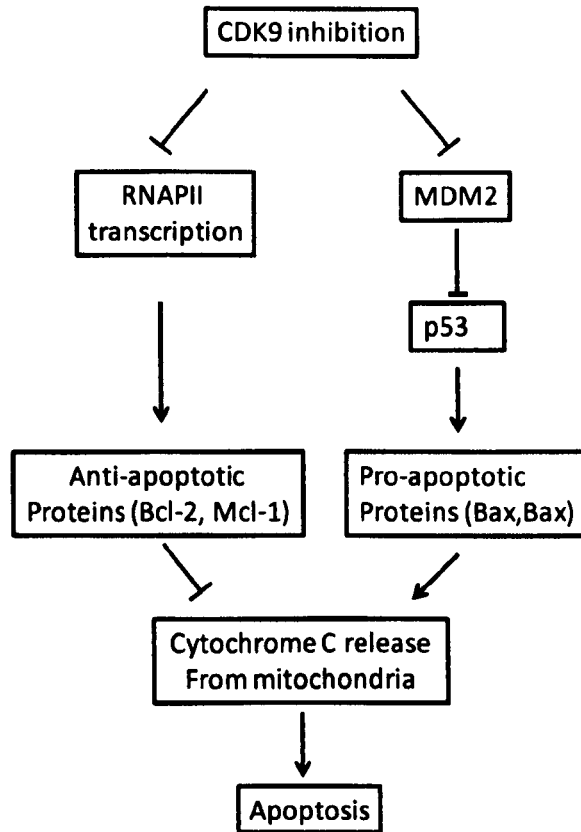


**Figure 1.20 Apoptosis induced by CDK9 inhibition.** In the intrinsic pathway, apoptosis occurs after the release of cytochrome C from mitochondria, which is regulated by Bcl-2 family members including pro- and anti- apoptotic proteins. CDK9 activates pro-apoptotic proteins BAK and BAX through down-regulation of anti-apoptotic proteins (Bcl-2, Bcl-XL, Mcl-1). By reducing MDM2 levels, CDK9 inhibition stabilizes p53, which could also induce apoptosis.

### 1.3.3.2 CDK inhibitors in clinical trials

Since inhibition of CDK9 has emerged as a potential cancer therapy, numerous CDK inhibitors have been developed. Many of them were originally designed

to target cell cycle CDKs, but it was found later that their anti-tumour activity was consistent with cellular CDK9 mediated RNAPII inhibition. This is why these drug candidates are cross-reactive toward multiple CDKs.

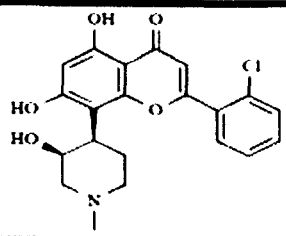
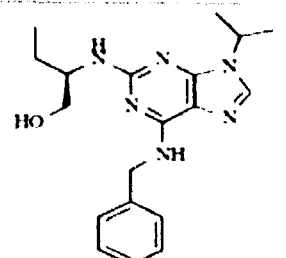
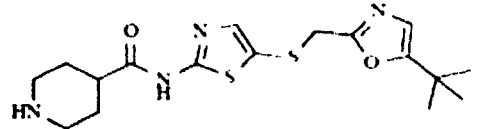
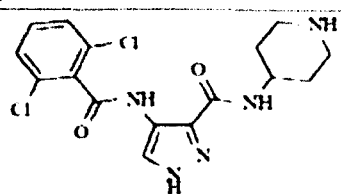
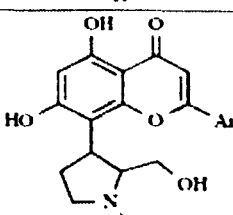
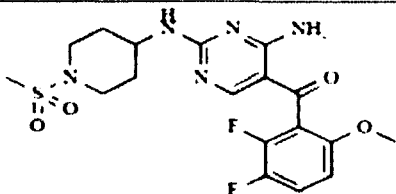
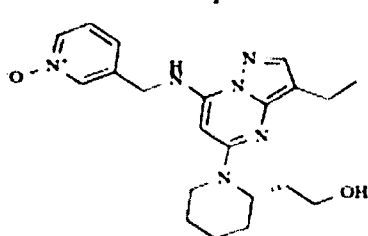
Many different classes of ATP competitive CDK inhibitors have been developed, (Rizzolio et al., 2010). Currently, some of them are under clinical evaluation (**Table 1.3**).

### **Flavopiridol**

The first CDK inhibitor to enter clinical trials was flavopiridol, which is a semi-synthetic flavonoid with potent inhibitory activity against a variety of cyclin-dependent kinases (CDK1, 2, 4, 6, 7 and 9). Being the most potent known inhibitor of CDK9, flavopiridol binds tightly to the ATP binding site of CDK9, with a  $K_i$  value of 3 nM (Shapiro, 2006).

At least 15 trials have been done in phase I and phase II aimed at evaluating the anti-tumour efficacy of flavopiridol (Lu et al., 2004). A phase I study in chronic lymphocytic leukemia (CLL) demonstrated marked activity with a 40% overall response rate (Phelps et al., 2009). In CLL cells, flavopiridol decreases transcription by inhibiting the phosphorylation of CTD of RNAPII at ser2 and ser5 (Chen et al., 2005). Since CLL cells are largely quiescent and normally do not need the cell cycle CDKs, the effect of flavopiridol is believed to be mainly through CDK9 inhibition, leading to down-regulation of anti-apoptotic proteins, such as Mcl-1 (Chen et al., 2005).

**Table 1. 3 Small-molecule CDK inhibitors with activity against CDK9 in clinical trials**  
(Rizzolio et al., 2010).

Compound	Structure	Phase
Flavopindol		II
(R)-roscovitine		II
BMS 387032		I
AT7519		I
P27600		I
R547		I
SCH 727965		II

Discouraging results were obtained when flavopiridol was administered as a single agent in phase II clinical trials for multiple myeloma (Dispenzieri et al., 2006), metastatic malignant melanoma (Burdette-Radoux et al., 2004) and endometrial carcinoma (Grendys et al., 2005). The major toxicity effects of flavopiridol include diarrhoea and myelosuppression, while the main problems which limit the clinical use of flavopiridol as a single agent are due to its poor absorption and narrow therapeutic window. Currently, a number of clinical trials for a combination of flavopiridol with other drugs are in progress.

Flavopiridol has also been reported to target DNA, intercalating into the molecule and comparison analysis reveals that flavopiridol shares similar mechanisms of action with DNA intercalating or damaging agents, such as ecteinascidin 729, chromomycin A3, actinomycin D (Bible et al., 2000). However, the biological significance of DNA binding has not been determined. In addition, the cytotoxicity of flavopiridol was reported to have no cell type selectivity (Liu et al., 2011b) and the reason for that needs to be further investigated.

### **Roscovitrine**

Roscovitrine (Seliciclib) is a purine derivative that inhibits CDK2, 7 and 9 (McClue et al., 2002). Similar to flavopiridol, roscovitrine inhibits RNAPII CTD phosphorylation, which results in a decrease in Mcl-1 and other anti-apoptotic proteins in CLL cells (Alvi et al., 2005; Hahntow et al., 2004). In contrast to flavopiridol, roscovitrine shows a higher degree of selectivity,

targeting only 11 kinases ( $K_i$  5 $\mu$ M) across a panel of 317 kinases (D'Andrea et al., 2005).

Several phase I and phase II clinical trials for roscovitine alone or with other agents have been done in non-small cell lung cancer (NSCLC) and other malignant solid tumours. The common side effects are hypokalemia, hyponatremis, hyperglycemia, elevated gamma-glutamyl transpeptidase and skin rash (Rizzolio et al., 2010).

### **SNS-032**

SNS-032 (formerly known as BMS-387032), is a thiazole derivative which was originally synthesized by Bristol-Myers Squibb Pharmaceutical Research Institute as a selective inhibitor of CDK2 (Misra et al., 2004). It was later realized that SNS-032 was also potent against CDK9 ( $IC_{50}$  = 4 nM) and CDK7 ( $IC_{50}$  = 62 nM) after this compound was licensed by Sunesis Pharmaceuticals.

Phase I trials of SNS-032 against advanced solid tumours (Heath et al., 2008) and advanced B-lymphoid malignancies, including CLL and multiple myeloma (Chen et al., 2009). Transcription inhibition by SNS-032 reduced anti-apoptotic proteins Mcl-1 and XIAP, resulting in cell death. Removal of SNS-032 reactivated RNAPII, leading to re-synthesis of Mcl-1 (Chen et al., 2009).

#### **1.3.3.3 Discovery of novel CDK9 inhibitors**

Structure-based design and analogue modification are often used to identify kinase inhibitors. Most of the CDK inhibitors under evaluation are ATP

competitive molecules. The x-ray crystal structure of CDK2 indicates that three regions in the ATP-active binding domains are crucial for ATP mimetics: the hinge region, the ribose binding domain and the hydrophobic binding pocket. The hydrophobic binding pocket plays the key role for designing inhibitors with specificity for individual CDKs (Wang et al., 2004).

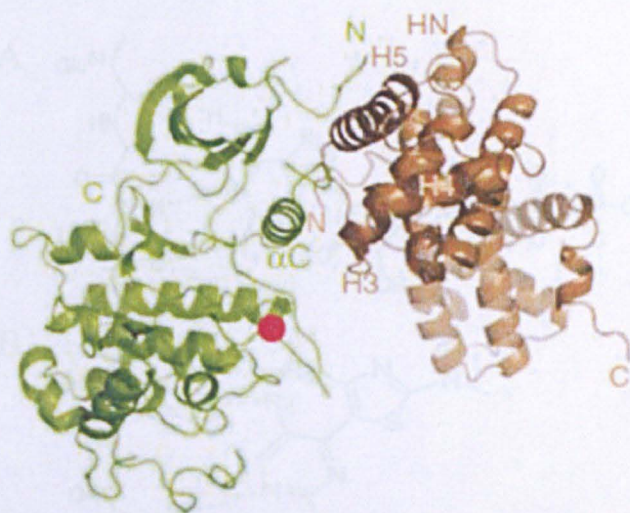


**Figure 1.21** The crystal structure of the CDK9 (green) /cyclin T1 (brown) complex (Baumli et al., 2008). The phospho-threonine residue in the activation segments is indicated by the red dot.

The structure of the ATP binding domain is particularly conserved among the CDKs, especially between CDK2 and CDK9. Recently, the crystal structure of CDK9/Cyclin T1 has been determined (Baumli et al., 2008) (**Figure 1.21**), showing a relative 26° rotation of Cyclin T1 with CDK9. ATP antagonistic CDK9 inhibitors, such as flavopiridol, bind to the ATP binding site in CDK9 and induce un-anticipated structural rearrangement.

Our novel CDK9 inhibitors, based on the structure of 2, 4, 5-trisubstituted pyrimidine, are designed as ATP antagonists against the ATP binding pocket of the kinase domain (**Figure 1.22**). Inspection of the binding mode of this class of CDK inhibitors in the ATP pocket of CDK2 indicated that they bound similarly to ATP itself.

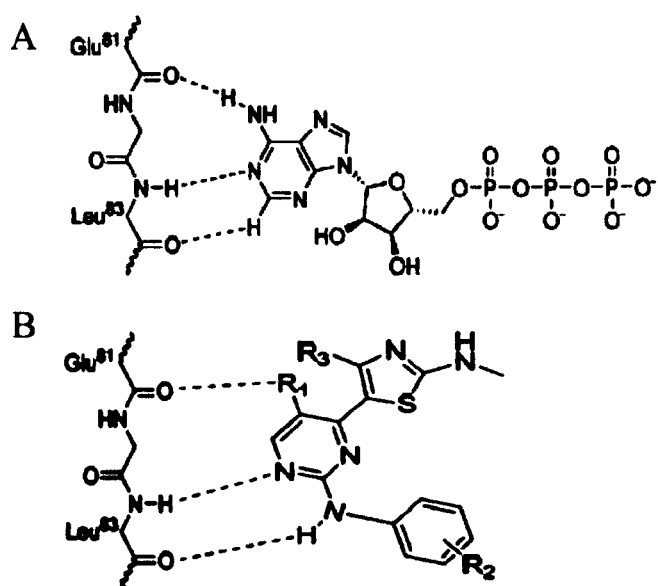


**Figure 1.22** Similar binding modes of 2,4,5-trisubstituted pyrimidine and ATP to ATP binding pocket of CDK2. A The three hydrogen bonds in this ATP-CDK complex are: NH<sub>2</sub>: Glu 81 CO; pyrimidine N1: Leu 83 NH; pyrimidine H6: Leu 83 CO. B The proposed binding of 2,4,5-trisubstituted pyrimidine to the ATP binding pocket of CDK2. R<sub>1</sub> binds to Glu 81 CO. R<sub>2</sub> and R<sub>3</sub> are designed to improve the potency and selectivity against CDK9.

## 1.4 Aims and objectives

Over the past decade, an intensive search for small molecule CDK inhibitors has resulted in development of several CDK inhibitors in clinical trials. A

novel class of 2,4,5-trisubstituted pyrimidine CDK inhibitors has been developed in our group. The project described was undertaken with the following specific aims:

- 1) To develop a screening cascade to classify compounds on the basis of their effects on proliferation, transcription, cell-cycle regulation and apoptosis. This cascade could then be used to screen and identify lead compounds.
- 2) To study the detailed cellular mode of action for lead compounds. Confirming the primary cellular mechanism of action.
- 3) To select a pre-clinic candidate using the drug flavopiridol as a benchmark.

This project involves cellular anti-cancer drug screening, *in vitro* biological evaluation and mechanistic study of these novel kinase inhibitors in the early stages of the drug discovery process.

# Chapter Two: Materials and Methods

## 2.1 Materials

### MTT assay

MTT Sigma-aldrich (cat: M2128-1G); DMSO Sigma-aldrich (cat: D5879-1L).

### Caspase 3 assay

Sigma Caspase 3 Assay Kit, Fluorimetric cat: (CASP3F-1KT).

### p53 protein stabilization assay

Reagents: Packard View 96-well microplates (Perkin-Elmer, cat: 6005182); Mouse anti-human p53 antiserum (Dako, cat: M7001); Alexafluor 488 goat anti-mouse IgG secondary antibody (Invitrogen, cat: 449349); Bisbenzimidide H33258, (Sigma, cat: B2883)

Buffers and Solutions: PBST (137 mM NaCl, 2.7 mM KCl, 10 mM Sodium Phosphate dibasic, 2mM Potassium Phosphate monobasic, 0.1% Triton×100, pH 7.4); Block buffer (PBST containing 1% BSA); 50:50 v:v methanol/acetone stored at -20°C; Hoechst dye (10mg/ml in water store at -20°C)

### Mitotic index assay

Reagents: Cellomics Mitotic Index Kits (cat K0500011); Vinblastine (Sigma,

cat: V1377); Formaldehyde (37%) (Sigma, cat: D8779); Packard View 96-well microplates (Perkin-Elmer, cat: 6005182)

### **Cell cycle analysis**

Reagents: Hypotonic Fluorochrome solution (0.1% sodium citrate; 0.1% Triton X-100; 50µg/ml propidium iodide; 100ug/ml RNaseA in dH<sub>2</sub>O)

### **Annexin V/PI staining assay**

Reagents: FITC Annexin V (BD Biosciences, cat: 556420); propidium iodide (Sigma, cat: P4170)

Buffers and Solutions: 10× binding buffer (0.1 M HEPES, Ph 7.4; 1.3 M NaCl; 25 mM CaCl<sub>2</sub>); propidium iodide solution (50 µg/ml in PBS).

### **Western blot analysis**

Reagents: Precision Plus Protein WesternC Standards (Bio-Rad, cat: #161-0376); Immun-Blot PVDF Membrane (Bio-Rad, cat: 9274011); Cassettes 1.5mm (Invitrogen, cat: NC2015); Albumin (Sigma, cat: A4503); SuperBlock T20 Blocking Buffer (Thermo, cat:#37536); DC Protein Assay Reagent A/B/S (Bio-Rad, cat:500-0113/0114/0115); 30% Acrylamide solution (Severn Biotech, cat: 9352); complete Mini protease inhibitor cocktail tablet (Roche Diagnostics, cat: 11836153001); Amersham<sup>™</sup> ECL<sup>™</sup> Western Blotting Detection Reagents (GE Healthcare, cat: RPN2106); Amersham Hyperfilm<sup>™</sup> ECL High performance chemi-luminescence film (GE Healthcare, cat: 28906837)

Buffers and Solutions: Resolving gel buffer (1.5M Tris.Cl, pH 8.8, 0.4% SDS); Stacking gel buffer (1M Tris.Cl, pH 6.8, 0.8% SDS); Resolving gel 7.5% / 10ml (30% acrylamide 2.5 ml, resolving buffer 2.51 ml, dH<sub>2</sub>O 4.99 ml); Resolving gel 10% /10 ml (30% acrylamide 3.33 ml, resolving buffer 2.51 ml, dH<sub>2</sub>O 4.16 ml); Resolving gel 15% / 10 ml (30% acrylamide 5 ml, resolving buffer 2.51 ml, dH<sub>2</sub>O 2.49 ml); Stacking gel 4% / 5 ml (30% acrylamide 0.67ml, stacking buffer 0.63 ml, dH<sub>2</sub>O 3.70 ml); Running buffer 1L (3.03g Trizma Base, 14.4 g glycine, 1 g SDS); Transfer buffer 1L (3.03 g Trizma Base, 14.4 g glycine, 0.375 g SDS, 200 ml methanol); TBST 1L (6.6 g NaCl, 25ml 1M Tris.Cl pH7.5, 0.05% Tween 20); 4×Laemmli simple buffer 10 ml (2.4 ml 1 M Tris pH 6.8, 0.8 g SDS stock, 4 ml 100% glycerol, 0.01% bromophenol blue, 1 ml β-mercaptoethanol, 2.8 ml water); lysis buffer (5 mM HEPES pH 7.5, 300 mM NaCl, 1.5 mM MgCl<sub>2</sub>, 0.5% sodium deoxycholate, 20 mM β-glycerophosphate, 1% Triton X-100, 0.1% sodium dodecyl sulfate (SDS), 0.2 mM EDTA pH 8, 0.5 mM DTT, 1mM sodium orthovanadate pH 10, 1 mM phenylmethylsulfonyl fluoride, 20 μg/mL aprotinin, and 20 μg/mL leupeptin); 100ml stripping buffer (0.76g Trizma base, 2g SDS and 0.7ml β-mercaptoethanol).

## Antibodies:

Antibody	Blocking buffer	Dilution	Storage	Company	Cat.
RNAP II ser 2	5% BSA	1:500	-20 °C	Covance	MMS-129R
RNAP II ser 5	5% BSA	1:500	-20 °C	Covance	MMS-134R
Total RNAP II	5% BSA	1:500	-20 °C	Covance	MMS-129R
Mcl-1	5% BSA	1:1000	-20 °C	Cell signaling	#4572
Bcl-2	10% milk	1:1000	4 °C	Dako	M0887
XIAP	5% BSA	1:1000	-20 °C	Cell signaling	#2045
p53	10% milk	1:1000	4 °C	Dako	M7001
p21	5% BSA	1:1000	-20 °C	Santa Cruz	sc-397
MDM2	10% milk	1:1000	-20 °C	Sigma	M-7815
PARP	10% milk	1:1000	-20 °C	Cell signaling	#9542
Cleaved PARP	10% milk	1:1000	-20 °C	Cell signaling	#9546
PP1 $\alpha$	5% BSA	1:1000	-20 °C	Cell signaling	#2582
Phospho-PP1 $\alpha$	5% BSA	1:1000	-20 °C	Cell signaling	#2581
Total Rb	5% BSA	1:1000	-20 °C	Cell signaling	#9309
Rb (PT821)	5% BSA	1:1000	-20 °C	Invitrogen	44-582G
$\gamma$ -H2AX	5% BSA	1:2000	4 °C	Millipore	#05-636
$\beta$ -actin	10% milk	1:2000	-20 °C	Sigma	A1978
goat anti-mouse		1:4000	4 °C	Dako	P0447
swine anti-rabbit		1:4000	4 °C	Dako	P0399

## Comet assay

Reagents: CometAssay kit (Trevigen cat: 4250-050-K).

## **RT-PCR**

Reagents: Oligo (dT)<sub>18</sub> Primers (Bioline cat: Bio-38029); High resolution agarose (Invitrogen); RNeasy<sup>®</sup> mini kit (Qiagen cat: 74104); Transcriptor Reverse Transcriptase (Roche cat: 03531317001); Taq DNA polymerase (Roche cat: 11146165001).

## **Microarray**

Reagents: Human cot-1 DNA (Invitrogen, cat: 15279-011); Cy5 mono-reactive dye pack (GE Healthcare, cat: PA25001); Cy3 mono-reactive dye pack (GE Healthcare, cat: PA25001);

## **2.2 Methods**

### **2.2.1 Cell culture**

In a Class II microbiological safety cabinet, the cell culture techniques were performed before swabbing with 70% IMS in distilled water. MRC-5 and WI-38 cell lines were cultured in minimum essential medium with 10% FBS, 1% of 7.5% Sodium bicarbonate, 1% 0.1mM non-essential amino acids, 1% 1M HEPES, 1% 200mM L-glutamine and 1% penicillin. All other cell lines were maintained in RPMI-1640 with 10% FBS. The FBS was inactivated by heating (55 - 60° C) for 1 hour to denature complement proteins which would evoke cellular immune responses. All of the cells were incubated in a humidified incubator at 37° C with 5% CO<sub>2</sub>. Cells were sub-cultured when growth achieved approximately 80% confluence. During the sub-culture, the medium

was aspirated from the flask completely and 0.75 ml 1x trypsin-EDTA solution was added. The cells were put back to the incubator until most of them detached from the bottom of the flask, normally less than 5 minutes. The cells were re-suspended in 10ml medium and 0.5-1ml of the cell suspension was transferred to a new flask depending on the growth rate of the cells. The final medium volume in the new flask was adjusted to 10ml. In order to minimize the phenotypic drift, cells need to be discarded before passageing 40 times. For thawing cells, the cell vial was removed from liquid nitrogen storage and immersed into a 37° C water bath immediately. When the cells pulled away from the vial wall, the contents of the vial were transferred into a 25cm<sup>2</sup> flask with 10ml pre-warmed medium. Two passages were needed to resume normal growth. For long-term storage, cells at approximately 80% confluence were detached by minimal trypsin/EDTA and suspended in freezing medium (FBS containing 5% DMSO), transferred to sterile cryogenic vials and kept at -20°C overnight followed by -80°C for 1-2 days and removed into liquid nitrogen storage.

### **2.2.2 Compound solution**

Newly synthesized compounds were dissolved in DMSO to make up 10mM stock solutions. Flavopiridol stock solution was prepared in DMSO and the final concentration was 1mM. All compound stock solutions were stored at -20° C for up to 3 months.

### 2.2.3 MTT cell viability assay

MTT (3-(4,5-Dimethylthiazol-2-yl)-2,5-diphenyltetrazolium bromide) is a yellow tetrazole which is reduced by mitochondrial dehydrogenases to insoluble purple formazan in living cells. DMSO is added to dissolve the insoluble purple formazan product into a coloured solution. The absorbance which reflects the amount of living cells can be quantified by measuring at a certain wavelength (usually between 500 and 600 nm) by a spectrophotometer or plate reader.

72h MTT assay: Dependent on different cell lines, 1500-3000 cells were added to each well from column 2 to 11 of each 96-well plate on the first day. The final volume was made up to 180 $\mu$ l with blank medium. 180 $\mu$ l medium was added to Columns 1 and 12 as blank controls. 2 columns of cells were plated in the T<sub>0</sub> plate for each cell line. All plates were incubated at 37°C with 5% CO<sub>2</sub> overnight. In the morning of the second day, 50 $\mu$ l MTT solution (2mg/ml in PBS phosphate buffered saline) was added to each well of the T<sub>0</sub> plate. At the same time, compounds for test in 10mmol DMSO stock solution were diluted from 1mM to 100nM with media. For each concentration, 20 $\mu$ l dilution was added per well in triplicate for each cell line resulting in a dilution range from 100 $\mu$ M to 10nM. After 2-6 hours treatment in 37°C with 5% CO<sub>2</sub>, all medium was removed from the T<sub>0</sub> plate and 150 $\mu$ l DMSO was added to each well. The T<sub>0</sub> plate was analyzed after incubating in a shaker for 10 minutes. Absorbance of each well was quantified at 550 nm using Perkin Elmer plate reader and the data was transferred to Microsoft Excel which was used to calculate the GI<sub>50</sub> value. Except for the T<sub>0</sub> plate, all plates were incubated for 72 hours at 37°C

with 5% CO<sub>2</sub>. After 72 hours from drug addition, the plates were treated in the same way as the T<sub>0</sub> plate on the second day. In 48h and 24h MTT assay, 2000-4000 and 5000-8000 cells were added to each well on the first day depending on different cell types, respectively. Each assay was performed at least 2 times for candidate screening and at least 3 times for the mechanism studies of lead compounds. The mean value and standard deviation of each compound were calculated by Excel.

## **2.2.4 Caspase activation assay**

### **2.2.4.1 Caspase-3 assay**

Caspase-3 activity was determined using the Sigma caspase-3 fluorimetric assay kit under the manufacturer's instructions. Briefly,  $2 \times 10^4$  HCT-116 cells were plated into each well in a 96 well plate and incubated at 37°C and 5% CO<sub>2</sub>. After 24 hours, 10mM DMSO compound stocks were diluted to 100µM, 20µM, 5µM and 1µM in a separate standard 96-well plate, then a multichannel pipette was used to transfer 20µl of diluted compound solutions to the cell assay plate which already contains 180µl of medium giving final concentrations of compounds of 10µM, 2µM, 0.5µM and 0.1µM. Growth medium was used as blank and 0.5% DMSO in growth medium was used as negative control. Cell culture media was removed after compound treatment for 24 or 48 hours. Then, 25µl 1×Lysis Buffer was added to each well and the plate was incubated on ice for 15–20 minutes. After that, 200µl/well 1×Assay Buffer containing substrate was added and mixed by pipetting. Finally, 200µl/well of the solution was transferred to a fluorimeter multiwell plate and

the plate was read within 60 minutes. Activities were calculated using the AMC standard curve and each test was performed in triplicate.

#### **2.2.4.2 Caspase 3/7 activity assay**

Activity of caspase 3/7 was measured using the Apo-ONE Homogeneous Caspase 3/7 kit from Promega following the manufacturer's instructions.

#### **2.2.5 p53 stabilization assay**

HCT-116 cells were seeded at  $1 \times 10^4$  cells/well in Packard ViewPlate black clear bottom 96-well microtitre plates. After 18h, cells were incubated with compounds with different concentrations (10 $\mu$ M, 2 $\mu$ M, 0.5 $\mu$ M, 0.1 $\mu$ M and 0.02 $\mu$ M) for 7h at 37°C and 5% CO<sub>2</sub>. At the end of treatment, Medium was removed and 100 $\mu$ l/well cold 50:50 methanol: acetone (-20°C) was added for a 3-min fixation at -20°C. The fixation solution was removed and the fixed cells were dried briefly, then washed once with 100 $\mu$ l/well PBST (PBS, 0.1% triton X-100) and incubated with 50 $\mu$ l primary antibody solution containing mouse anti-human p53 antiserum diluted 1:1000 in block buffer for 1 hour. After that, the primary antibody solution was removed and wells were washed 3 times with 100 $\mu$ l PBST. After incubation with 50 $\mu$ l secondary antibody and Hoechst dye solution containing Alexafluor 488 goat anti-mouse antibody (1:300) and Hoechst dye (1 $\mu$ g/ml) for 1h at room temperature in the dark, cells were washed 3 times with 100 $\mu$ l PBST and analyzed using a ImageXpress<sup>MICRO</sup><sup>TM</sup> automated fluorescent microscope (Molecular Devices). The percentages of cell nuclei stained with p53-specific antibody versus total cell nuclei stained with Hoechst were calculated automatically using Multi Wavelength Cell

Scoring application module.

### **2.2.6 Mitotic index assay**

The assay was performed using the Cellomics Mitotic index kit from Thermo following the manufacturer's instructions. In brief, HCT-116 cells were seeded at  $1 \times 10^4$  cells/well in Packard ViewPlate black clear bottom 96-well microtitre plates. After 18h, cells were incubated with compounds with different concentrations (10 $\mu$ M, 2 $\mu$ M, 0.5 $\mu$ M, 0.1 $\mu$ M and 0.02 $\mu$ M) for 7h at 37°C and 5% CO<sub>2</sub>. After a 10-min fixation in 100 $\mu$ l of fixation solution at 37°C, cells were washed once with 100 $\mu$ l / well of 1 $\times$  blocking buffer and permeabilized in 100  $\mu$ l of 1 $\times$  permeabilization buffer for 15 minutes. After washing, cells were incubated with 50 $\mu$ l/well primary antibody solution for 1 hour, and then with staining solution for another 1 hour. Finally, plates were sealed and evaluated on a ImageXpress<sup>MICRO</sup><sup>TM</sup> automated fluorescent microscope (Molecular Devices) to calculate the mitotic index which is the percentage of cell nuclei stained with the mitosis-specific antibody (anti-phospho-Histone H3) versus total cell nuclei stained with Hoechst. Vinblastine (0.5 $\mu$ M) was used as a positive control and DMSO (0.2%) was used as a negative control. Assays were carried out using duplicate plates.

### **2.2.7 Kinase assay**

Inhibition of CDKs and other kinases was measured by radiometric assay using the Millipore KinaseProfiler services. Half-maximal inhibition (IC<sub>50</sub>) values were calculated from 10-point dose-response curves and apparent inhibition

constants ( $K_i$ ) were calculated from the  $IC_{50}$  values and appropriate ATP values.

### **2.2.8 Cell cycle analysis**

The analysis of cell cycle distribution was performed by flow cytometric measurement of cellular DNA contents. HCT-116, A2780 or MRC-5 cells were seeded at a density of  $4 \times 10^5$  / well in 6-well plates and incubated at 37°C, 5% CO<sub>2</sub> overnight. Cells were treated with CDKI-71 or CDKI-83 at different concentrations and harvested with the medium at appropriate time points, washed with PBS (Phosphate Buffer Saline) (Sigma) and centrifuged at 1200rpm for 5 minutes at 4°C. Supernatants were discarded and 300µl fluorochrome solution was added to each sample. Cells were suspended and transferred to FACS tubes, protected from light and stored at 4°C overnight. Prior to flow cytometric analysis, the cell suspension was syringed using a 23g needle at least 3 times to obtain a single cell suspension. Fluorescence of PI stained nuclei was analyzed on a Beckman Coulter EPIS-XL MCL™ flow cytometer and the data analysis was performed using EXPO32™ software.

### **2.2.9 Annexin V/PI staining assay**

HCT-116, A2780 or MRC-5 cells was seeded at a density of  $4 \times 10^5$  / well in 6-well plates and incubated at 37°C, 5% CO<sub>2</sub> overnight. After the treatment with CDKI-71 or CDKI-83 at appropriate concentrations and time points, cells were collected in a FACS tube, together with the culture media. The supernatants were discarded and the cells were re-suspended with 1ml fresh media after 5-min centrifuge at 1200rpm. Cells were counted and  $1 \times 10^5$  cells were

transferred into a fresh FACS tube with 1ml PBS, and centrifuged at 1200rpm for another 5 minutes. Supernatants were discarded again and the cell pellet was re-suspended in 100µl binding buffer and 5 µl Annexin V-FITC. Samples were incubated at room temperature for 15 minutes in the dark and 400µl binding buffer was added, together with 10µl propidium iodide (50 µl/ml in PBS). Samples were kept on ice and protected from light for a further 10 minutes and analyzed using FACS after vortex within 1h.

## **2.2.10 Western blot analysis**

### **2.2.10.1 Preparation of cell lysate**

Cells were treated with compounds when the growth reached 50-70% confluent at 37°C with 5% CO<sub>2</sub> atmosphere. At appropriate time points, cells were collected and centrifuged at 1200rpm for 5 minutes, 4°C. The pellet was washed with PBS and re-suspended in lysis buffer which contained a complete Mini protease inhibitor cocktail tablet in every 10ml. Cell lysates were stored at -20° C until use. After thawing, the lysates were centrifuged (12000rpm, 4°C, 10min) to remove insoluble proteins and cell debris before protein analysis.

### **2.2.10.2 Protein assay**

Protein concentrations in cell lysates were determined using DC Protein Assay Reagents A/B/S following the manufacturer's instructions.

### **2.2.10.3 SDS PAGE**

SDS PAGE was used to separate protein mixtures based on their molecular

mass by passing them electrophoretically through a polyacrylamide gel. Depending on the molecular mass of the protein of interest, different concentrations of acrylamide were used in the gels (7.5-15%). Polymerisation was initiated after the addition of APS and TEMED in a gel cassette. Stacking gel buffer with APS and TEMED was added after the resolving gel had polymerised. A comb was added immediately to create sample wells.

Cell lysate samples with loading buffer, each containing 50-200µg proteins depending on cell lines, were denatured at 95°C for 5 minutes. Each sample was then loaded into a well in the stacking gel. 5µl Precision Plus Protein WesternC Standards were added to the first well. Protein samples were separated by SDS-PAGE at a voltage between 60-150V using running buffer. After electrophoresis, gels were removed from cassettes and prepared for electro-transfer onto a PVDF membrane.

#### **2.2.10.4 Immunoblotting**

Proteins separated by SDS-PAGE in gels were electro-transferred onto PVDF membranes using transfer buffer (25V overnight). Membranes were blocked in TBST with either 5-10% BSA or 10% dried non-fat milk (dependant on primary antibodies) for 1h at room temperature with gentle shaking, followed by incubation with primary antibody solutions overnight at 4°C. To remove excess unbound primary antibodies, membranes were washed with TBST 3 times, 5-10min each. Incubation with appropriate secondary antibodies conjugated to horseradish peroxidase for 1h was followed at room temperature. Membranes were rinsed again before visualisation using ECL system.

#### **2.2.10.5 Enhanced chemiluminescence (ECL) reaction**

Following the procedures in the manufacturer's instruction of Amersham™ ECL™ Western Blotting Detection Reagents, membranes were exposed to high performance chemiluminescence films in the dark for appropriate exposure times. Films were developed manually.

#### **2.2.10.6 Membrane stripping**

Membranes were incubated with stripping buffer for 30 minutes at 50°C, followed by rinsing under running water for 1h and 3×10min with TBST.

#### **2.2.11 $\gamma$ -H2AX foci**

Cells were seeded at  $1 \times 10^4$  cells/well in Packard ViewPlate black clear bottom 96-well microtitre plates and incubated overnight at 37°C and 5% CO<sub>2</sub>. Cells were treated with 0.2 $\mu$ M flavopiridol or 5 $\mu$ M CDKI-71 for 6h, the medium was removed and 100 $\mu$ l/well cold 50:50 methanol: acetone (-20°C) was added for a 5-min fixation at -20°C. The fixation solution was removed and the fixed cells were washed once with 100 $\mu$ l/well cold PBS and incubated with permeabilization buffer for 15 mins at room temperature. After washing and incubating with blocking buffer, cells were incubated with mouse monoclonal anti- $\gamma$ -H2AX (Ser 139) at 1:1000 dilutions in blocking buffer for 1h at room temperature. Cells were then washed 3 times with blocking buffer and then incubated with Alexafluor 488 goat anti-mouse secondary antibody (Molecular Probes) at a dilution of 1:1000 and Hoechst dye (1 $\mu$ g/ml) in blocking buffer for 1h at room temperature in the dark, followed by washing with PBS. Images

were taken through a ImageXpress<sup>MICRO™</sup> automated fluorescent microscope (Molecular Devices). Cisplatin (5 $\mu$ M) was used as a positive control and DMSO (0.2%) was used as a negative control. Assays were carried out in duplicate plates.

### **2.2.12 Comet assay**

The comet assay or single cell gel electrophoresis assay is used to detect DNA damage in individual cells. The assay is based on the ability of denatured or cleaved DNA fragments to migrate out of the cell under an electric field, whereas undamaged DNA migrates slower and remains within the nucleoid under electrophoresis.

The comet assay was performed using the Trevigen CometAssay kit under alkaline conditions, following the manufacturer's instruction. After treatment, MRC-5 cells at  $1 \times 10^5$ /ml were combined with molten LMAgarose (37°C) at a ratio of 1:10 (v/v) and 50 $\mu$ M was added onto each Comet slide. After 20 minutes, slides were immersed in cold lysis solution at 4°C for 30 minutes. Then, excess buffer was removed and slides were incubated in freshly prepared Alkaline Solution for 20 minutes at room temperature, in the dark. Electrophoresis was performed for 40 minutes (1 volt/cm, current about 300mA) in alkaline electrophoresis solution (1mM EDTA and 300mM NaOH, pH > 13). All steps beginning with the cell lysis were conducted under dim light to prevent additional DNA damage. Samples were washed with distilled water and 70% ethanol and dried at 40°C for 15 minutes. Onto each circle of dried agarose, 100 $\mu$ l of diluted SYBR Green I nucleic acid gel stain was added.

Nikon Eclipse TS100 fluorescence microscopy equipped with fluorescein filter and camera was used to record images. Analysis was performed using the Comet Assay IV program. Typically, 50 cells were analyzed per slide with two slides for each treatment.

### **2.2.13 Reverse Transcription polymerase chain reaction (RT-PCR)**

This experiment was performed with the help of Dr Frankie Lam.

#### **2.2.13.1 RNA preparation and quantification**

A2780 cells were treated with CDKI-83 when the growth reached 50-70% confluence at 37°C with 5% CO<sub>2</sub> atmosphere. At appropriate time points, cells were collected and RNA was extracted using RNeasy<sup>®</sup> mini kit according to the manufacturer's instruction. The concentrations of RNA samples were determined by a NanoDrop<sup>®</sup> ND-1000 spectrophotometer (Thermo Fisher Scientific).

#### **2.2.13.2 Reverse transcription and PCR**

Reverse transcription and PCR were performed according to the standard operating procedures provided by Roche. Oligo (dT) 18 primers were provided by Bioline. Reverse transcriptase and PCR grade nucleotide mix were obtained from Roche. The primers for amplifying  $\beta$ -actin were purchased from MGW Biotech AG and the primers for Mcl-1 and Bcl-2 were designed by Dr Scott Roberts and produced by Sigma. The designed primers for Mcl-1 were

5'GAAGGCGCTGGAGACCTTAC3' (forward) and  
5'CATTCTGATGCCACCTCT3' (reverse). For Bcl-2, the primers were  
5'ATGTGTGTGGAGAGCGTCAA3' (forward) and  
5'GCCGTACAGTTCCACAAAGG3' (reverse).

### **2.2.13.3 Agarose gel electrophoresis and visualization of bands**

Agarose gel (2.5%) was prepared in TBE buffer (0.89M Trizma base, 0.02M EDTA, 0.89M Boric acid) and heated by microwave to dissolve the agarose. The gel was cooled down to around 60° C and ethidium bromide (EtBr) was added to a concentration of 0.2µg/ml. The mixture was poured into a gel plate with casting combs inserted. After the gel was set, the combs were removed and 5µl PCR product was loaded to each well with 1µl loading buffer. Samples were separated by electrophoresis at 100V for 1h and visualised under UV. Images were recorded digitally using a Benchtop 3UV<sup>TM</sup> Transilluminator (UVP).

### **2.2.14 Microarray**

A2780 cells were treated with CDKI-71 (1µM) or flavopiridol (0.2µM) for 6 hours. After treatment, RNA samples were prepared and quantified as described in 2.2.13.1. The 30,000 gene probe pan human Array (MWG Biotech) slides were purchased from Genomics Facility, QMC, University of Nottingham. Reverse transcription, cDNA purification, probes labelling and hybridization were performed by Miss Adeline Barthet-Barateig. The arrays were scanned on an Axon Genepix 4000b scanner and quantified using Genepix Pro 6. For each gene, a log<sub>2</sub> ratio was calculated automatically

between its treatment and control intensities. The features with high background or which were significantly uniform were removed from analysis. Then the R program with the "Limma" package was used to analyze expression of the microarray data and the 158 probe sets whose expression changes more than 1 log ( $|\log_2| > 1$ ) by CDKI-71 treatment were chosen for further analysis. Hierarchical clustering was performed and visualized using MeV version 4.6.2 for the 158 probe sets. The web-based Database for Annotation, Visualization and Intergrated Discovery (DAVID) was used for functional annotation.

# **Chapter Three: Screening and classification of an inhibitor compound library**

## **3.1 Introduction**

Because of similarities in structure of kinases, particular in the ATP-binding motif among all protein kinases, target specificity is the main problem in the development of ATP-antagonistic inhibitors. Furthermore, identify the primary target of designed anti-cancer kinase inhibitors in cancer cells plays a key role in kinase drug development.

Hundreds of compounds designed to target diverse kinases have been synthesized by our group. These include CDK9 inhibitors (S-, S2-, S3-, SW-, D- and E-series), CDK7 inhibitors (coded PL4-series) and Polo-like kinase 1 (Plk1) inhibitors (OC-series). A cell-based screening cascade was developed to classify compounds and identify effective transcription CDK (CDK7 and especially CDK9) inhibitors as lead candidates.

This screening cascade comprised an MTT assay, a Caspase-3 activation assay, a p53 stabilization assay and a mitotic index assay. SW-32, a potent CDK9 inhibitor (Wang et al., 2004), was used as a positive control. 5,6-Dichloro-1-beta-d-ribofuranosylbenzimidazole (DRB), the most selective CDK9 inhibitor known (Wang and Fischer, 2008), was used as a further positive control in this screening cascade.

## 3.2 Results and Discussion

### 3.2.1 Cell viability

Effective anti-cancer drugs normally induce cancer cell death or inhibit proliferative activity, both of which decrease cancer cell viability. MTT is a water soluble yellow dye which can be converted to insoluble purple crystal formazan by mitochondrial dehydrogenases in viable cells. At the first stage of the screening cascade, the anti-proliferative activity of more than 100 new synthesized compounds was tested using 72h-MTT assay on HCT-116 cells.

Compounds with  $GI_{50}$  values below  $1\mu\text{M}$  are summarized in **Figure 3.1**. A number of compounds including SW-32, SW-130, SW-118, S3-41, S3-53, S2-123, S2-122, S2-104, S-134, S-64 and OC-21 showed potent anti-proliferative activity with  $GI_{50}$  values below 100 nM. In similar experiments, DRB has modest cytotoxicity with a  $GI_{50}$  value of  $32.86 \pm 6.85\mu\text{M}$ .

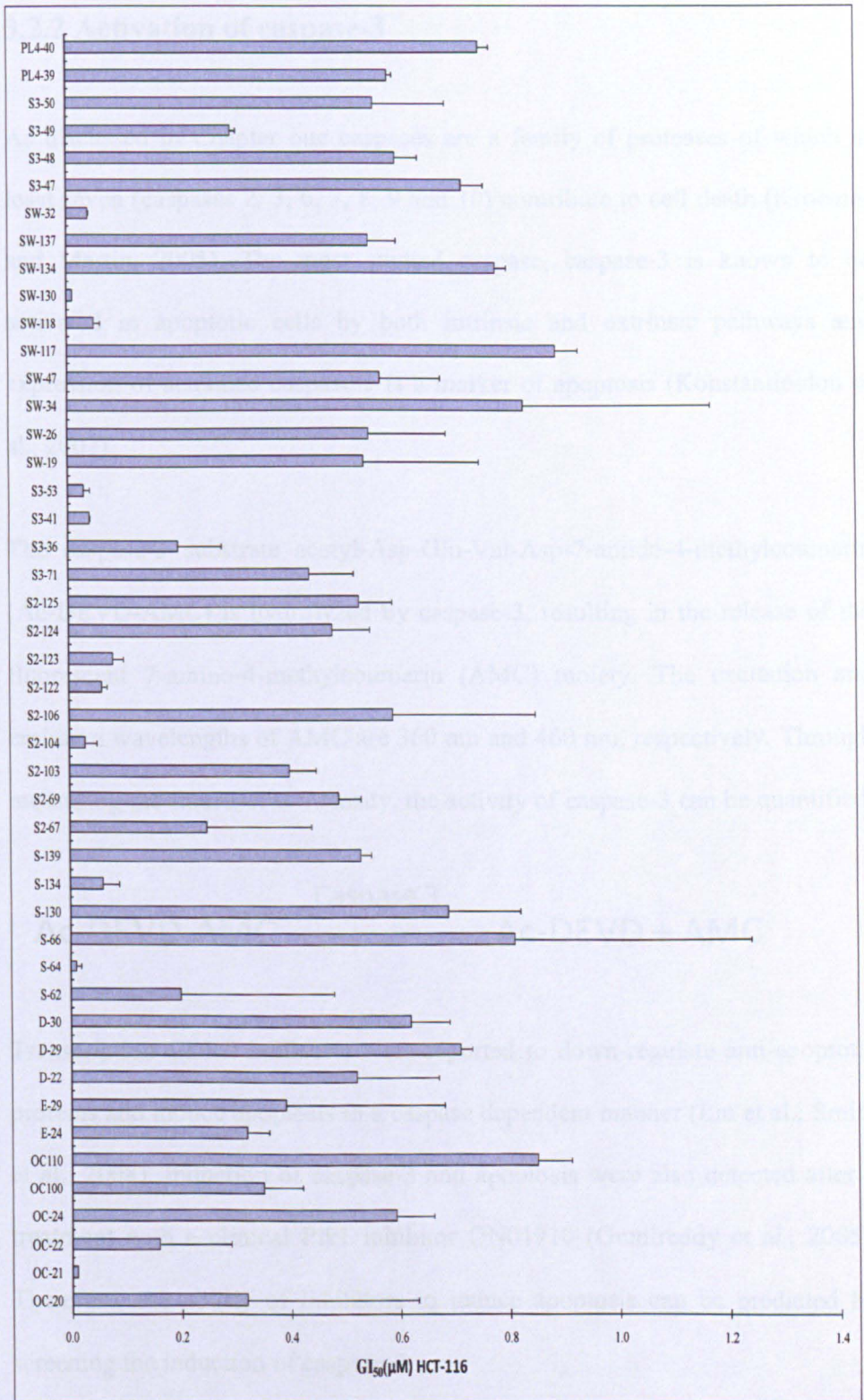
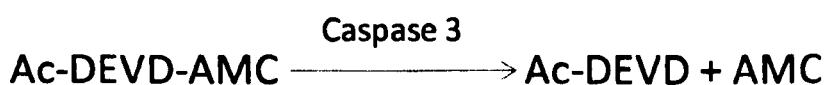


**Figure 3.1** GI<sub>50</sub> values of 46 compounds in HCT-116 cells (MTT assay). HCT-116 cells were treated with different compounds for 72 hours. Horizontal bars represent the mean GI<sub>50</sub> values ± SD of at least two independent experiments

### 3.2.2 Activation of caspase-3

As discussed in Chapter one caspases are a family of proteases of which at least seven (caspases 2, 3, 6, 7, 8, 9 and 10) contribute to cell death (Kroemer and Martin, 2005). The most studied caspase, caspase-3 is known to be activated in apoptotic cells by both intrinsic and extrinsic pathways and expression of activated caspase-3 is a marker of apoptosis (Konstantinidou et al., 2007).

The caspase-3 substrate acetyl-Asp-Glu-Val-Asp-7-amido-4-methylcoumarin (Ac-DEVD-AMC) is hydrolyzed by caspase-3, resulting in the release of the fluorescent 7-amino-4-methylcoumarin (AMC) moiety. The excitation and emission wavelengths of AMC are 360 nm and 460 nm, respectively. Through measuring the fluorescent intensity, the activity of caspase-3 can be quantified.



Transcription CDK9 inhibitors were reported to down-regulate anti-apoptotic proteins and induce apoptosis in a caspase dependent manner (Liu et al.; Smith et al., 2008). Induction of caspase-3 and apoptosis were also detected after a treatment with a clinical Plk1 inhibitor ON01910 (Gumireddy et al., 2005). Therefore, the ability of inhibitors to induce apoptosis can be predicted by screening the induction of caspase-3.

The caspase-3 activity after treatment was determined for compounds with  $GI_{50}$  values below  $1\mu\text{M}$ . Figure 3.2 shows the induction of caspase-3 in HCT-116

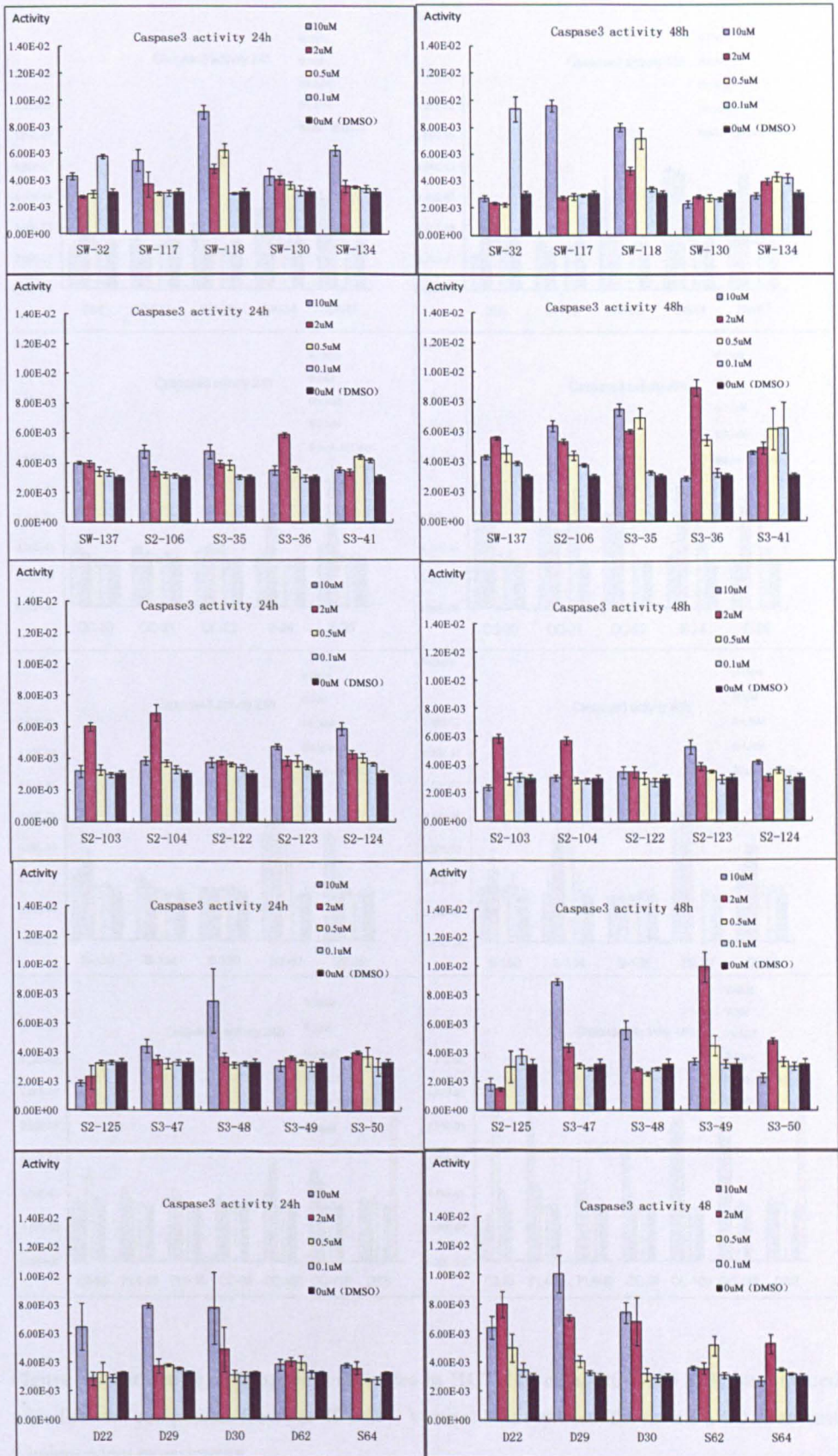
cells after treatment with 46 compounds for 24 or 48 hours. DRB was used as a positive control in this experiment. As shown in **Figure 3.2**, 48h treatment induced higher caspase-3 activity for the majority of compounds. Based on the results of 48h treatments, the 46 compounds were classified into 3 groups:

Group 1: Compounds induced caspase-3 activities at concentrations  $\leq 0.5\mu\text{M}$  (OC-21, S3-53, S3-71, S3-41, SW-32, SW-118, S-134, OC-22, S-62, S3-36, S2-67, E-24, E-29 and S2-106).

Group 2: Compounds induced caspase-3 activities at concentrations between  $2\mu\text{M}$  and  $10\mu\text{M}$  (S-64, S2-123, S3-49, OC-20, OC-100, S2-103, S2-124, S2-69, D-22, SW-26, SW-137, S3-50, SW-47, PL4-39, OC-24, S3-48, D-30, S-130, D-29, S3-47, PL4-40, SW-134, S-66, SW-34, OC110 and SW-117)

Group 3: Compounds do not induce caspase-3 activities (SW-130, S2-122, S-139, S2-125 and SW-19).

As a lead compound, SW-32 induced caspase-3 activity at a very low concentration ( $0.1\mu\text{M}$ ). This is consistent with its  $\text{GI}_{50}$  value obtained in the MTT assay. However, SW-32 treatment at higher concentrations did not increase the level of caspase-3 activity. This also occurred with other inhibitors, such as E-24, S3-36, and S3-53. Since these compounds were very cytotoxic, at the higher concentrations they induced significant cell death. This may be the reason why induction of caspase-3 has not been detected. As shown in **Figure 3.2** DRB induced caspase-3 activity significantly at  $50\mu\text{M}$ , which is similar to its  $\text{GI}_{50}$  value in the MTT assay ( $32.86\mu\text{M}$ ), indicating the anti-proliferative effect of DRB is mainly due to the induction of apoptosis.



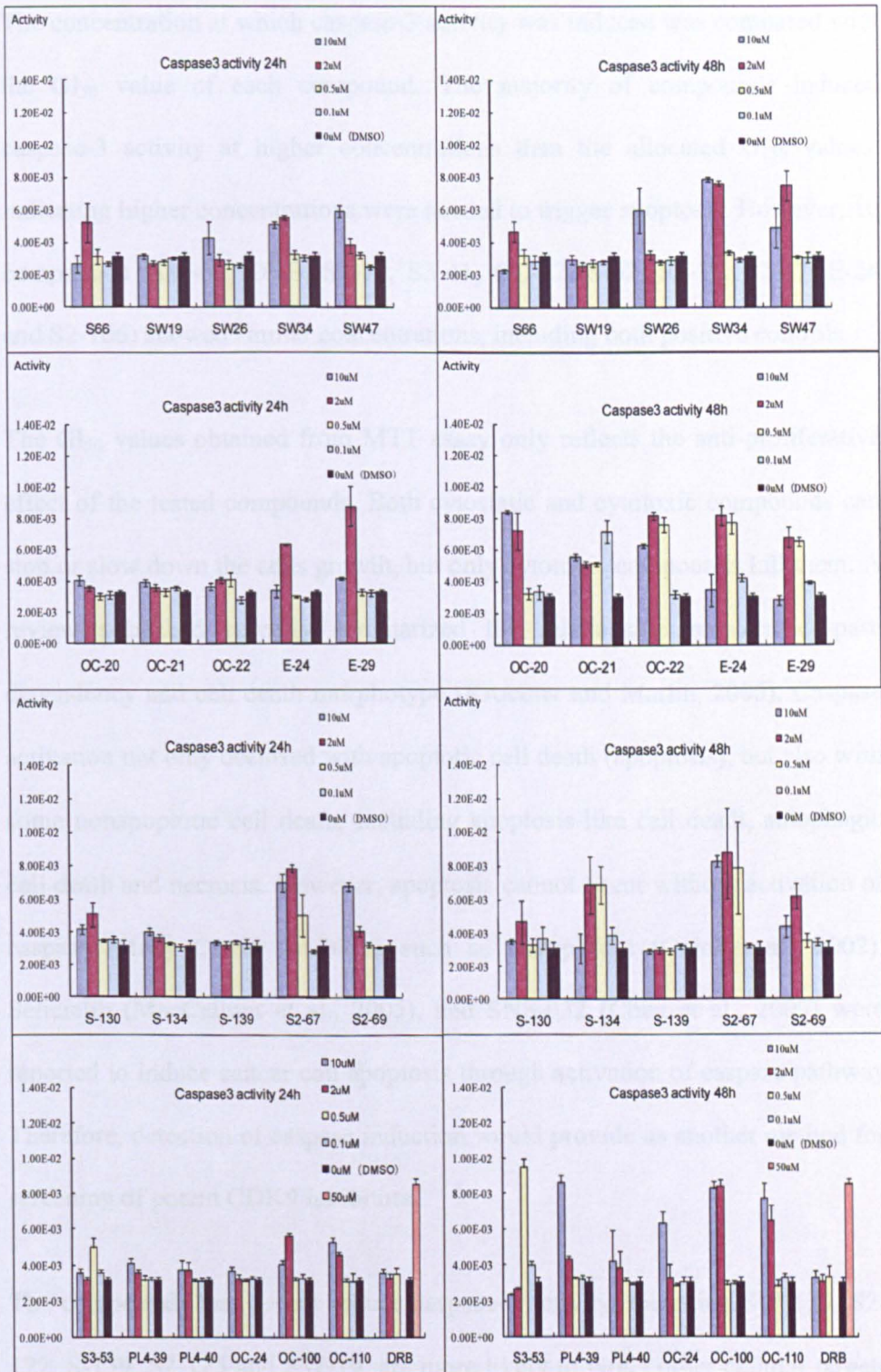


**Figure 3.2 Induction of Caspase-3 activities in HCT-116 cells.** HCT-116 cells were treated with different compounds for 24 or 48 hours. Vertical bars represent the means  $\pm$  SD of at least 2 independent experiments.

The concentration at which caspase-3 activity was induced was compared with the GI<sub>50</sub> value of each compound. The majority of compounds induced caspase-3 activity at higher concentrations than the allocated GI<sub>50</sub> values, indicating higher concentrations were needed to trigger apoptosis. However, 10 compounds (SW-32, DRB, S3-71, S3-41, OC-22, S-62, S3-36, S2-67, E-24 and S2-106) showed similar concentrations, including both positive controls.

The GI<sub>50</sub> values obtained from MTT assay only reflects the anti-proliferative effect of the tested compounds. Both cytostatic and cytotoxic compounds can stop or slow down the cells growth, but only cytotoxic compounds kill them. A review published recently summarized the relationship between caspase dependency and cell death morphotype (Kroemer and Martin, 2005). Caspase activation not only occurred with apoptotic cell death (apoptosis), but also with some nonapoptotic cell death, including apoptosis-like cell death, autophagic cell death and necrosis. However, apoptosis cannot occur without activation of caspase. Many CDK9 inhibitors such as flavopiridol (Gojo et al., 2002), Seliciclib (MacCallum et al., 2005), and SNS-032 (Chen et al., 2009) were reported to induce cancer cell apoptosis through activation of caspase pathway. Therefore, detection of caspase induction would provide us another method for screening of potent CDK9 inhibitors.

The compounds that do not induce caspase-3 activity, including SW-130, S2-122, S-139, S2-125 and SW-19, are more likely to target other cellular targets other than or in addition to CDK9. However, induction of caspase is highly dependent on the amount of cells. If compounds tested are extremely toxic and kill the cells in a short time, no caspase induction would be detected. Therefore,

further tests might be worth to perform for the compounds which kill the cells immediately without caspase induction. Targeting other kinases, for example cell cycle kinases, may inhibit cell proliferation while CDK9 inhibition induces apoptosis through caspase activation. Thus, compounds S3-71, S3-41, OC-22, S-62, S3-36, S2-67, E-24 and S2-106, with similar GI<sub>50</sub> values and Caspase induction concentrations, have the largest potential to be selective CDK9 inhibitors.

### **3.2.3 Induction of p53 protein**

CDK9 inhibitors were reported to reduce the expression of MDM2, a well-established negative regulator of p53, resulting in p53 stabilization (Alonso et al., 2003; Demidenko and Blagosklonny, 2004; Liu et al., 2011b) . Induction of p53 protein levels has been considered a marker of CDK7/9 inhibition (Shapiro, 2006) and detection of nuclear p53 protein accumulation was used to screen and identify transcription CDK7/9 inhibitors (Wang et al., 2010).

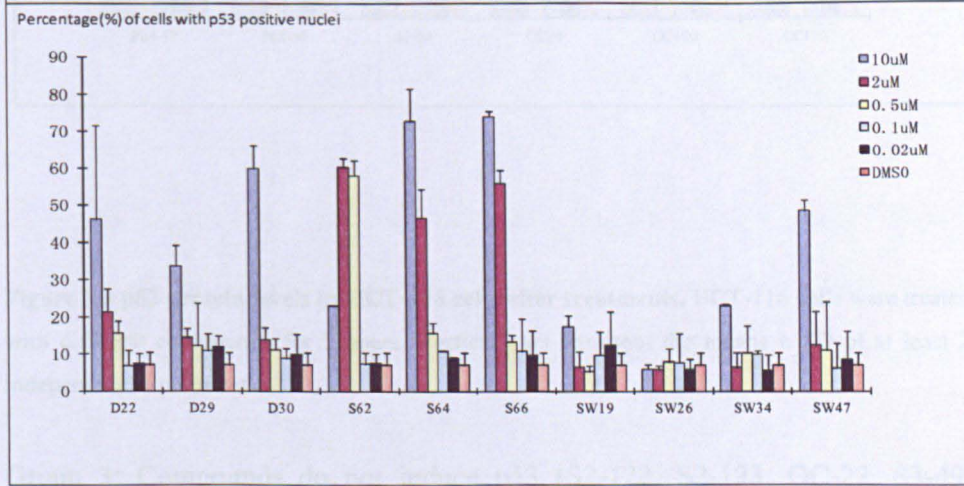
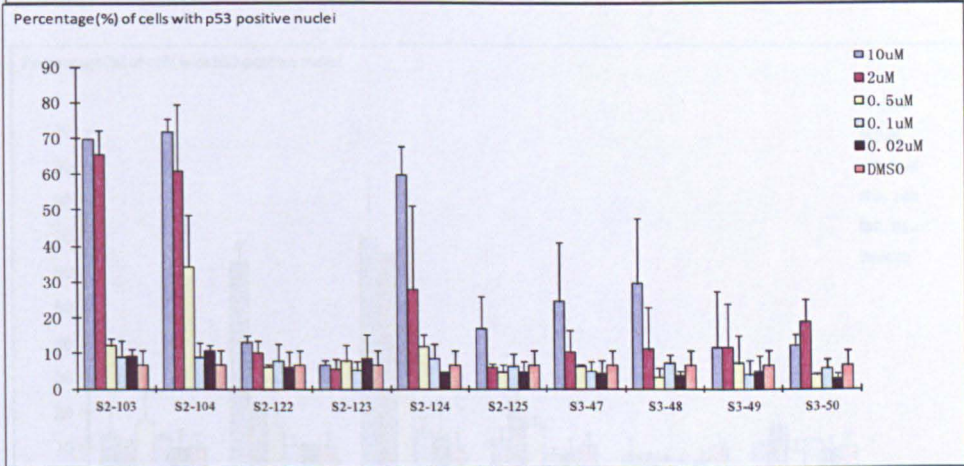
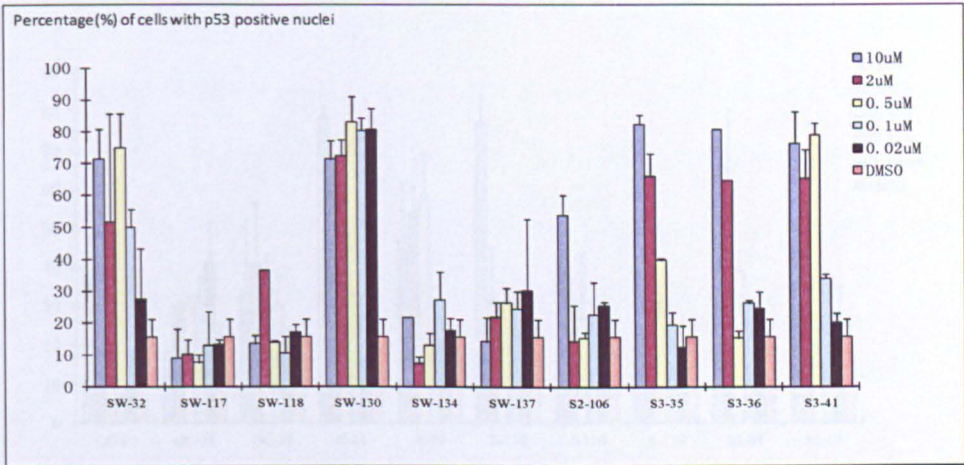
In order to identify potent CDK9 inhibitors, the effects of the 46 compounds with GI<sub>50</sub> values below 1 $\mu$ M on p53 protein were further assessed using a relevant high-throughput automated microscopy system. Nuclear accumulation of p53 was assessed by immunofluorescent staining and the percentage of cells with p53 positive nuclei versus total cell nuclei stained with Hoechst was calculated.

Based on previous data (Wang et al., 2010), 7h treatment was chosen to identify the maximum effects on induction of p53 protein levels.

Figure 3.3 illustrates the response of HCT-116 cells p53 levels after treatment with each compound, the 46 test compounds falling into 3 groups:

Group 1: Compounds induced p53 at concentrations  $\leq 0.5\mu\text{M}$  (SW-130, OC-21, S3-53, S2-104, S3-71, S3-41, SW-32, S-62, S2-67, E-24 and E-29).

Group 2: Compounds induced p53 at concentrations between  $2\mu\text{M}$  and  $10\mu\text{M}$  (S-64, SW-118, S-134, S3-36, OC-20, S2-103, S2-124, S2-69, D-22, S2-125, SW-19, SW-137, SW-47, OC-24, S2-106, S3-48, D-30, S-130, D-29, S3-47, PL4-40, SW-134, S-66 and SW-34).



OC100, S3-119, SW-36, S3-38, S3-39, D2110 and SW-137).  
 It can be seen clearly that SW-32, as a test compound and positive control,  
 increased p53 level at 0.1uM which is the same concentration required to  
 induce caspase-3 activity. It also has been reported that DNR induced p53 by

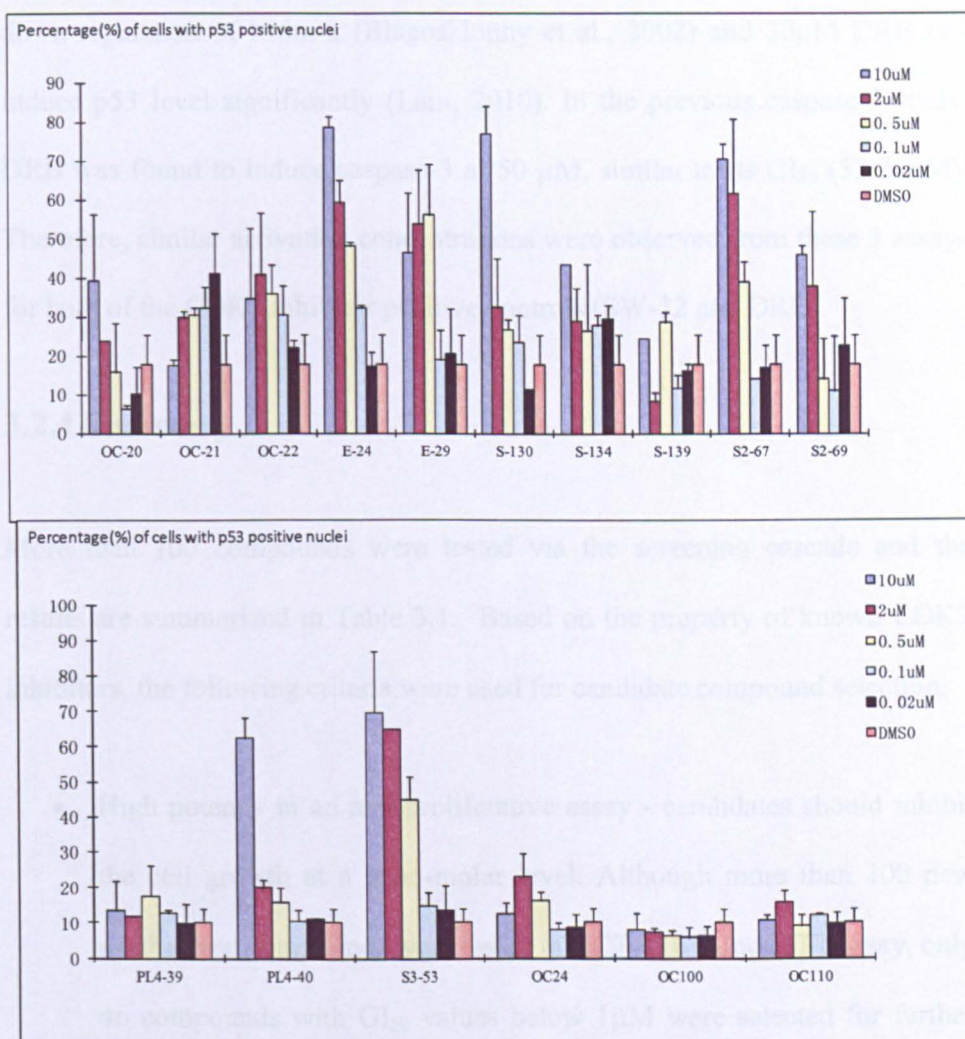


**Figure 3.3 p53 protein levels in HCT-116 cells after treatments.** HCT-116 cells were treated with different compounds for 7 hours. Vertical bars represent the means  $\pm$  SD of at least 2 independent experiments.

Group 3: Compounds do not induce p53 (S2-122, S2-123, OC-22, S3-49, OC100, S-139, SW-26, S3-50, PL4-39, OC110 and SW-117).

It can be seen clearly that SW-32, as a lead compound and positive control, increased p53 level at 0.1 $\mu$ M which is the same concentration required to induce caspase-3 activity. It also has been reported that DRB induced p53 by

down-regulation of Mdm-2 (Blagosklonny et al., 2002) and 30 $\mu$ M DRB can induce p53 level significantly (Lam, 2010). In the previous caspase-3 study, DRB was found to induce caspase-3 at 50  $\mu$ M, similar to its GI<sub>50</sub> (32.86 $\mu$ M). Therefore, similar activation concentrations were observed from these 3 assays for both of the CDK9 inhibitor positive controls (SW-32 and DRB).

### **3.2.4 Summary**

More than 100 compounds were tested via the screening cascade and the results are summarized in Table 3.1. Based on the property of known CDK9 inhibitors, the following criteria were used for candidate compound selection:

- High potency in an anti-proliferative assay - candidates should inhibit the cell growth at a nano-molar level. Although more than 100 new synthesized compounds were tested in HCT-116 using MTT assay, only 46 compounds with GI<sub>50</sub> values below 1 $\mu$ M were selected for further assays (Table 3.1).
- Effective induction of both caspase-3 and p53. Compounds S2-122 and S-139 had no effects on either, while 14 compounds only affected either caspase-3 activity or p53 protein level. Therefore, these 16 compounds have less potential to be potent CDK9 inhibitors (Table 3.1).
- Comparative potency cross all three assays. Compounds S3-41, S2-67, E-24, E-29, S3-71 and S-62, designed for inhibition of CDK9, and compound OC-21, designed as a Plk-1 inhibitor followed this rule. Each of them inhibited cell growth, induced caspase-3 activity and increased p53 protein level at similar concentration (Table 3.1).

**Table 3.1 Summary of MTT, caspase-3 activity and p53 stabilization assays.**

Compounds	MTT GI <sub>50</sub> *	Cell-based assays, (μM)		candidate
		Caspase 3 activity #	p53 stabilization#	
OC-21	0.01	0.1	0.02	✓
S3-41	0.04	0.1	0.1	✓
SW-32	0.04	0.1	0.1	control
S2-67	0.25	0.5	0.5	✓
E-24	0.32	0.5	0.5	✓
E-29	0.39	0.5	0.5	✓
S3-71	0.40	0.5	0.5	✓
S-62	0.20	0.5	0.5	✓
S3-53	0.03	0.5	0.5	
SW-118	0.05	0.5	2	
S-134	0.06	0.5	10	
S3-36	0.20	0.5	2	
S2-106	0.59	0.5	10	
S-64	0.01	2	2	
S2-104	0.03	2	0.5	
OC-20	0.32	2	10	
S2-103	0.40	2	2	
S2-69	0.49	2	2	
D-22	0.52	2	2	
SW-137	0.55	2	2	
SW-47	0.57	2	10	
OC-24	0.59	2	2	
D-30	0.62	2	10	
S-130	0.69	2	10μM	
D-29	0.71	2μM	2μM	
PL4-40	0.75	2μM	2μM	
S-66	0.81	2μM	2μM	
SW-34	0.83	2μM	10μM	
S2-124	0.48	10μM	2μM	
S3-48	0.60	10μM	10μM	
S3-47	0.72	10μM	10μM	

SW-134	0.78	10 $\mu$ M	2 $\mu$ M
OC-22	0.16	0.5 $\mu$ M	/
S3-49	0.30	2 $\mu$ M	/
OC100	0.35	2 $\mu$ M	/
S3-50	0.56	2 $\mu$ M	/
PL4-39	0.59	2 $\mu$ M	/
OC110	0.85	2 $\mu$ M	/
SW-117	0.89	2 $\mu$ M	/
S2-123	0.08	10 $\mu$ M	/
SW-26	0.55	10 $\mu$ M	/
SW-130	<0.01	/	0.02 $\mu$ M
S2-125	0.53	/	10 $\mu$ M
SW-19	0.54	/	10 $\mu$ M
S2-122	0.06	/	/
S-139	0.53	/	/

\*: 72 hours MTT assay

#: the concentration at which the activity was significantly induced

/: no effects even at the highest concentration

### 3.2.3 Cell cycle effects

As described previously, CDK9 regulates transcription. Reduction of CDK9 level by siRNA had no appreciable effects on cell cycle distribution (Cai et al., 2006b). Apoptosis was detected after treatment with a selective CDK9 inhibitor from all stages of the cell cycle (Wang et al., 2010), while SW-32, a potent inhibitor of CDK9 and CDK2 was reported to reduce mitotic index (Wang et al., 2004). In contrast, inhibition of Plk1 resulted in spindle

abnormalities and mitotic arrest followed by apoptosis (Gumireddy et al., 2005; Sumara et al., 2004).

To distinguish the transcriptional CDK inhibitor compounds from Plk1 inhibitors, a mitotic index assay was introduced. Mitotic index is the ratio between the number of cells in mitosis and the total number of cells. It's a valuable means of characterizing cell proliferation, and represents the cell fraction within a population undergoing cell division. In this study, HCT-116 cells were treated with selected inhibitor compounds for a period of 7 hours and the mitotic index was measured. Vincristine, which is known to target tubulin dimers and the capable of arresting cells in mitosis, was used as a positive control, and DMSO vehicle as a negative control. The mitotic index was calculated by measuring cell nuclei stained with the positive mitosis-specific antibody (anti-phospho-Histone H3) versus total cell nuclei stained with Hoechst. DRB was used as CDK9 inhibitor control. Compounds selected for the assay were E-29, S2-122, S3-71 and S3-41 which are designed to target CDK, while OC21, OC100 and OC110 are potential mitotic inhibitors.

As shown in Figure 3.4, compound series OC21, OC100 and OC110 increased mitotic index at 10  $\mu$ M, which is consistent with the effect of plk1 inhibitor ON01910 (Gumireddy et al., 2005). CDK9 inhibitor E-29 decreased mitotic index significantly at 2  $\mu$ M, which is similar to the CDK9 positive control DRB at 50  $\mu$ M. S3-71 also decreased mitotic index, but with less significance, while S3-41 showed no effects on the mitotic index.

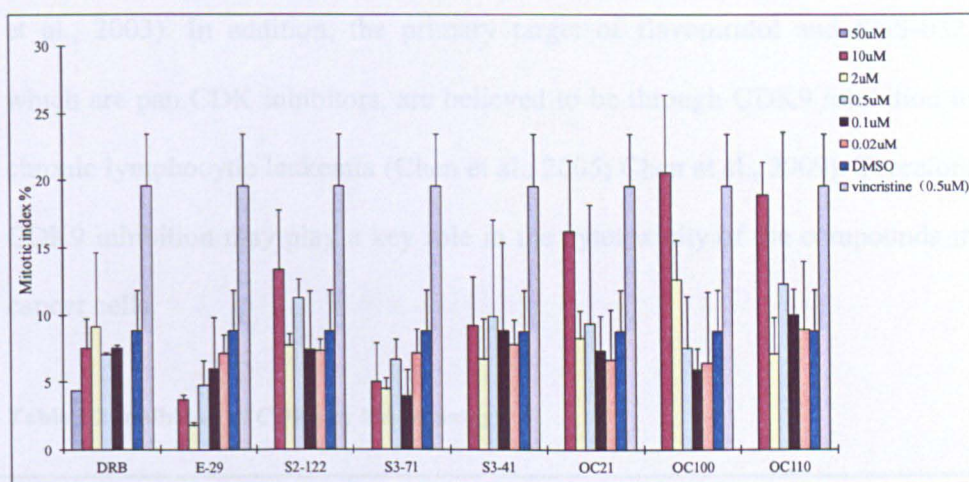


**Figure 3.4 Cell cycle status detected by mitotic index.** HCT-117 cells were treated with compounds with a range of concentrations for 7 hours. Vertical bars represent the means  $\pm$  SD of at least 2 independent experiments.

The kinase inhibition activities of compounds E-29, S2-122, S3-71, S3-41 and DRB were tested at 1  $\mu$ M for 6 CDKs and the  $K_i$  values against CDK9 were obtained (**Table 3.2**). Candidates S3-41, S3-71 and E-29 inhibited CDK9 and CDK2 potently and the  $K_i$  values for CDK9 were 6, 6 and 27 nM, respectively, indicating the efficacy of our screening cascade. Through the compound screening, S2-122 was not selected as a CDK9 inhibitor candidate because it failed to induce caspase-3 and p53. Kinase assay shows S2-122 had no activity against CDK9 and other CDKs, further confirming the practicality of the screening cascade.

CDK2 binds to CyclinE or CyclinA, regulating G1/S transition and S phase progress (Knockaert et al., 2002). However, recent studies show a variety of cancer cell lines are able to proliferate after specific and acute depletion of CDK2, suggesting CDK2 inhibition may not be useful therapeutically (Ortega

et al., 2003). In addition, the primary target of flavopiridol and SNS-032, which are pan CDK inhibitors, are believed to be through CDK9 inhibition in chronic lymphocytic leukemia (Chen et al., 2005; Chen et al., 2009). Therefore, CDK9 inhibition may play a key role in the cytotoxicity of the compounds in cancer cells.

**Table 3.2 Inhibition of CDKs by kinase assay\***

	CDK1/B	CDK2/A	CDK4/D	CDK5/p25	CDK7/H	CDK9/T	CDK9/T**
<b>S3-41</b>	89	98	51	83	45	96	6
<b>S3-71</b>	94	99	92	95	80	99	6
<b>E-29</b>	66	89	22	54	58	92	27
<b>DRB</b>	0	0	0	0	10	64	304
<b>S2-122</b>	0	0	0	0	0	0	>10

\* Percentages of inhibition at 1 $\mu$ M against 6 CDKs were obtained. Half-maximal inhibition (IC<sub>50</sub>) values for CDK9 were calculated from 10-point dose-response curves. \*\* K<sub>i</sub> in nM represented by the means of two independent measurements.

### 3.3 Conclusion

More than 100 new synthesized compounds were tested by MTT assay and 46 compounds were further screened using caspase-3 activation assay and p53 stabilization assay to identify potent CDK9 inhibitors. The cell cycle effects

were detected by mitotic index assay. Based on the above results, compounds S3-41, S2-67, E-24, E-29, S3-71 and S-62 were chosen as key CDK9 inhibitors. Compounds S3-41 and S3-71 are the most potent CDK9 inhibitors identified. They have potent anti-proliferative activity; induce both caspase-3 activity and p53 protein level, which are the cellular marker of CDK9 inhibition. Most importantly, these two compounds showed comparative potency across all the three assays in our screening cascade without significant effects on mitotic index, suggesting their anti-proliferative effect would be due to CDK9 inhibition .

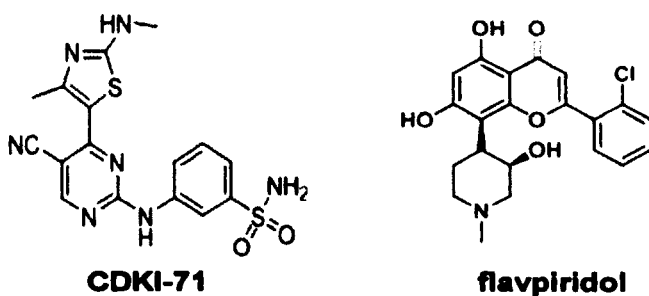
# Chapter Four: Cellular mechanism of action of a novel CDK9 inhibitor CDKI-71

## 4.1 Structure and kinase activity

Through our screening assays, CDKI-71 (S3-71) was chosen as a lead CDK9 inhibitor. The cellular effects of CDKI-71 were compared with the clinic compound flavopiridol to verify the mechanism of action (Liu et al., 2011b).

The structures and CDK inhibitory activity of CDKI-71 and flavopiridol are summarized in Table 4.1. The CDK inhibitory activity was measured by radiometric assay from Millipore. Similar activities were determined for CDKI-71 and flavopiridol against CDK9, CDK7, CDK1 and CDK6, with the highest potency being against CDK9 ( $K_i = 6$  and  $3$  nM for CDKI-71 and flavopiridol respectively). However, CDKI-71 is more potent against CDK2 ( $K_i = 4$  nM) than flavopiridol ( $K_i = 79$  nM).

Table 4. 1 Chemical structures and summary of CDK inhibitory activity.



Compounds	Kinase inhibition, <i>K<sub>i</sub></i> (nM)					
	CDK9/T1	CDK7/H	CDK1/B	CDK2/E	CDK5/p53	CDK6/D3
Flavopiridol	3	113	13	79	100	265
CDKI-71	6	114	12	4	920	205

Inhibition of CDKs was measured by radiometric assay using the Millipore KinaseProfiler services. Apparent inhibition constants (*K<sub>i</sub>*) were calculated from IC<sub>50</sub> values and the appropriate K<sub>m</sub> (ATP) values for each kinase (Cheng Y, 1973).

## 4.2 Growth inhibition effect

CDKI-71 and flavopiridol were widely tested using 48h MTT anti-proliferation assay on a panel of 12 tumour cell lines and two normal human diploid fibroblast cell lines. The half-maximal growth inhibition (GI<sub>50</sub>) values are summarized in **Table 4.2**. Tumour cell lines from different origins were introduced, such as colon, breast, renal, ovarian, pancreatic and cervical. To investigate whether the cell growth inhibition effect is p53 or Rb dependent, cell lines with different p53 and Rb status were also included in our cell panel (**Table 4.2**). MRC-5 and WI-38 cells are well characterized normal diploid fibroblasts and are the most commonly used non-cancerous cell lines (Jacobs et al., 1970).

Flavopiridol was reported to induce cancer cell apoptosis in a p53 and Rb independent manner (Alonso et al., 2003). In our MTT assay, both compounds show similar sensitivity for cells with different p53 and Rb status, indicating p53 and Rb independent anti-proliferative activity. CDKI-71 suppressed tumour cell growth with similar GI<sub>50</sub> values ranging from 287 to 854 nM in

different tumour cells, but was about 10-fold less potent than flavopiridol in the same cell lines. However, MRC-5 and WI-38 cells were significantly less sensitive to CDKI-71 ( $GI_{50} = 4277$  and  $2265$  nM, respectively), showing the tumour cell selective effect of CDKI-71. In contrast, all cell lines were sensitive to flavopiridol, irrespective of cell type (tumour or non-transformed).

The tumour cell specific cytotoxicity of CDKI-71 was also observed in patient-derived CLL cells, as well as normal B- and T-cells, by Annexin V-FITC apoptosis assay carried out by Dr Chris Pepper. CDKI-71 showed its potency with  $LD_{50} = 0.43$   $\mu$ M against CLL cells, while little effect was observed in normal B- and T-cells ( $LD_{50} > 500$  and  $> 700$   $\mu$ M, respectively). In contrast, flavopiridol exhibited similar toxicity in the three cell lines ( $LD_{50} = 0.34$ ,  $0.59$  and  $0.81$   $\mu$ M, respectively).

**Table 4.2 Average GI<sub>50</sub> values (nmol/L) for CDKI-71/flavopiridol-mediated growth inhibition in a panel of human cell lines.**

Human cell line		GI <sub>50</sub> nmol/L ± SD <sup>a</sup>	
Origin	Designation	CDKI-71	Flavopiridol
Colon	HCT-116 (p53+/+)	472±25	46±4
	HCT-116 (p53-/-)	484±14	54±1
Melanoma	MDA-MB435(Rb+)(p53 mutant)	553±111	81±7
Breast	MDA-MB468(Rb-)(p53 mutant)	512±9	70±18
	MCF-7 (p53 wild type)	483±32	41±7
Renal	TK10	769±158	48±4
	CAK1-1	589±21	64±5
Ovarian	IGROV-1	854±168	59±12
	A2780	287±3	21±5
	SKOV-3	752±118	73±6
Pancreatic	Miapaca-2	650±16	78±7
Cervical	Hela	446±37	43±1
Embryonic Lung	WI-38	2265±744	77±20
Fibroblast	MRC-5	4277±761	49±9

<sup>a</sup>: Average values ± SD from three independent determinations

To find out the effect of treatment time on CDKI-71 anti-proliferative activity time-course MTT assays were performed using HCT-116, A2780 and MRC-5 for 24, 48 and 72h (Figure 4.1). Treatment for 24h was almost sufficient to achieve the highest growth inhibition for CDKI-71. Cell numbers decreased sharply between 0.1µM and 1µM treatment for all time points in HCT-116 and A2780 cancer cells. However, proliferation inhibition occurred only at 10µM

treatment in MRC-5 cells, indicating its specific activity towards cancer cells (Liu et al., 2011b).

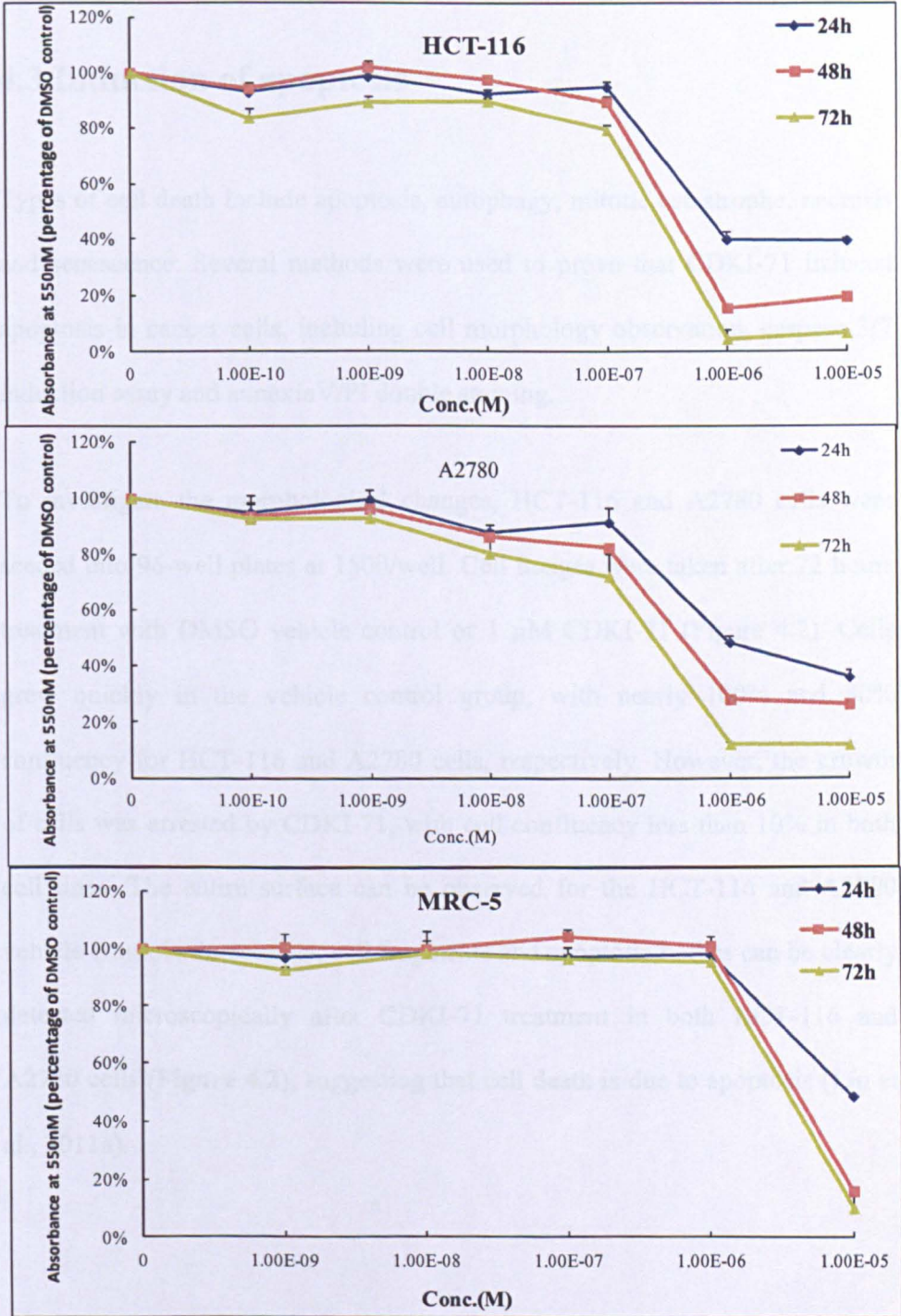


Figure 4.1 Growth inhibition curves of CDKI-71 for different treatment time points. HCT-116, A2780 and MRC-5 cells were treated with CDKI-71 for a range of concentrations at

24h, 48h or 72h, respectively. Mean values and SD were obtained from 3 independent experiments.

### 4.3 Induction of apoptosis

Types of cell death include apoptosis, autophagy, mitotic catastrophe, necrosis and senescence. Several methods were used to prove that CDKI-71 induced apoptosis in cancer cells, including cell morphology observation, caspase 3/7 induction assay and annexinV/PI double staining.

To investigate the morphological changes, HCT-116 and A2780 cells were seeded into 96-well plates at 1500/well. Cell images were taken after 72 hours treatment with DMSO vehicle control or 1  $\mu$ M CDKI-71 (Figure 4.2). Cells grew quickly in the vehicle control group, with nearly 100% and 80% confluency for HCT-116 and A2780 cells, respectively. However, the growth of cells was arrested by CDKI-71, with cell confluency less than 10% in both cell lines. The entire surface can be observed for the HCT-116 and A2780 vehicle controls. In contrast, cell fragments and apoptotic bodies can be clearly detected microscopically after CDKI-71 treatment in both HCT-116 and A2780 cells (**Figure 4.2**), suggesting that cell death is due to apoptosis (Liu et al., 2011a).

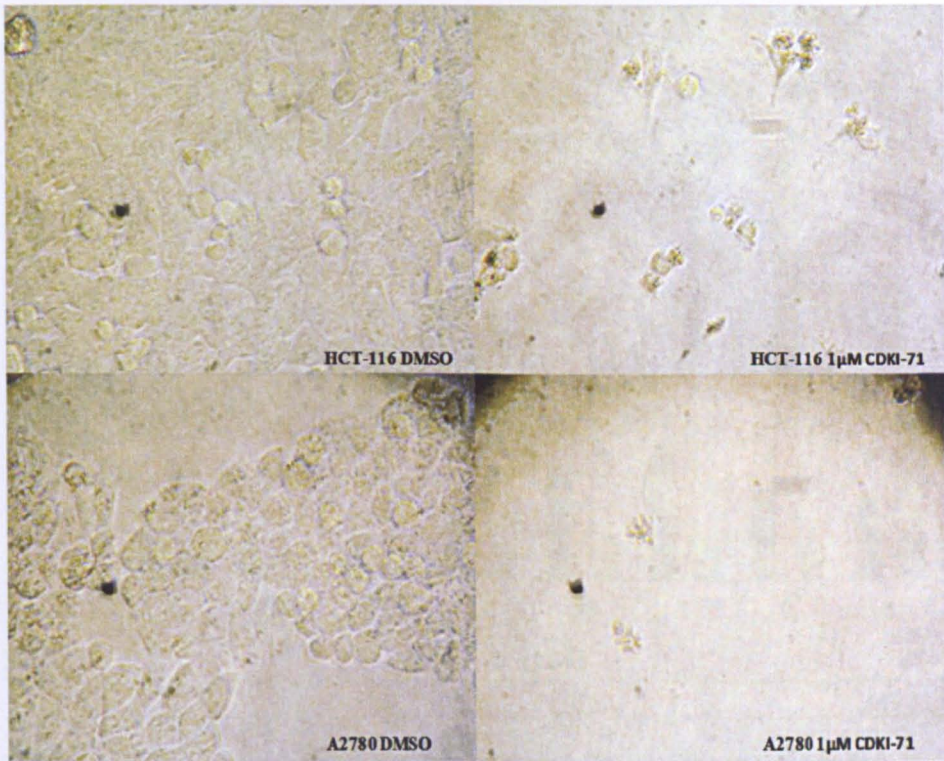


**Figure 4.2 Images of cell death after CDKI-71 treatment.** HCT-116 or A2780 cells were treated with 1µM CDKI-71 for 72 hours. DMSO vehicle treatment was used as negative control.

Caspase activation is an important biochemical feature of apoptosis. Induction of caspase 3/7 activity was also observed in HCT-116, A2780 or MRC-5 cells after treatment with either CDKI-71 or flavopiridol following 24 hours exposure (**Figure 4.3**).

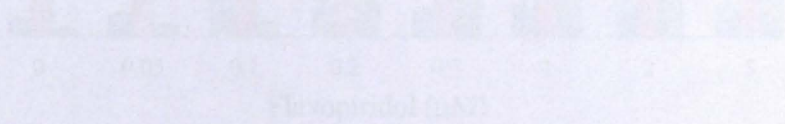


**Figure 4.3 Induction of caspase 3/7 activity in cancer cell lines HCT-116 and A2780 and Noncancer MRC-5 after treatment with CDKI-71 (1µM) or Flavopiridol (1µM) for 24 hours.** Cell lines were exposed to either 1 µM of drug or vehicle. Values represent mean ± SD (n=3) in triplicate from DMSO vehicle control (used as control with 1 µM DMSO).

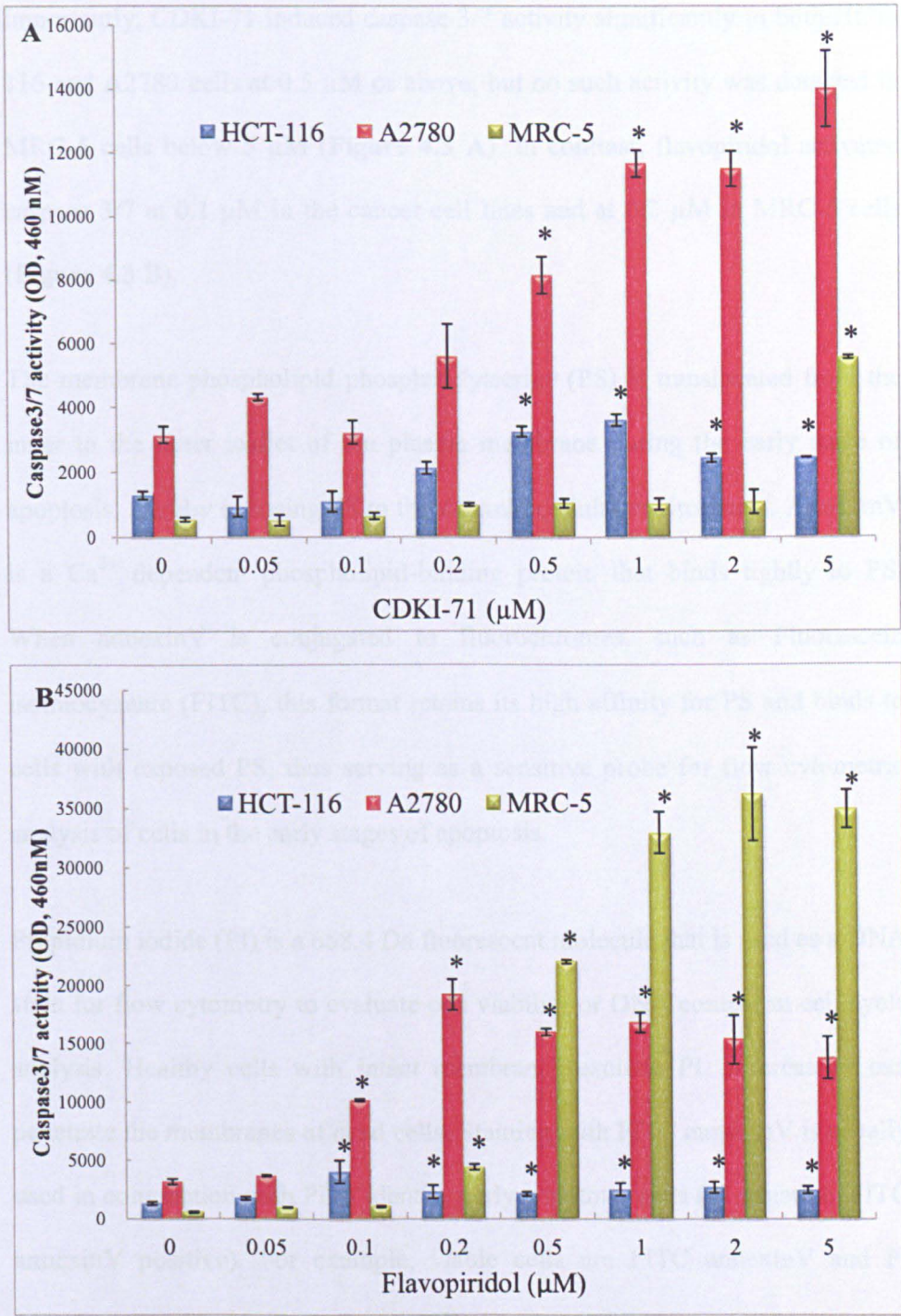


**Figure 4.3** Induction of caspase 3/7 activity in cancer cell lines HCT-116 and A2780, and fibroblast MRC-5 after treatment with CDKI-71 (A) or flavopiridol (B) for 24 hours. Vertical bars represent the mean  $\pm$  SD of three replicates. Values significantly ( $p \leq 0.05$ ) different from DMSO vehicle control were marked with an asterisk (\*).

Importantly, CDKI-71 induced caspase 3/7 activity significantly in both HCT-116 and A2780 cells at 0.5  $\mu\text{M}$  or above, but no such activity was detected in MRC-5 cells below 5  $\mu\text{M}$  (**Figure 4.3 A**). In contrast, flavopiridol activated caspase 3/7 at 0.1  $\mu\text{M}$  in the cancer cell lines and at 0.2  $\mu\text{M}$  in MRC-5 cells (**Figure 4.3 B**).

The membrane phospholipid phosphatidylserine (PS) is translocated from the inner to the outer leaflet of the plasma membrane during the early stage of apoptosis, thereby exposing PS to the external cellular environment. AnnexinV is a  $\text{Ca}^{2+}$  dependent phospholipid-binding protein that binds tightly to PS. When annexinV is conjugated to fluorochromes, such as Fluorescein isothiocyanate (FITC), this format retains its high affinity for PS and binds to cells with exposed PS, thus serving as a sensitive probe for flow cytometric analysis of cells in the early stages of apoptosis.

Propidium iodide (PI) is a 668.4 Da fluorescent molecule that is used as a DNA stain for flow cytometry to evaluate cell viability or DNA content in cell cycle analysis. Healthy cells with intact membranes exclude PI, whereas PI can penetrate the membranes of dead cells. Staining with FITC annexinV is usually used in conjunction with PI to identify early apoptotic cells (PI negative, FITC annexinV positive). For example, viable cells are FITC annexinV and PI negative; early apoptotic cells are FITC annexin V positive and PI negative; and late apoptotic or dead cells are FITC annexin V and PI positive. During long time treatment, apoptotic cells usually move from FITC annexinV and PI double negative (viable), to FITC Annexin V positive and PI negative (early apoptosis, membrane integrity is retained) and finally to FITC Annexin V and

PI double positive (end stage apoptosis and death). Progression through these three stages can be used to confirm cell apoptosis.

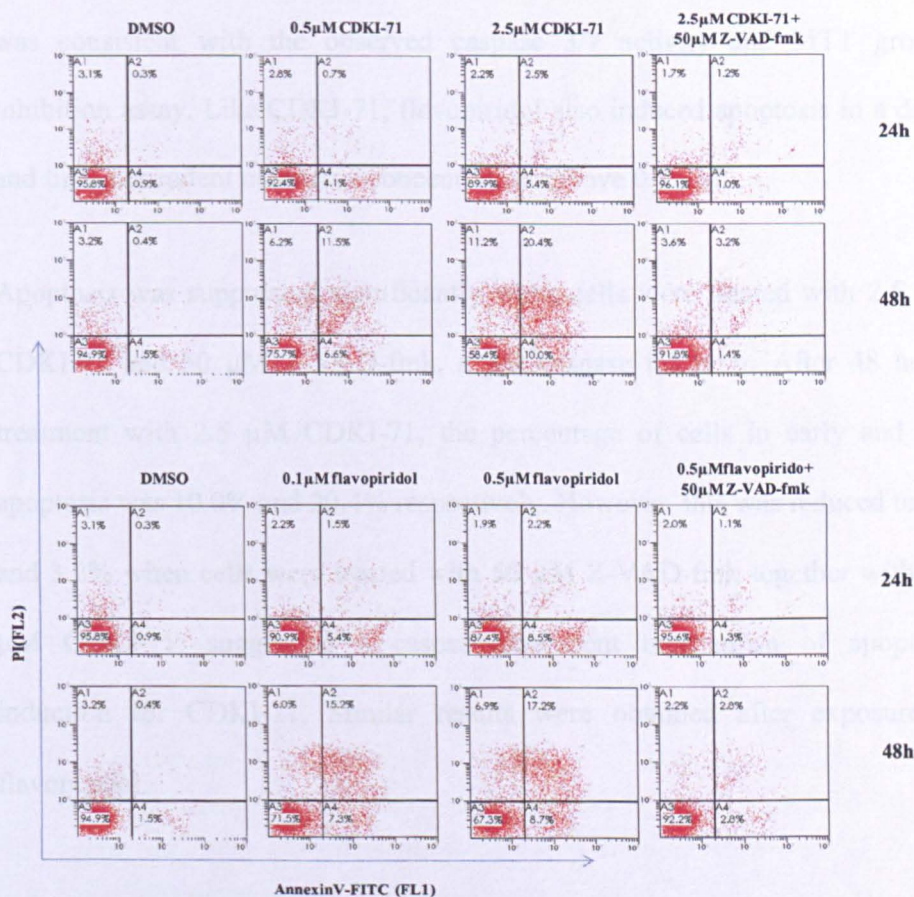


**Figure 4.4 Induction of caspase-dependent apoptosis in HCT-116 cells.** HCT-116 cells were exposed to different doses of CDKI-71 or flavopiridol, with or without Z-VAD-fmk, for 24 h or 48 h and analysed by annexinV/PI stained DNA content (The data are representative of three replicate experiments).

Induction of apoptosis by CDKI-71 or flavopiridol was analyzed by annexinV/PI double staining in HCT-116 (Figure 4.4), A2780 (Figure 4.5) and MRC-5 cells (Figure 4.6). In HCT-116 cells, both CDKI-71 and flavopiridol induced dose- and time- dependent apoptosis. CDKI-71 induced early apoptosis starting from 0.5 μM (GI<sub>50</sub> concentration) after 24 hours, which is indicated by significant increase of FITC annexinV in the bottom right

chamber (A4). After 48 hours treatment, increased late cell death population was also detected (11.5% and 20.4% for 0.5  $\mu$ M and 2.5  $\mu$ M treatment, respectively) in the top right chamber (A2). The starting concentration (0.5  $\mu$ M) was consistent with the observed caspase 3/7 activity and MTT growth inhibition assay. Like CDKI-71, flavopiridol also induced apoptosis in a dose- and time-dependent manner at concentrations above 0.1  $\mu$ M.

Apoptosis was suppressed significantly when cells were treated with 2.5  $\mu$ M CDKI-71 and 50  $\mu$ M Z-VAD-fmk, a pan-caspase inhibitor. After 48 hours treatment with 2.5  $\mu$ M CDKI-71, the percentage of cells in early and late apoptosis was 10.0% and 20.4% respectively. However, this was reduced to 1.4% and 3.2% when cells were treated with 50  $\mu$ M Z-VAD-fmk together with 2.5  $\mu$ M CDKI-71, suggesting a caspase-dependent mechanism of apoptosis induction for CDKI-71. Similar results were obtained after exposure to flavopiridol.

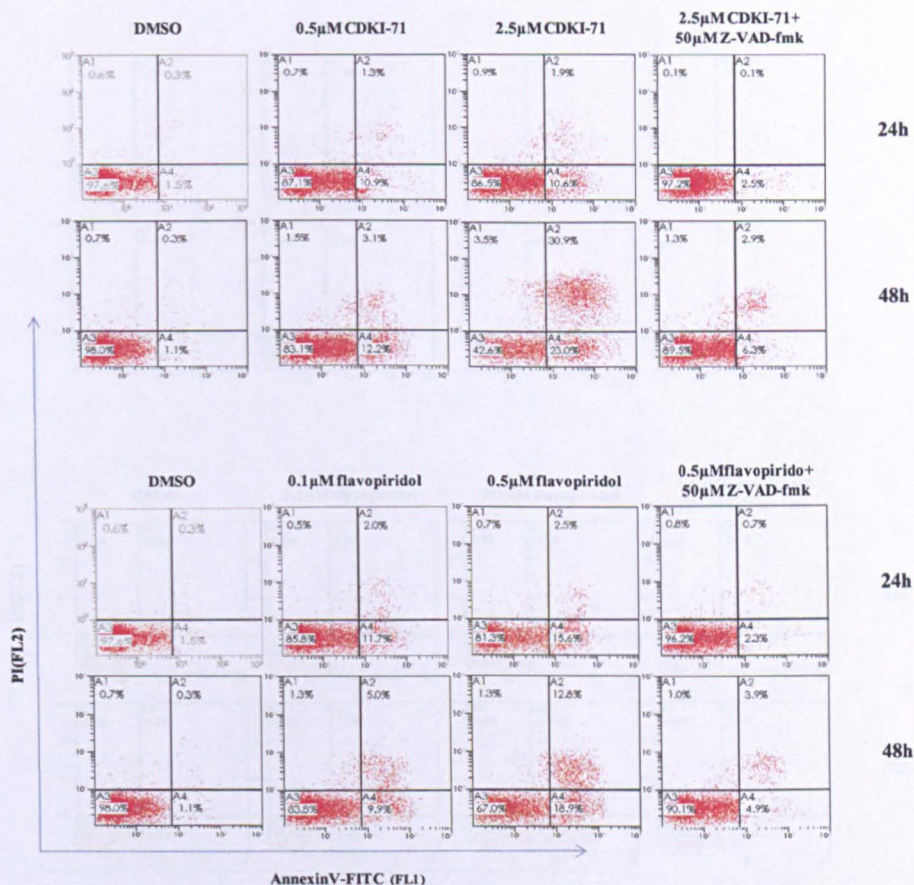


**Figure 4.5 Induction of caspase-dependent apoptosis in A2780 cells.** A2780 cells were exposed to different doses of CDKI-71 or flavopiridol, with or without Z-VAD-fmk, for 24 h or 48 h and analysed by annexinV/PI stained DNA content (The data are representative of three replicate experiments).

Induction of caspase-dependent apoptosis was also observed in A2780 cells after CDKI-71 or flavopiridol treatment at the same concentrations (**Figure 4.5**). Importantly, MRC-5 cells were less sensitive to CDKI-71 treatment compared to the cancer cell lines, and apoptotic cells were only detected on treatment with CDKI-71 at 5  $\mu$ M, which was 10 times higher than the effective concentration in cancer cells (**Figure 4.6**). This result is consistent with the MTT assay. In contrast, flavopiridol induced apoptosis in MRC-5 cells after exposure to concentrations from 0.2  $\mu$ M, showing similar potency in cancer and normal cell lines (Liu et al., 2011b).

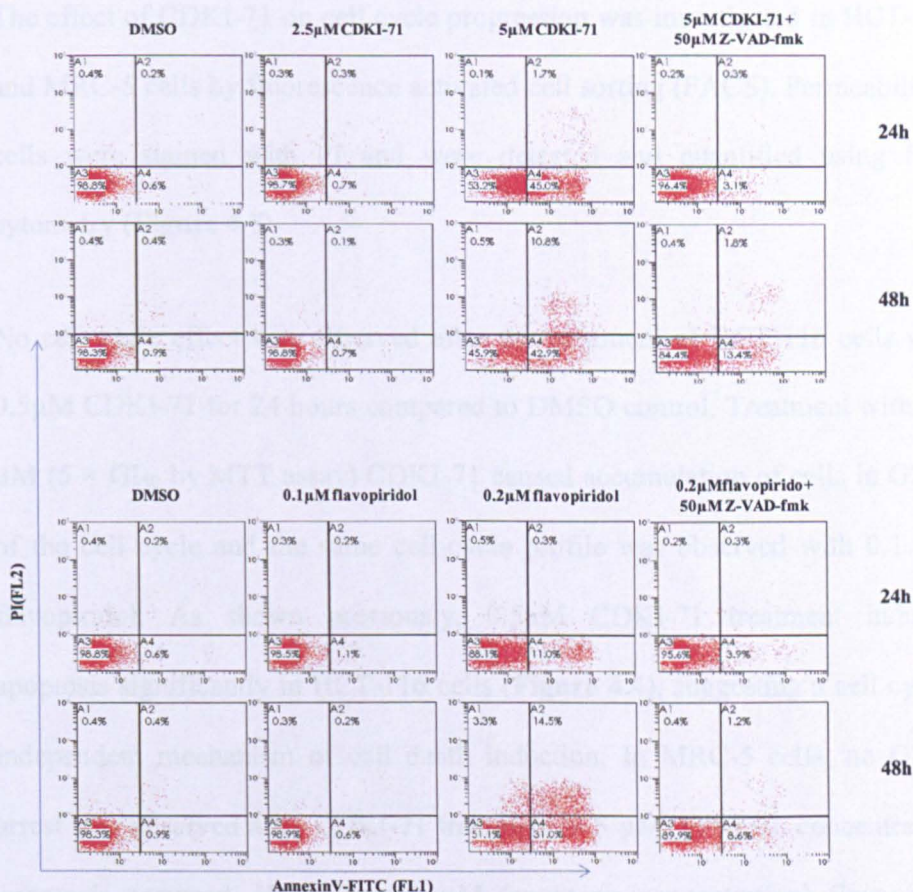


**Figure 4.6 Induction of caspase-dependent apoptosis in MRC-5 cells.** MRC-5 cells were exposed to different doses of CDKI-71 or flavopiridol, with or without Z-VAD-fmk, for 24 h or 48 h and analysed by annexinV/PI stained DNA content (The data are representative of three replicate experiments).

#### 4.4 Cell cycle effect

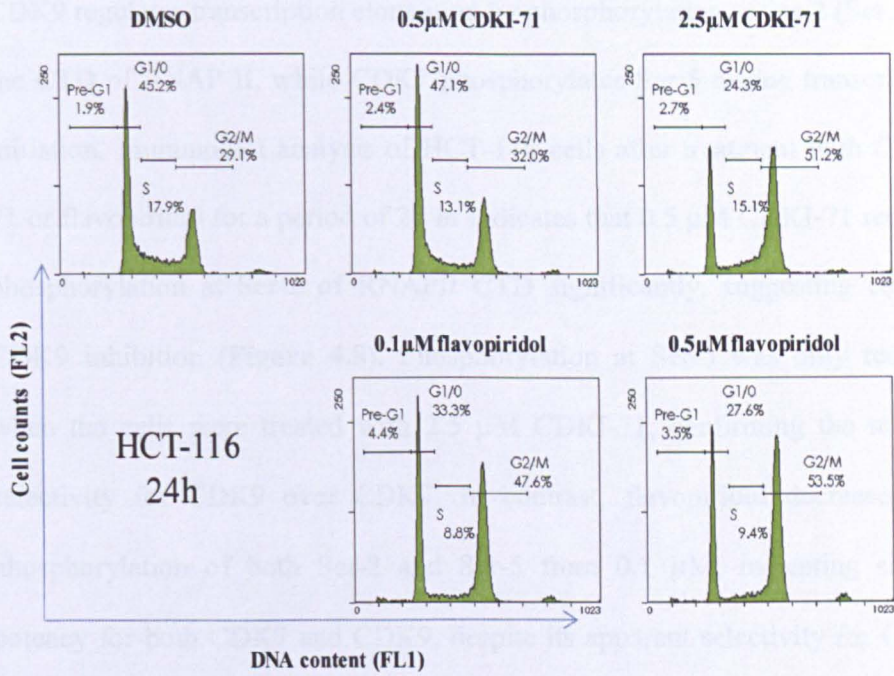
Lacking cell cycle roles, CDK9 regulates RNAPII transcription. Reduction of CDK9 levels by siRNA had no appreciable effect on cell cycle distribution (Cai et al., 2006b), whereas inhibition of CDK1 and CDK2 may arrest cells at G2/M boundary and G1 phase respectively (Lapenna and Giordano, 2009; Shapiro, 2006).

The effect of CDKI-71 on cell cycle progression was investigated in HCT-116 and MRC-5 cells by fluorescence activated cell sorting (FACS). Permeabilized cells were stained with PI and were detected and quantified using flow cytometry (**Figure 4.7**).

No cell cycle effect was observed after the treatment of HCT-116 cells with 0.5 $\mu$ M CDKI-71 for 24 hours compared to DMSO control. Treatment with 2.5  $\mu$ M ( $5 \times GI_{50}$  by MTT assay) CDKI-71 caused accumulation of cells in G2/M of the cell cycle and the same cell-cycle profile was observed with 0.1  $\mu$ M flavopiridol. As shown previously, 0.5 $\mu$ M CDKI-71 treatment induced apoptosis significantly in HCT-116 cells (**Figure 4.4**), suggesting a cell cycle-independent mechanism of cell death induction. In MRC-5 cells, no G2/M arrest was observed after CDKI-71 treatment at 5  $\mu$ M, at which concentration apoptosis occurred. However, 0.2  $\mu$ M (apoptosis concentration) flavopiridol induced G2/M accumulation (Liu et al., 2011b).

## 4.5 Inhibition of cellular RNAPII CTD phosphorylation

A



B

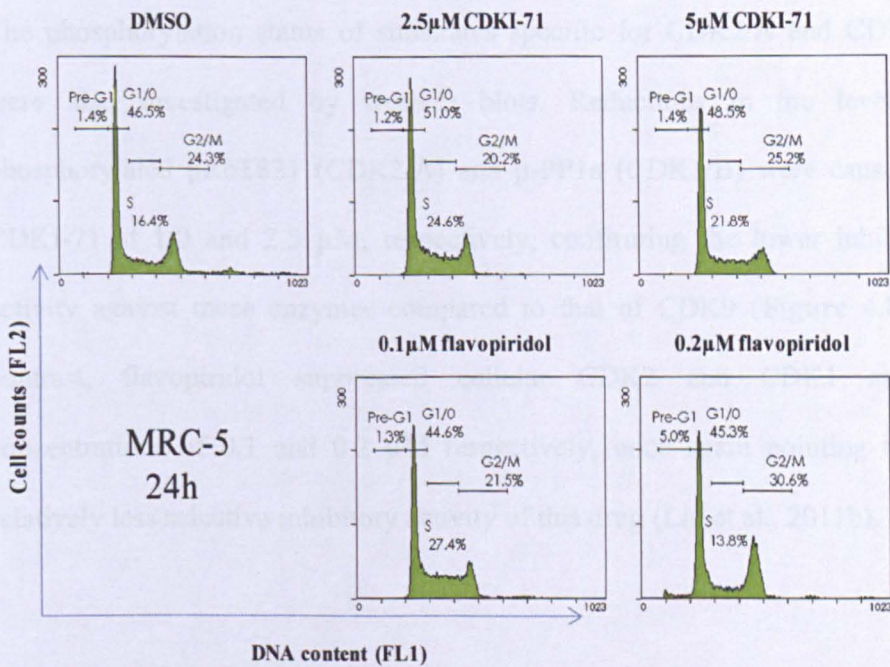


**Figure 4.7 Cell cycle effects of CDKI-71 or flavopiridol.** HCT-116 (A) or MRC-5 (B) cells were treated with different concentrations of CDKI-71 or flavopiridol for 24 hours (The data are representative of three replicate experiments).

## 4.5 Inhibition of cellular RNAPII CTD phosphorylation

CDK9 regulates transcription elongation by phosphorylating serine 2 (Ser 2) on the CTD of RNAP II, while CDK7 phosphorylates Ser 5 during transcription initiation. Immunoblot analysis of HCT-116 cells after treatment with CDKI-71 or flavopiridol for a period of 24 hr indicates that 0.5  $\mu\text{M}$  CDKI-71 reduced phosphorylation at Ser-2 of RNAPII CTD significantly, suggesting cellular CDK9 inhibition (**Figure 4.8**). Phosphorylation at Ser-5 was only reduced when the cells were treated with 2.5  $\mu\text{M}$  CDKI-71, confirming the relative selectivity for CDK9 over CDK7. In contrast, flavopiridol decreased the phosphorylation of both Ser-2 and Ser-5 from 0.1  $\mu\text{M}$ , indicating similar potency for both CDK7 and CDK9, despite its apparent selectivity for CDK9 over CDK7 in the kinase assays.

The phosphorylation status of substrates specific for CDK2/A and CDK1/B were also investigated by western blots. Reductions in the levels of phosphorylated pRbT821 (CDK2/A) and p-PP1a (CDK1/B) were caused by CDKI-71 at 1.0 and 2.5  $\mu\text{M}$ , respectively, confirming the lower inhibitory activity against these enzymes compared to that of CDK9 (**Figure 4.8**). In contrast, flavopiridol suppressed cellular CDK2 and CDK1 at the concentrations of 0.1 and 0.2  $\mu\text{M}$  respectively, once again pointing to the relatively less selective inhibitory activity of this drug (Liu et al., 2011b).

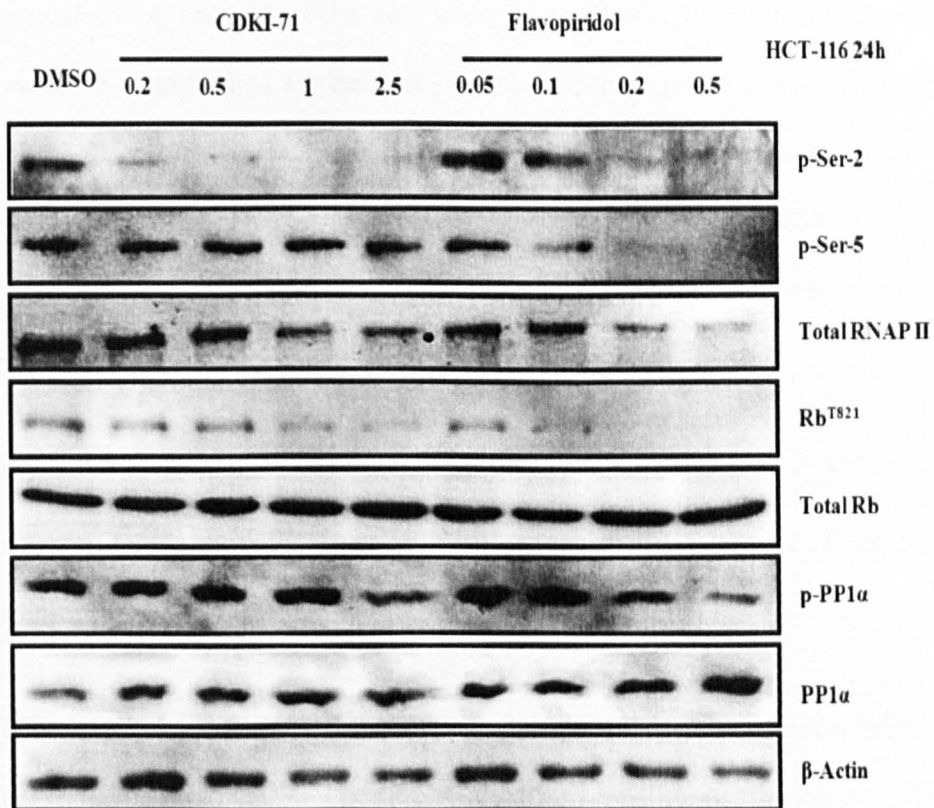


**Figure 4.8 Inhibition of RNAPII CTD phosphorylation and other cell cycle CDKs by Western blot analysis.** HCT-116 cells were treated with indicated concentrations of CDKI-71 or flavopiridol for 24 hr.

## 4.6 Effect on gene transcription

Since CDK9 regulates transcription elongation, CDK9 inhibition should suppress the synthesis of messenger RNA (mRNA) from genes regulated by CDK9. To investigate the effect of CDKI-71 treatment on gene transcription, DNA microarray (30,000 gene probe) was performed on A2780 cells after treatment with CDKI-71 (1  $\mu$ M) or flavopiridol (0.2  $\mu$ M) for 4 hours. In comparison to untreated A2780 cells, CDKI-71 changed expression of 158 probes by at least two fold ( $|\log_2| > 1$ ) (Appendix One). The lowest  $\log_2$  ratio was -1.77 and the highest was 1.29. Of note, 141 probe sets were down-

regulated and only 17 probe sets were up-regulated. Hierarchical clustering was further performed for the 158 probe sets to compare the gene changes of CDKI-71 and flavopiridol (**Figure 4.9 A**). EASE software (Hosack et al., 2003) was used to identify over-represented gene categories. These 158 probe sets were further divided into 4 clusters depending on different changes in gene expression induced by CDKI-71 or flavopiridol.

Cluster 1 (green) includes 138 probes downregulated by both CDKI-71 and flavopiridol. The main gene categories enriched in cluster 1 contains: transcription (26 hits), regulation of transcription (23 hits).

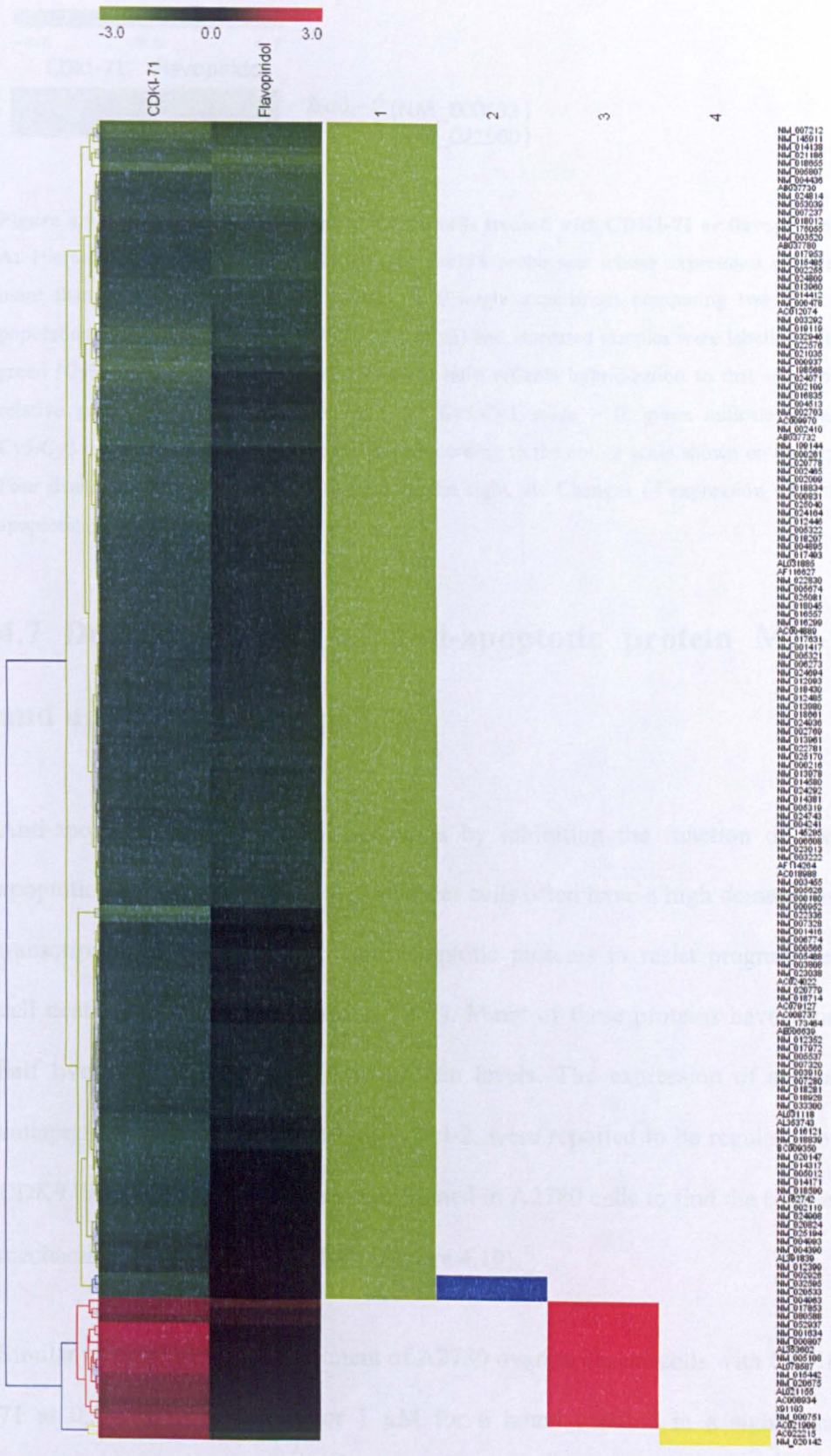
Cluster 2 (blue) exhibits the 3 probes (NM\_032595: protein phosphatase 1, regulatory subunit 9B, spinophilin, NM\_020533: mucolipin 1 and NM-004963: guanylate cyclase 2C) which were only down-regulated by CDKI-71. However, it's not accurate to analyze the gene category due to the low probe quantity.

Cluster 3 (red) includes probes up-regulated by CDKI-71 that were also up-regulated or not regulated by flavopiridol. 10 genes were obtained from EASE. Cluster 3 maximally enriched biological process gene ontology (GO) includes: transport (3 hits), catalytic activity (5 hits) and transporter activity (4 hits). Since many functional genes were down-regulated, the cellular feedback loop may facilitate the over-expression of genes regulating catalytic or transporter activity to overcome the lack of down-regulated genes. It is also possible that these up-regulated genes were negatively regulated by some genes which were decreased by the treatment.

Cluster 4 (yellows) contains two probe sets (AC022215 and NM\_020142) which were up-regulated by CDKI-71 but down-regulated by flavopiridol. The function of AC022215 is still not clear, while NM\_020142 gene encode NADH: ubiquinone oxidoreductase MLRQ subunit homolog and may transport electrons from NADH to ubiquinone. However, no further analysis can be performed because of the very low probe amount.

Flavopiridol was reported to inhibit transcription globally in a similar way to two transcription inhibitors, actinomycin D and DRB (Lam et al., 2001). The majority of genes were down-regulated after CDKI-71 (141 out of 158 genes) or flavopiridol (142 out of 158 genes) treatment, suggesting CDKI-71 is also a transcription inhibitor.

A



B

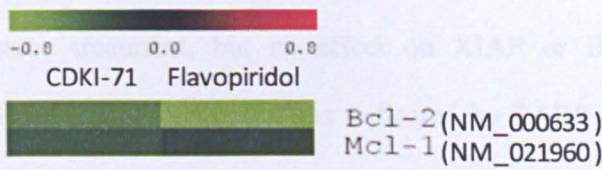


**Figure 4.9 Gene expression patterns of A2780 cells treated with CDKI-71 or flavopiridol.** **A:** Hierarchical clustering was performed for the 158 probe sets whose expression changes more than 1 log ( $|\log_2| > 1$ ). Each column is a single experiment comparing two cDNA populations; treated samples were labelled red (Cy5) and untreated samples were labelled with green (Cy3). The red-to-green ( $\log_2 \text{ Cy5/Cy3}$ ) ratio reflects hybridization to that spot and relative gene expression. Red indicates  $\log_2 \text{ Cy5/Cy3}$  value  $> 0$ , green indicates  $\log_2 \text{ Cy5/Cy3}$  value  $< 0$ . The values were depicted according to the colour scale shown on the top. Four distinct clusters of genes are marked on the right. **B:** Changes of expression of anti-apoptotic proteins Bcl-2 and Mcl-1

## 4.7 Down-regulation of anti-apoptotic protein Mcl-1 and up-regulation of p53

Anti-apoptotic proteins inhibit apoptosis by inhibiting the function of pro-apoptotic proteins (section 1.1.4.2). Cancer cells often have a high demand for transcription and translation of anti-apoptotic proteins to resist programmed cell death (Koumenis and Giaccia, 1997). Many of these proteins have short half lives at both the mRNA and protein levels. The expression of several antiapoptotic proteins, such as Mcl-1, Bcl-2, were reported to be regulated by CDK9. Western blot analysis was performed in A2780 cells to find the cellular mechanism of action for CDKI-71 (**Figure 4.10**).

Similar to HCT-116 cells, treatment of A2780 ovarian cancer cells with CDKI-71 at 0.5  $\mu\text{M}$  for 24 hours or 1  $\mu\text{M}$  for 6 hours resulted in a significant

reduction in the phosphorylation of Ser-2, but not Ser-5, suggesting selective CDK9 inhibition. Mcl-1 anti-apoptotic protein was reduced significantly by the same treatment, but no effect on XIAP or Bcl-2 proteins was detected. Induction of apoptosis was indicated by PARP cleavage at 0.5  $\mu$ M. Similar

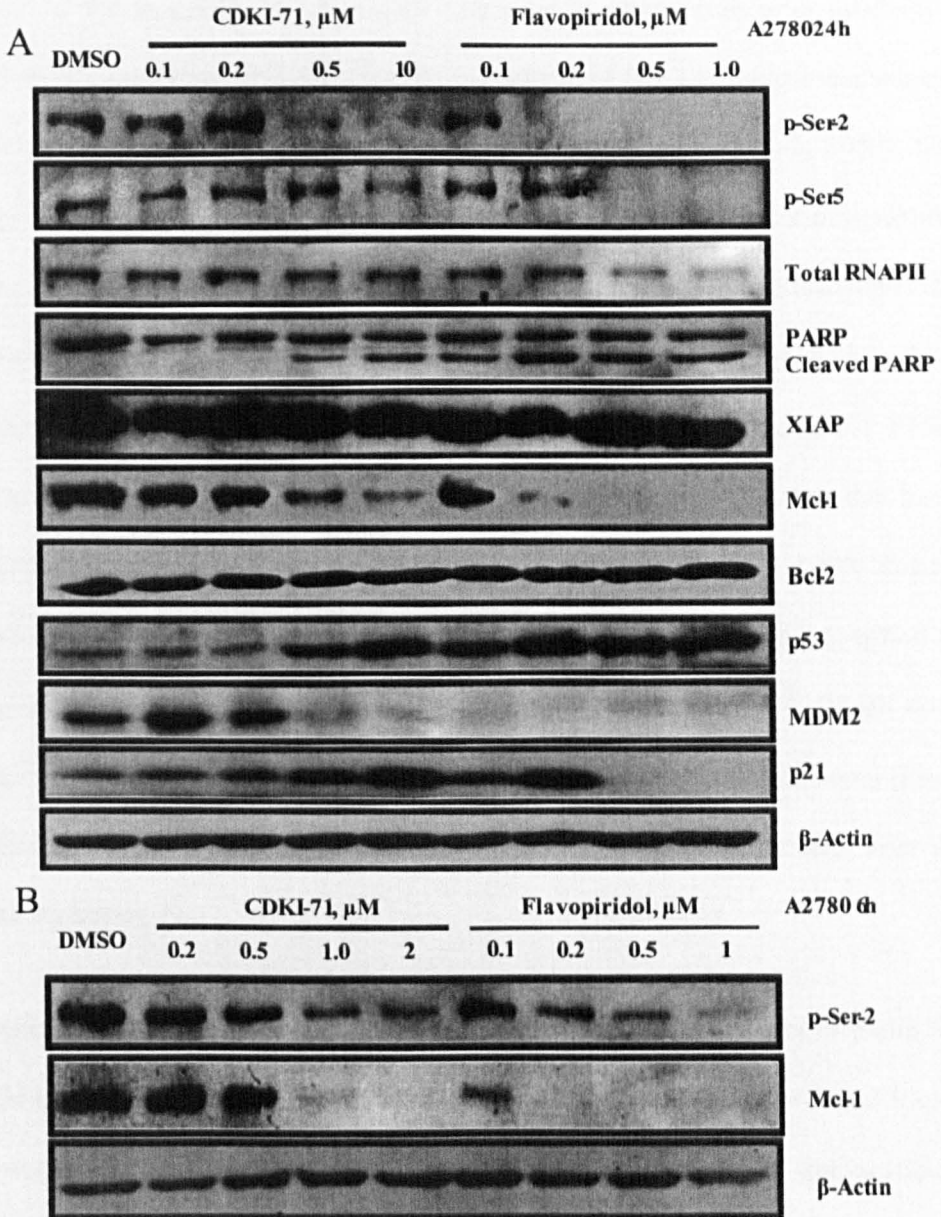


**Figure 4.10** Effects on anti-apoptotic proteins and the p53 pathway by Western blot analysis in A2780 cells. Cells were treated with indicated concentrations of CDKI-71 or flavopiridol for 24 hours (A) or 6 hours (B).

results were obtained after flavopiridol treatment. Blockade of RNAPII transcriptional activity reduced the levels of the transcripts and their encoded proteins. Mcl-1 but not Bcl-1 protein was found to be particularly sensitive to CDKI-71 or flavopiridol treatment. This is consistent with the results reported before. For example, Mcl-1 protein decreased in cancer cells after incubation with flavopiridol or SNS-032, but the expression of Bcl-2 remained unchanged, even though its mRNA was reduced (Chen et al., 2005; Chen et al., 2009). The specific motifs of the mRNA or protein sequences signalling for degradation may be responsible for the different responses. The adenylate/uridylate-rich elements (ARE) -mediated Mcl-1 and Bcl-2 mRNA decay may explain their short mRNA half lives (Chen and Shyu, 1995; Schiavone et al., 2000). PEST regions (rich in proline, glutamic acid, serine, and threonine), on the other hand, identify proteins for rapid destruction (Rechsteiner and Rogers, 1996; Rogers et al., 1986). The primary protein structure of Mcl-1 confirms its susceptibility to rapid intracellular proteolysis ( $t_{1/2} = 0.5 - 1$  hour) while Bcl-2, which does not have a PEST region, is a long-lived protein with  $t_{1/2} = 10 - 24$  hours (Reed et al., 1987). This may explain why only Mcl-1 protein was reduced after 24 hours treatment.

MRC-5 fibroblast cells were treated with CDKI-71, flavopiridol or cisplatin for 24 hr (Figure 4.11). CDKI-71 reduced phosphorylated Ser-2, Ser-5 and Mcl-1 protein at 5  $\mu$ M. Induction of apoptosis also occurred at 5  $\mu$ M, demonstrated by PARP cleavage and annexin V/PI assays. These data confirmed that the cancer cells were more sensitive (10-fold) to CDKI-71 than the untransformed MRC-5 cells. However, MRC-5 cells also seem to rely on Mcl-1, but the reasons for this remain unresolved. In contrast, treatment with 0.2  $\mu$ M

flavopiridol resulted in reduced levels of phosphorylated Ser-2 and Ser-5 as well as a reduction in Mcl-1 expression, demonstrating less selectivity compared to CDKI-71.

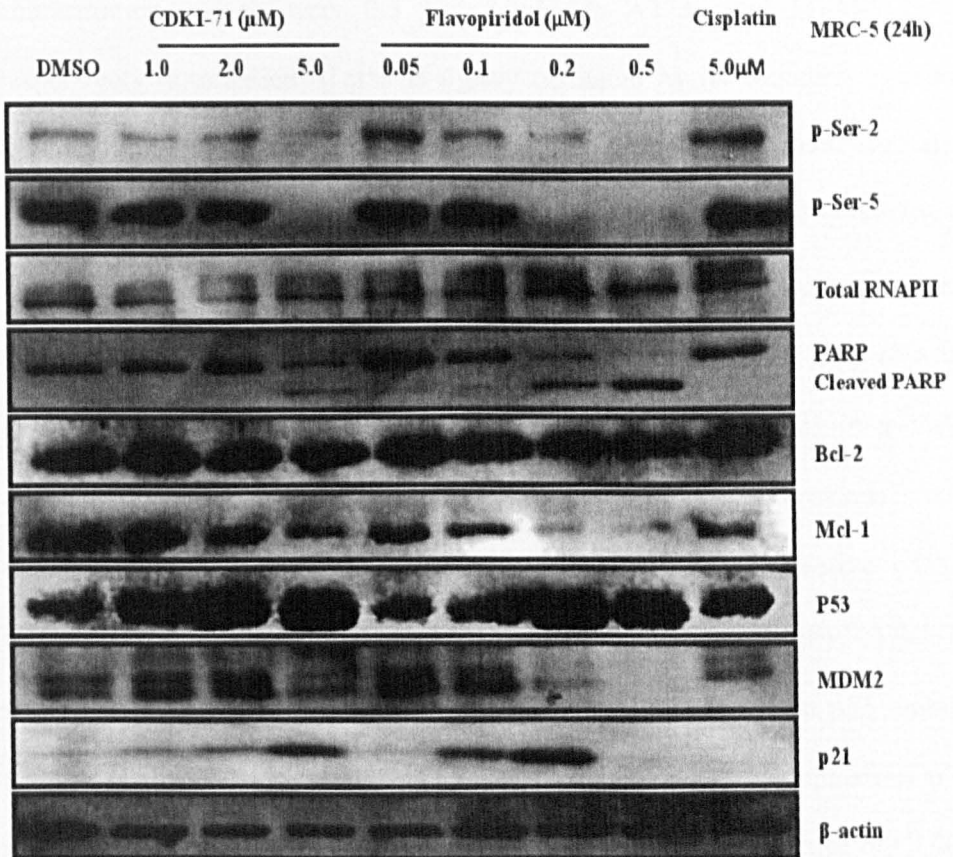


**Figure 4.11** Effects on anti-apoptotic proteins and the p53 pathway by Western blot analysis in MRC-5 cells. Cells were treated with indicated concentrations of CDKI-71 or flavopiridol for 24 hours.

Mcl-1 prevents mitochondrial outer membrane permeabilization and cytochrome C release (Danial, 2007; Danial and Korsmeyer, 2004); down-regulation of Mcl-1 by CDKI-71 and flavopiridol may therefore facilitate the release of cytochrome C from mitochondria leading to induction of apoptosis. As tumour cells appear to be dependent on Mcl-1 for survival (Michels et al.,

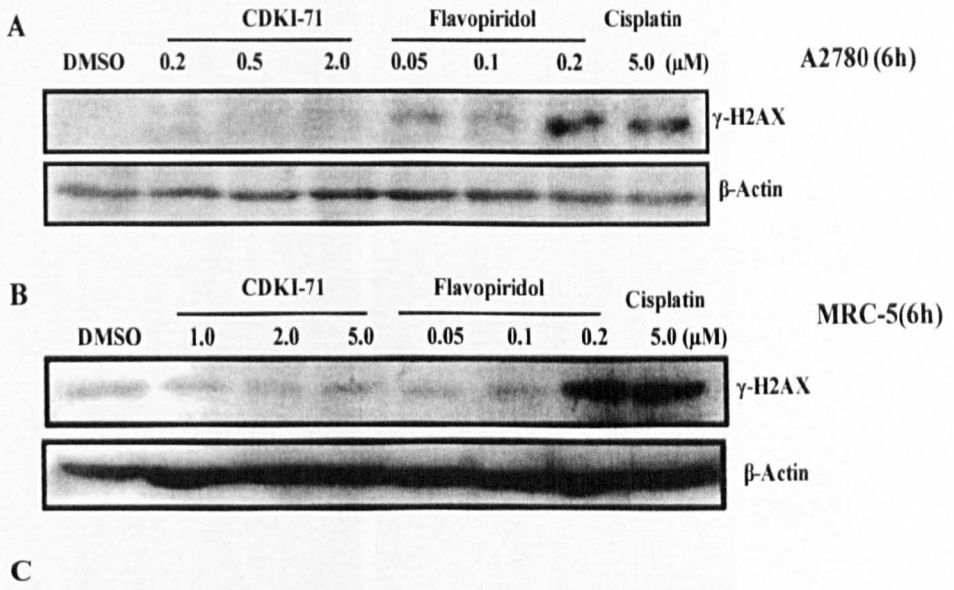
2005), this is an excellent target for CDK9 inhibitors for the induction of apoptosis.

Induction of p53 was observed on treatment with CDKI-71 at apoptotic concentrations which were 0.5 and 5  $\mu$ M in A2780 and MRC-5 cells, respectively. Expression of p53 is tightly regulated by its negative regulator MDM2, a short half-life protein targeting p53 degradation, which was also reduced by CDKI-71 and flavopiridol (Figure 4.10 and 4.11). Importantly, CDKI-71 decreased Ser-2 phosphorylation, Mcl-1 and MDM2 protein at the same concentration, suggesting the down-regulation of MDM2 may also be due to CDK9 inhibition. In addition, CDKI-71 up-regulated p21 in a dose-dependent manner. This is consistent with the result of a previous study demonstrating that p21 was induced by DRB, the most selective CDK9 inhibitor identified to date (Blagosklonny et al., 2002). Importantly, CDKI-71 showed similar sensitivity between p53 wild type, p53 null, and p53 mutant cells in our MTT assays, suggesting that CDKI-71-induced apoptosis is p53 independent and that the increase of p53 is a molecular consequence of CDK9 inhibition-mediated MDM2 down-regulation.

## **4.8 Flavopiridol induces DNA double-strand breaks**

Flavopiridol demonstrated potent anti-proliferation effects ( $GI_{50} < 100$ nM) in the cell lines tested, with no obvious tumour-type or tumour selectivity, which is consistent with reported data using the US National Cancer Institute (NCI) 60 human tumour cell lines (Dai and Grant, 2003). Flavopiridol also killed

CLL cells and normal mononuclear cells at similar concentrations (Byrd et al., 1998).



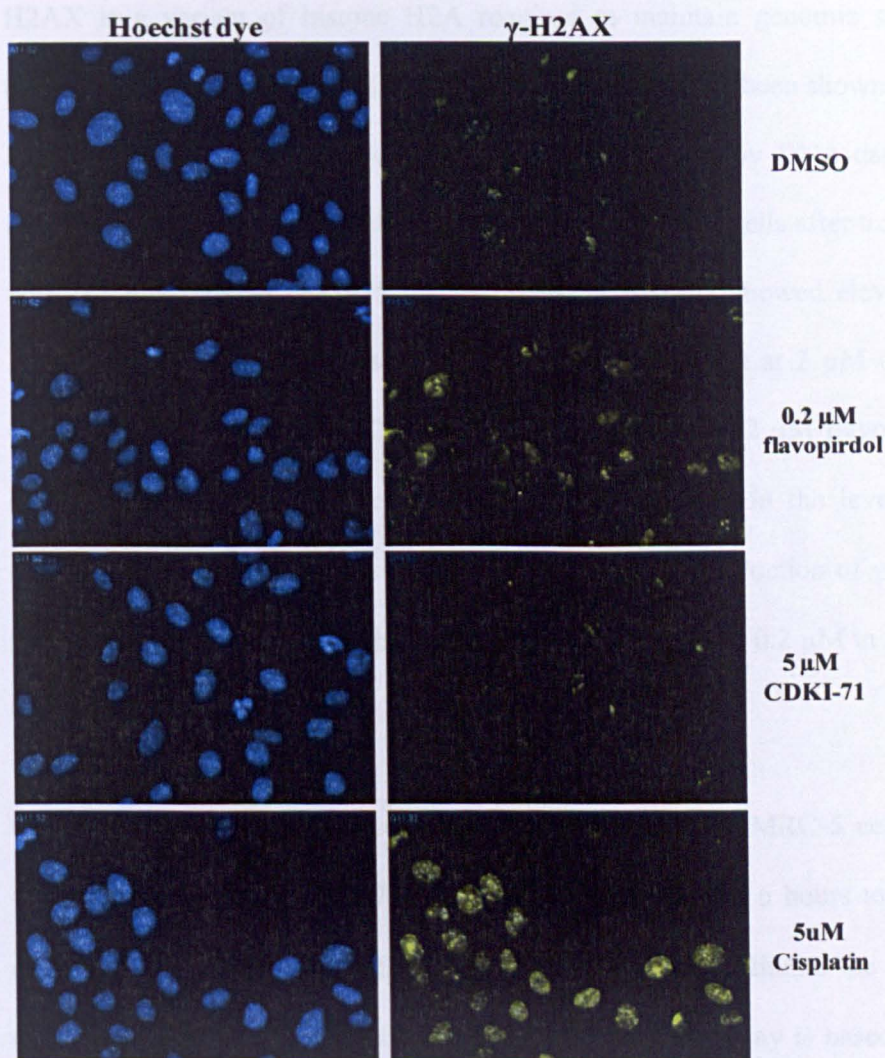


**Figure 4.12 Induction of  $\gamma$ -H2AX by flavopiridol.** Western blot analysis was performed in A2780 (A) or MRC-5 (B) cells after CDKI-71, flavopiridol or cisplatin treatment for 6 hours. Images of permeabilized MRC-5 cells were taken after labelling with a  $\gamma$ H2AX primary antibody and an Alexa Fluor 488 secondary antibody (C) DNA was counterstained with Hoechst dye.

Given that the kinase inhibition profile of CDKI-71 and flavopiridol were similar but their cytotoxicity profiles were not, we suspected that DNA damage may be another outcome of flavopiridol treatment. Consequently, we investigated the effects of flavopiridol and CDKI-71 on the expression of  $\gamma$ -H2AX (Figure 4.12).

H2AX is a variant of histone H2A required to maintain genomic stability (Celeste et al., 2002).  $\gamma$ -H2AX (phosphorylated H2AX) has been shown to be a sensitive marker of DNA double strand breaks induced by DNA-damaging agents (Paull et al., 2000). Western blot analysis of A2780 cells after treatment with 0.2  $\mu$ M flavopiridol or 5  $\mu$ M cisplatin for 6 hours showed elevated  $\gamma$ -H2AX, but no effect was observed for CDKI-71 treatment at 2  $\mu$ M (**Figure 4.12 A**). In MRC-5 cells  $\gamma$ -H2AX was also increased by 0.2  $\mu$ M flavopiridol, while 5  $\mu$ M CDKI-71 showed no significant differences in the level of  $\gamma$ -H2AX compared to DMSO treatment (**Figure 4.12 B**). Induction of  $\gamma$ -H2AX foci was also detected after 6 hours flavopiridol treatment at 0.2  $\mu$ M in MRC-5 cells (**Figure 4.12 C**).

Comet assay under alkaline conditions was performed on MRC-5 cells after treatment with 5  $\mu$ M CDKI-71 or 0.2  $\mu$ M flavopiridol for 6 hours to further confirm the DNA damage effect of flavopiridol, and to estimate the damage distribution in a population of cells (**Figure 4.13**). This assay is based on the ability of denatured or cleaved DNA fragments to migrate out of the nucleus, whereas undamaged DNA strands are too large and do not leave the cavity under electrophoresis. Significant numbers of cells with DNA double-strand breaks were observed, as evidenced by the formation of the comet, enlarged tail and increased tail intensity, after treatment with flavopiridol (**Table 4.4**). In contrast, no comet cells can be detected after CDKI-71 or DMSO vehicle control treatment.

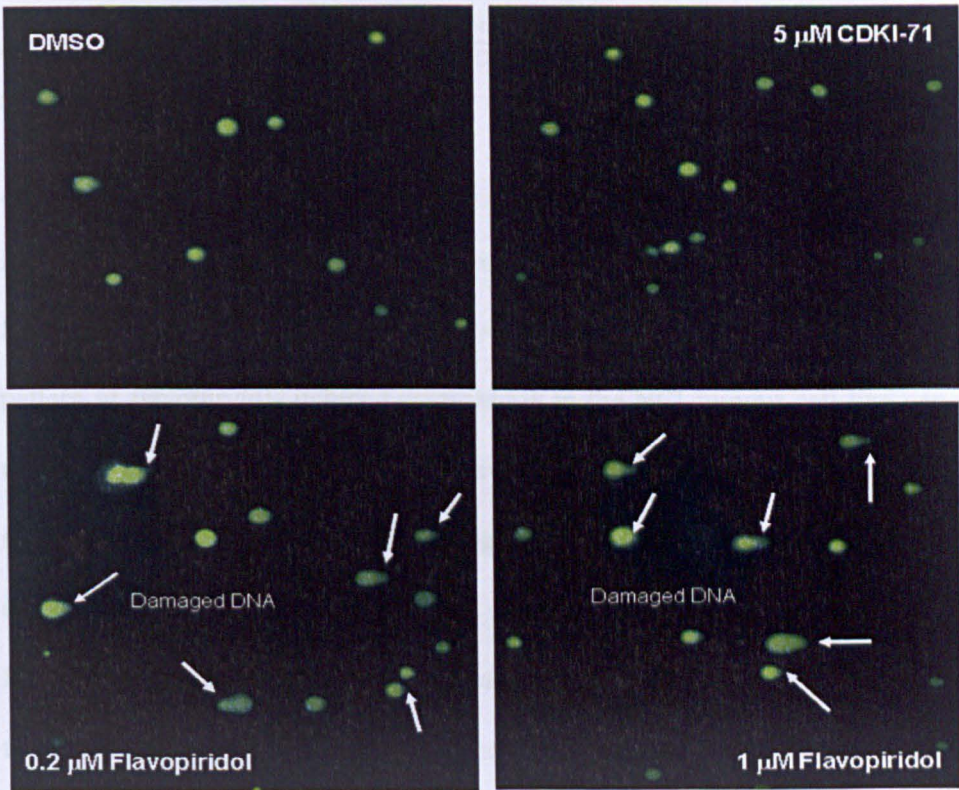


**Figure 4.13** Comet assay (single-cell gel electrophoresis) on MRC-5 cells treated with DMSO vehicle, CDKI-71 or flavopiridol for 2 hours. The comet cells with DNA double-strand breaks were detected by tail length and intensity, and some of these cells can be visualized (indicated with the arrows).

No significant indication was observed in the microarray. It might be due to the genes related to DNA damage were down-regulated by CDK9 inhibition or the response maybe at the translation level.

**Table 4.3** Tail length and Tail intensity after CDKI-71 or flavopiridol treatment in the comet assay.

Treatments	Tail Length $\mu\text{m}$	Tail Intensity %
DMSO	15.94 $\pm$ 5.98	8.38 $\pm$ 6.78
5 $\mu\text{M}$ CDKI-71	15.47 $\pm$ 5.65	8.41 $\pm$ 8.55
0.2 $\mu\text{M}$ flavopiridol	29.29 $\pm$ 13.13*	24.14 $\pm$ 20.68*

1 $\mu$ M flavopiridol      26.97 $\pm$ 8.99\*      24.97 $\pm$ 19.31\*  
Values significantly different ( $p < 0.05$ ) from DMSO treated cells are marked with an asterisk (\*).

As the first CDK inhibitor in clinical trials, flavopiridol has attracted much interest in the past decade. Previous studies showed the evidence that flavopiridol interacts with DNA *in vitro* (Bible et al., 2000). Analysis of the pattern of flavopiridol- induced cytotoxicity in the NCI-tumour cell line panel using the COMPARE algorithm showed that flavopiridol shares similar mechanisms of action to intercalating or DNA-damaging agents, such as ecteinascidin 729, chromomycin A3, actinomycin D (Bible et al., 2000). However, the biological significance has not been determined. Here we report the first cellular evidence that flavopiridol induces DNA double-strand breaks in cancer cells and fibroblasts.

## **4.9 Cellular model of action of CDKI-71 and flavopiridol**

It has been observed that CDKI-71 and flavopiridol have similar activity at the kinase level, but flavopiridol is more potent in cells. In addition, flavopiridol appears to have no selectivity between CDK9 and CDK7 in cells. These observations may arise from the ability of flavopiridol to intercalate into the DNA double strands, which may serve as a template to facilitate the association of flavopiridol with the RNAPII CTD and therefore inhibit activity of CDKs 9 and 7 (**Figure 4.14**). However, the cellular distribution model is only a hypothesis and further experiments are needed to prove it. Alternatively, the DNA damage response of flavopiridol may down regulate CDK7 activity

and the DNA intercalated flavopiridol would also arrest the function of RNAPII.

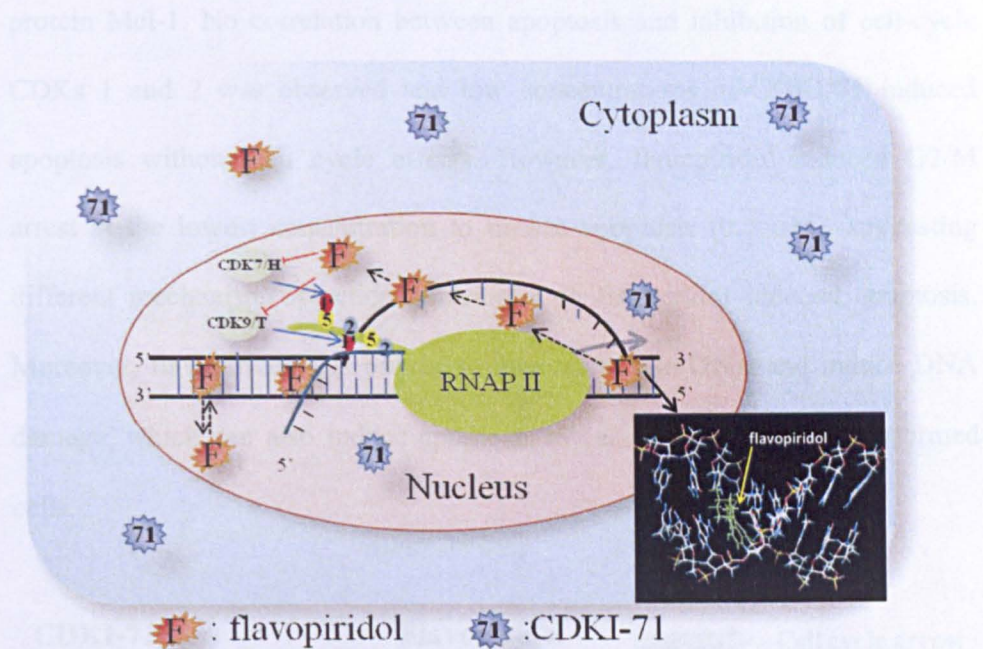


**Figure 4.14 Cellular distribution model for CDKI-71 and flavopiridol.** As flavopiridol binds to double strand DNA, DNA double strands may form a reservoir for flavopiridol. Due to equilibrium effect, the concentration of unbound flavopiridol around the DNA strands should be higher than other areas outside the nucleus. After transcription initiation, RNAPII traverses one strand of DNA (the template strand) and uses base pairing complementarity with the DNA template to create an RNA copy. Therefore, RNAPII is in close proximity to DNA which is the reservoir of flavopiridol. CDK7/Cyclin H and CDK9/Cyclin T phosphorylate Ser5 and Ser2 sites of RNAPII, respectively. The locally high concentration of flavopiridol facilitates its inhibitory activity and conceals flavopiridol's selectivity towards CDK7 and CDK9. As a transcription inhibitor, flavopiridol or CDKI-71 must enter the nucleus. As we know, different cell types should have different membrane penetration characteristics or organelle distribution for anti-cancer agents. The DNA binding effect for flavopiridol ensures the high concentration for flavopiridol in different cell types. This may explain why flavopiridol inhibits CDK9 at similar concentrations in HCT-116, A2780 and MRC-5 cells, but CDKI-71 has a 10-fold difference.

Based on the above experiments, the cellular similarity and difference between CDKI-71 and flavopiridol are shown in **Figure 4.15**. CDKI-71 induces caspase-dependent apoptosis potently which was closely associated with the

inhibition of RNAPII phosphorylation at serine-2. This was caused by effective CDK9 inhibition and resulted in the downstream inhibition of anti-apoptotic protein Mcl-1. No correlation between apoptosis and inhibition of cell-cycle CDKs 1 and 2 was observed and low concentrations of CDKI-71 induced apoptosis without cell cycle effects. However, flavopiridol induced G2/M arrest at the lowest concentration to induce apoptosis (0.1  $\mu$ M), suggesting different mechanism of action contributes to flavopiridol induced apoptosis. Moreover, flavopiridol was proved to intercalate into DNA and induce DNA damage, which can also induce apoptosis in cancer cells or non-transformed cells.

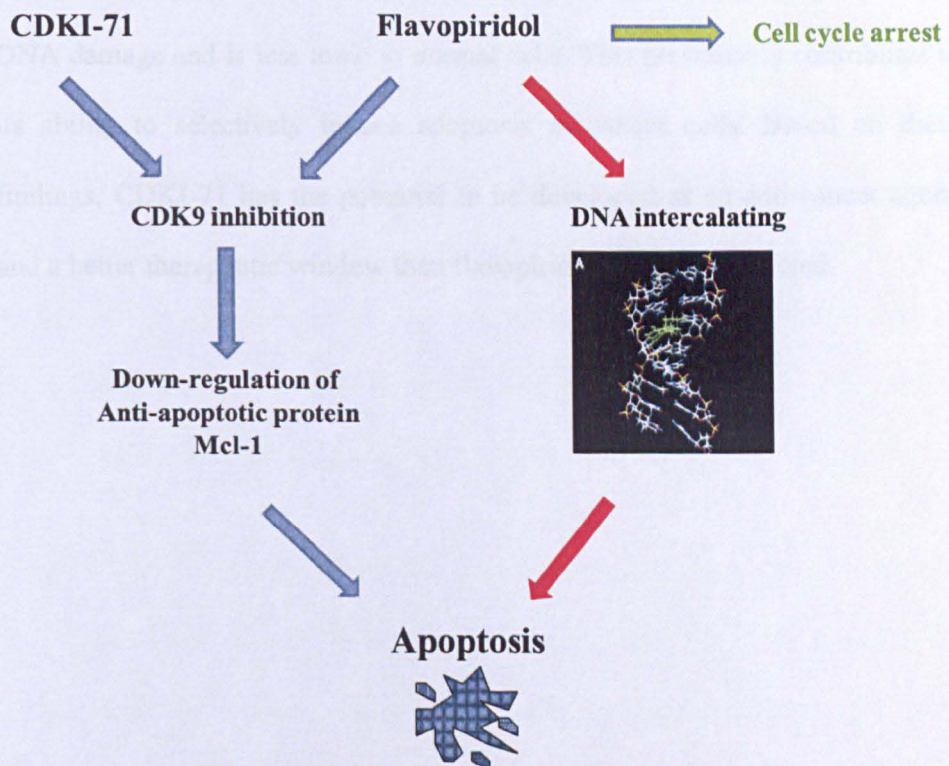


**Figure 4.15 Cellular model of action of CDKI-71 and flavopiridol.** Both CDKI-71 and flavopiridol are potent transcriptional CDK9 inhibitors. By reducing anti-apoptotic protein Mcl-1, they trigger apoptosis in cancer cells regardless of the p53 and Rb status. However, flavopiridol induces DNA double-strand breaks, which also can induce apoptosis in cancer or

non-transformed cells. The apoptosis induced by CDKI-71 is not related to cell cycle effects. In contrast, flavopiridol causes G2/M.

## **4.10 Conclusion**

In this section, it has been demonstrated that by inhibiting CDK9 regulated RNAPII transcription, CDKI-71 reduces anti-apoptotic protein Mcl-1 and thereby renders cells sensitive to apoptosis, which is caspase-dependent but p53-independent. This comparative study also shows similar CDKI-71 concentrations cause significant reduction in the levels of the anti-apoptotic protein Mcl-1 and MDM-2 in cancer cells, which is also observed after flavopiridol treatment. However, unlike flavopiridol, CDKI-71 does not induce DNA damage and is less toxic to normal cells. This presumably contributes to its ability to selectively induce apoptosis in cancer cells. Based on these findings, CDKI-71 has the potential to be developed as an anti-cancer agent, and a better therapeutic window than flavopiridol could be predicted.

# **Chapter Five: In vitro anti-tumour mechanism of a novel cyclin-dependent kinase inhibitor CDKI-83**

## **5.1 Introduction**

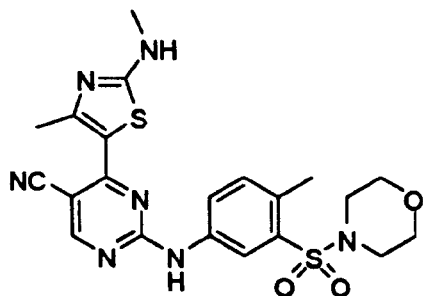
Targeting CDKs should counteract the unchecked proliferation of transformed cells by modulating the functions of CDKs in the regulation of the cell cycle. However, the conventional understanding of the roles of CDKs in the cell cycle regulation has been challenged (Cai et al., 2006b). Cancer cell lines and some embryonic fibroblasts lacking CDK2 proliferate normally and CDK2 knockout mice are viable, suggesting that CDK2 performs a nonessential role in cell cycle control (Barriere et al., 2007; Berthet et al., 2003). Furthermore, Mammalian cells without CDKs 4 and 6 enter the cell cycle normally (Malumbres et al., 2004). It has been demonstrated the catalytic activity of CDK1 is sufficient for cell-cycle progression (Santamaria et al., 2007).

Specific CDK1 depletion in some cancer cells results in accumulation of cells with G2/M DNA content, but causes only minimal cell death (Vassilev et al., 2006). It has been shown that the combined depletion of CDK9, CDK1 and CDK2 resulted in effective induction of apoptosis through both RNAPII CTD- and E2F mediated effects (Cai et al., 2006b).

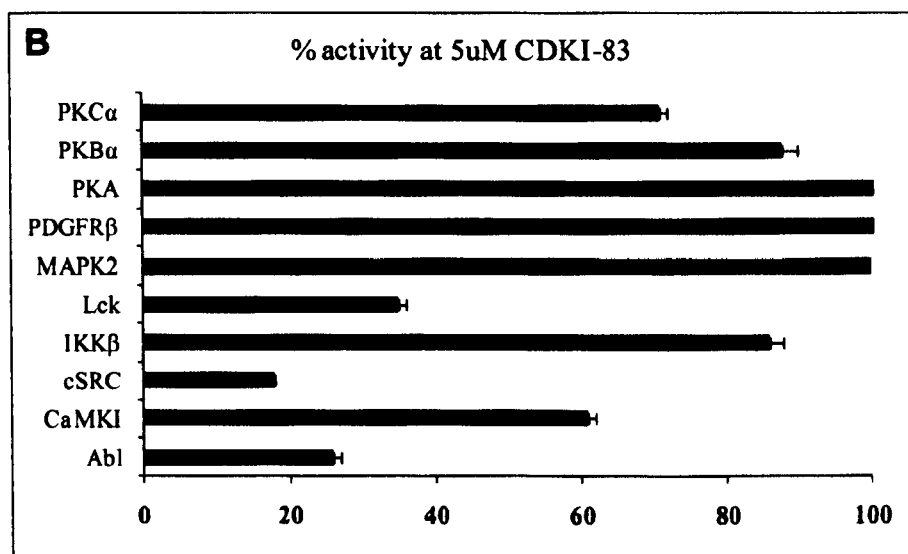
In an effort to discover novel CDK inhibitors, a class of 2,4,5-tri-substituted pyrimidines were identified using structure-guided and analogue design approaches in our group. A number of inhibitors exhibited anti-proliferative activity in human cancer cells. One of the lead compounds CDKI-83 was found to be a potent CDK inhibitor against CDK9 and CDK1 (Liu et al., 2011a).

## 5.2 CDKI-83 is a potent inhibitor of CDK9 and CDK1

The structure and inhibitory specificity of 4- (4-methyl-2-(methylamino)thiazol-5-yl)-2-(4-methyl-3-(morpholinosulfonyl)phenylamino)pyrimidine-5-carbonitrile (CDKI-83) is shown in **Figure 5.1**. CDKI-83 inhibited CDK9/T1 and CDK1/B potently with  $K_i$  values of 21 nM and 72 nM, respectively. This compound also targeted other CDKs but was less effective against CDK2/E, CDK4/D and CDK7/H with  $K_i$  values of 232, 290 and 405 nM, respectively. To determine the selectivity, CDKI-83 was also tested against a panel of non-CDK kinases (**Figure 5.1 B**) at 5  $\mu$ M. This compound was not active against protein kinase A, B, C, CaMKII, PDGF $\beta$  or MAPK, and showed low activity against Src, Lck and Abl.

**A**

Chemical Formula:  $C_{21}H_{23}N_7O_3S_2$   
 Molecular Weight: 485.6

**C**

Compound	Enzymatic assay $K_i$ nM				
	CDK9/T1	CDK7/H	CDK1/B	CDK2/E	CDK4/D3
CDKI-83	21	405	72	232	290

**Figure 5.1 Structure and in vitro kinase activity of CDKI-83.** A: chemical structure; B: Kinase activity after treatment with 5 $\mu$ M CDKI-83 as a percentage of untreated. C: Apparent inhibition constants ( $K_i$ ) of CDK inhibition. Kinase inhibition was measured by radiometric assay using the Millipore KinaseProfiler services.  $K_i$  values were calculated from  $IC_{50}$  values and the appropriate  $K_m$  (ATP) values for each kinase.

### 5.3 CDKI-83 is a potent anti-proliferative agent and an effective apoptotic inducer

The A2780 ovarian cancer cell line was used to investigate the cellular mechanism of action of CDKI-83. The anti-proliferative activity was measured using MTT assay after 24, 48 or 72 hours treatment (Figure 5.2). Sharp decreases in the growth inhibition curves were detected after 48 or 72 hours treatment with CDKI-83 between 0.1  $\mu\text{M}$  and 1  $\mu\text{M}$ . The  $\text{GI}_{50}$  values for 24, 48 or 72 hours treatment were  $0.97 \pm 0.06 \mu\text{M}$ ,  $0.46 \pm 0.02 \mu\text{M}$  and  $0.47 \pm 0.04 \mu\text{M}$ , respectively.

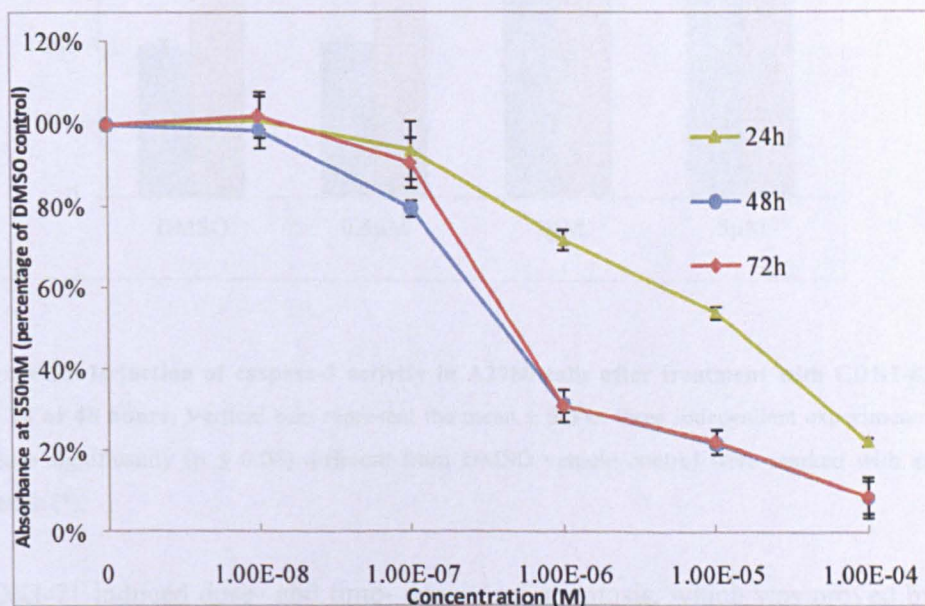
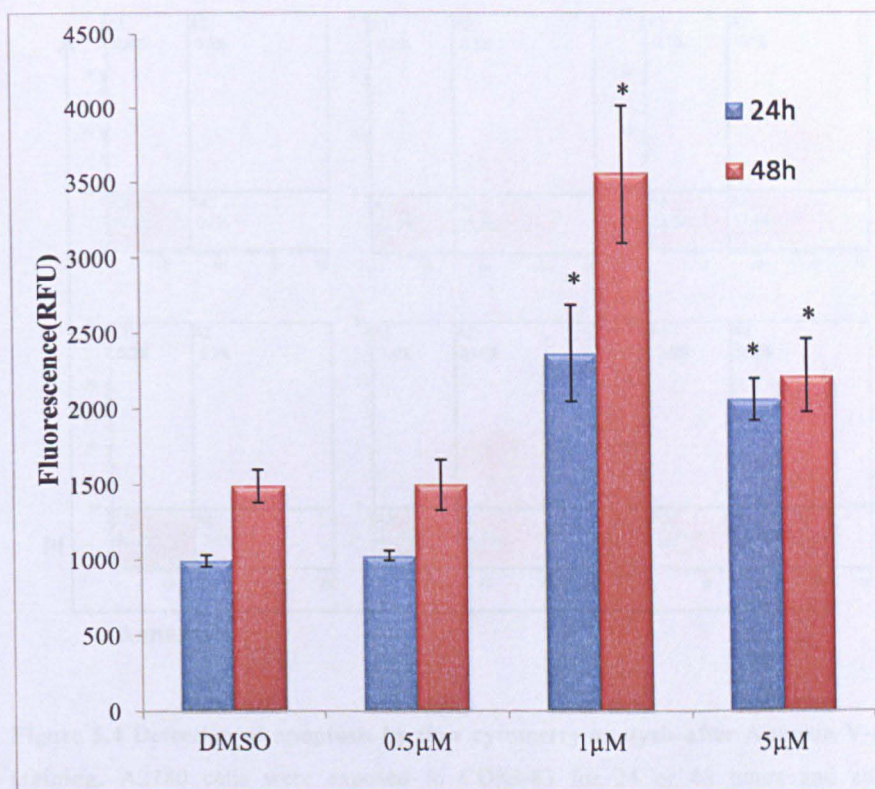


Figure 5.2 Growth inhibition curves of CDKI-83 for different treatment time points. A2780 cells were treated with CDKI-83 for a range of concentrations at 24h, 48h or 72h, respectively. Mean values and SD were obtained from 3 independent experiments.

Caspase-3 activity was measured in A2780 cells on treatment with CDKI-83 for 24 or 48 h to find out whether the anti-proliferative effect of CDKI-83 was

a consequence of induction of apoptosis. The caspase-3 activity was increased significantly after CDKI-83 treatment at 1  $\mu$ M or above, compared with DMSO vehicle control (**Figure 5.3**).



**Figure 5.3 Induction of caspase-3 activity in A2780 cells after treatment with CDKI-83 for 24 or 48 hours.** Vertical bars represent the mean  $\pm$  SD of three independent experiments. Values significantly ( $p \leq 0.05$ ) different from DMSO vehicle control were marked with an asterisk (\*).

CDKI-71 induced dose- and time- dependent apoptosis, which was proved by AnnexinV/PI double staining (**Figure 5.4**). Treatment of A2780 cells with 1  $\mu$ M CDKI-83 for 24 h resulted in 25% cells in early apoptosis and 6.3% in late apoptosis. On extending the treatment to 48 h the apoptotic cell population was significantly increased to 36.5% and 20.6% in early and late apoptosis,

respectively, while for the same time period 5  $\mu$ M CDKI-83 caused 76.9% cell death (48.1% and 38.8% in early and late apoptosis, respectively).

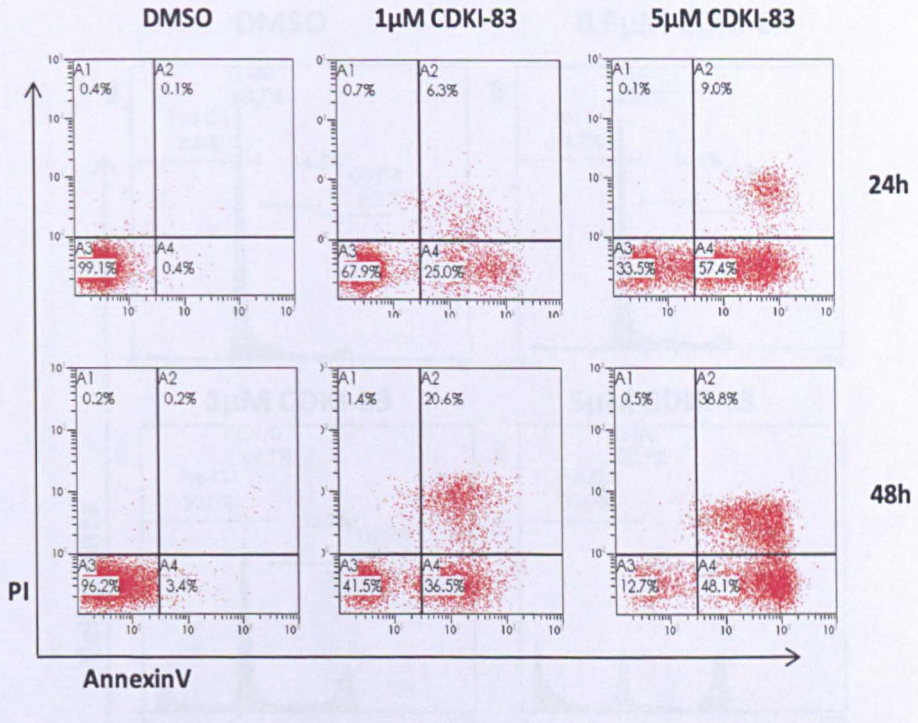


**Figure 5.4** Detection of apoptosis by flow cytometry analysis after Annexin V-PI double staining. A2780 cells were exposed to CDKI-83 for 24 or 48 hours and analysed by annexinV/PI stained DNA content.

These results obtained from CDKI-83 are consistent with those of CDKI-71, suggesting these two CDK inhibitors may have similar cellular mode of action (Liu et al., 2011a).

### 5.4 CDKI-83 induces cell arrest in G2 phase

As the only nonredundant cell cycle regulator, CDK1 plays key roles during late G2 and Mitosis (Nigg, 2001). CyclinB/CDK1 complex regulates late G2 and mitosis by phosphorylating substrates and facilitating G2/M transition.

Therefore, CDK1 inhibition would make cells incapable of initiating mitosis and should arrest cells at the G2/M border (Vassilev, 2006).

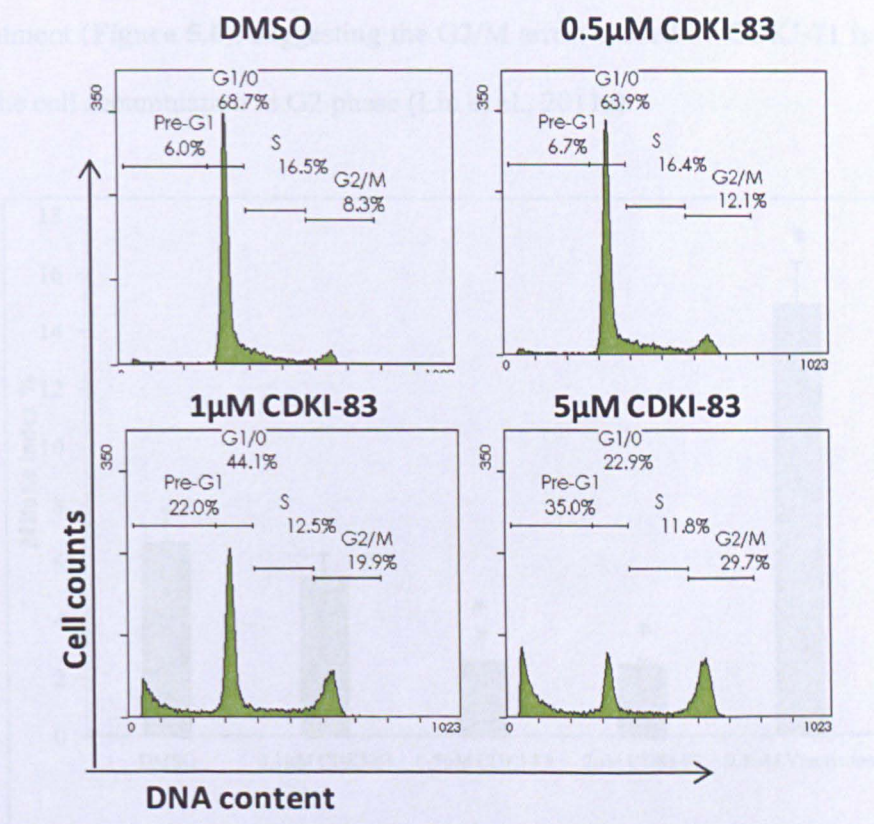


**Figure 5.5** Cell cycle effects in A2780 cells. A2780 Cells were treated with 0.5, 1 or 5µM CDKI-83 for 24 hours.

The effect of CDKI-83 on cell cycle progression was investigated by FACS. Human ovarian cancer A2780 cells were treated with CDKI-83 for 24 hours. Cell cycle analysis indicated that the treatment of A2780 cells with 0.5µM CDKI-83 slightly increased the number of G2/M cells comparing to DMSO treatment; 1µM CDKI-83 however resulted in significant accumulation of cells with G2/M DNA content (**Figure 5.5**). Increased population of cells containing sub-G1 amount of DNA was also observed, indicating that cell death was induced by the compound (Liu et al., 2011a).

Mitotic index assay was performed to identify whether CDKI-83 induced mitotic arrest. Vincristine, which is a mitotic inhibitor was used as a positive control. There was a decrease in mitotic index after 0.5 $\mu$ M or 2 $\mu$ M CDKI-83 treatment (**Figure 5.6**), suggesting the G2/M arrest caused by CDKI-71 is due to the cell accumulation in G2 phase (Liu et al., 2011a).

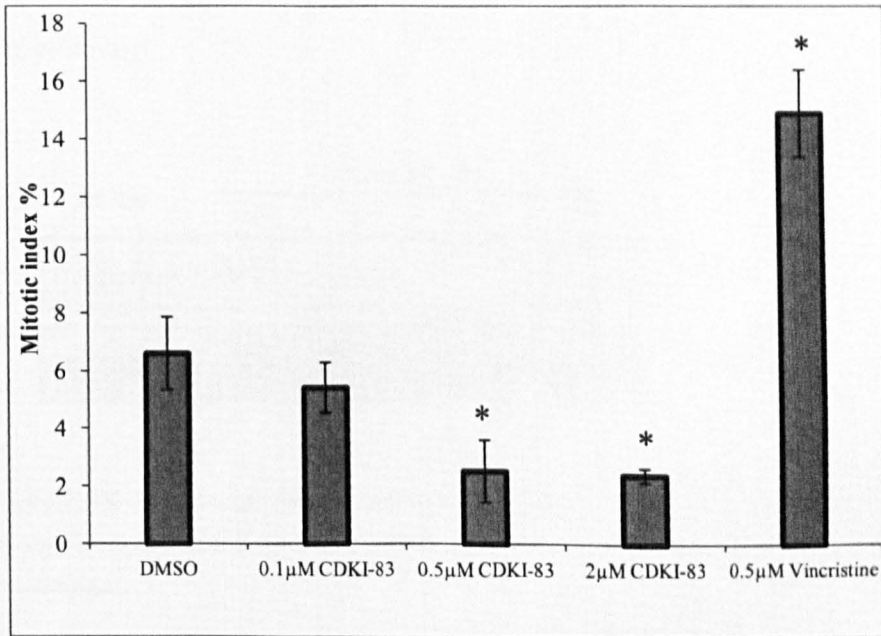


**Figure 5.6 Effect on Mitotic index in A2780 cells.** A2780 cells were treated with CDKI-83 for 7 hours and the percentages of cells in mitotic were measured. DMSO vehicle and 0.5 $\mu$ M vincristine were used as negative and positive controls respectively. Vertical bars represent the mean  $\pm$  SD of three independent experiments. Values significantly ( $p \leq 0.05$ ) different from DMSO vehicle control were marked with an asterisk (\*).

## 5.5 Cellular CDK1 inhibition of CDKI-83

During metaphase, PP1 $\alpha$  phosphatase, one of the substrates for CDK1 complex, is phosphorylated at Thr<sup>320</sup>. This phosphorylation inhibits PP1 $\alpha$  phosphatase

activity and increases phosphorylation of proteins critical in mitosis. CDKI-83 is shown to block the phosphorylation of PP-1 $\alpha$  at Thr<sup>320</sup> at  $\geq 1$   $\mu$ M concentrations (**Figure 5.7**), indicating cellular CDK1 inhibition (Liu et al., 2011a). In this experiment, inhibition of CDK1 was observed after 24h, which is the same period used in the previous cell cycle analysis. However a shorter treatment time (2h - 6h) would be better to detect the original effect on the cell cycle proteins.

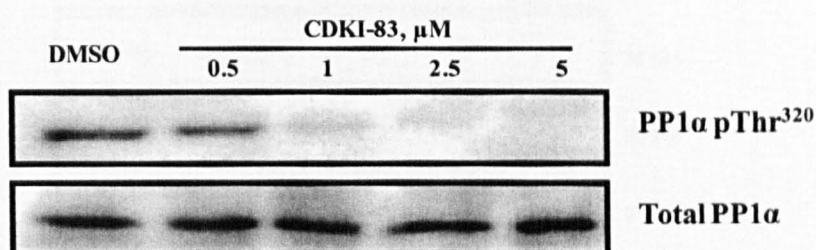
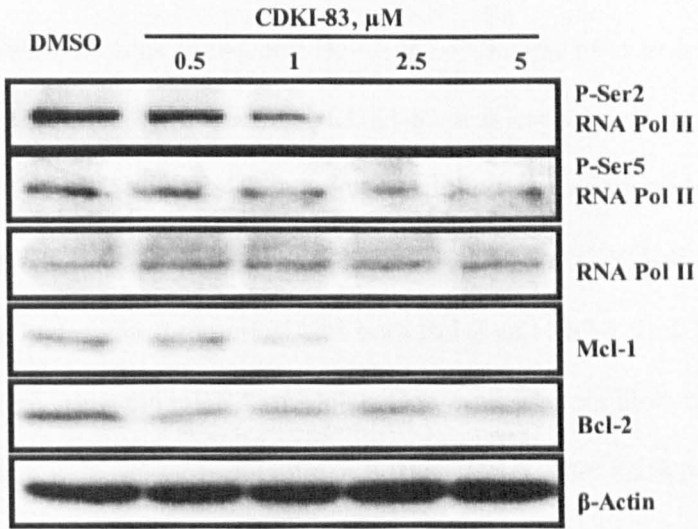


**Figure 5.7** Effect on the phosphorylation status of CDK1 substrate PP1 $\alpha$  at Thr<sup>320</sup>. A2780 cells were incubated with 0.5, 1, 2.5 or 5  $\mu$ M CDI-83 for 24 hours. Data are representative for 3 experiments.

## 5.6 CDKI-83 reduces both mRNA and protein level of Mcl-1 by targeting CDK9

The ability of CDKI-83 to inhibit cellular transcriptional CDK9/CDK7 activity was determined by measuring the phosphorylated Ser-2/Ser-5 of RNAPII CTD in A2780 cells. After 24 hours treatment, the phosphorylation of ser-2 was significantly reduced from 1 $\mu$ M and completely inhibited by 2.5  $\mu$ M (**Figure 5.8 A**). However, little effect was observed on the phosphorylation of Ser-5 and total RNA polymerase II, indicating CDKI-83 targeted the transcription by CDK9, but not CDK7.

A



B

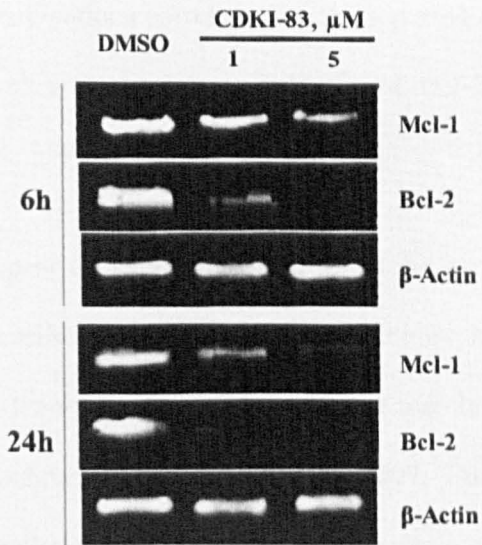


**Figure 5.8 Inhibition of CDK9 and reduction of survival factors in A2780 cells.** A: Cells were analysed by Western blot after 24h treatment with CDK-83 at the concentrations indicated. B: Effect on the levels of mRNAs determined by RT-PCR following treatment with

1 or 5  $\mu$ M CDKI-83 for 6 or 24 hours. DMSO vehicle was used for comparison and  $\beta$ -actin antibody was used as an internal control in each experiment.

We further investigated whether inhibition of CDK9 regulated RNAPII transcriptional reduced the levels of those mRNAs and proteins with rapid turnover rates, such as Mcl-1 and Bcl-2. RT-PCR was used to investigate the action of CDKI-83 on transcripts. CDKI-83 was capable of down-regulation the mRNA of Mcl-1 and Bcl-2 in a dose- and time-dependent manner as shown in **Figure 5.8 B**. Incubation of A2780 cells with 1 $\mu$ M CDKI-83 for 24 hours substantially decreased the mRNA of both Bcl-2 and Mcl-1. Bcl-2 mRNA was more affected than the mRNA of Mcl-1. However, western blots showed Mcl-1 protein was reduced more significantly than Bcl-1 after CDKI-83 treatment (**Figure 5.7 A**). This pattern corresponds to the effects of clinic CDK inhibitors flavopiridol and SNS-032, which have been shown to reduce the mRNA of Bcl-2, but are ineffective against its protein level (Chen et al., 2005),(Chen et al., 2009). These observations correlate with the reported short half-life of Bcl-2 mRNA (2.5–4 h) and the longer half-life of Bcl-2 protein (10–24 h) (Blagosklonny et al., 1996).

As tumour cells appear to be dependent on Mcl-1 for survival (Michels et al., 2005), it is an excellent target for CDK9 inhibitors and the induction of apoptosis. As Mcl-1 prevents mitochondrial outer membrane permeabilization (MOMP) and cytochrome c release (Danial, 2007; Danial and Korsmeyer, 2004), its downregulation by CDKI-83 may facilitate cytochrome c release from mitochondria and induce apoptosis through caspase activation.

## **5.7 Conclusion**

In order to cure complex disorders in cancer, absolute selectivity to one target might not be the best approach for cancer therapy. Combinations of targets rather than a single effect might yield better therapeutic agents (Knockaert et al., 2002). CDKI-83 is a nano-molar CDK1 and CDK9 inhibitor with potent anti-proliferative activity. This compound is capable of inducing apoptosis in cancer cells. By inhibiting cellular CDK1 and CDK9 activities, CDKI-83 arrests cells in G2 phase and reduces anti-apoptotic protein Mcl-1, respectively. This study suggests that the combination of CDK9 and CDK1 inhibition results in effective induction of apoptosis in A2780 cells and CDKI-83 has the potential to be further developed as a potent anti-cancer agent.

# Chapter Six

## General discussion and conclusion

The processes of hit-to-lead and preclinical candidate optimization often take a long time in the modern drug discovery program. Due to the high cost of compounds generated from structure-based approaches and high throughput screening (HTS), focused screen of compounds with similar structures to previously identified hits is widely used in academia. Hundreds of compounds designed to target diverse kinases, including CDK9, CDK7 and Plk1 have been synthesized by our group. In this project, a cell-based screening cascade was developed to classify compounds and identify effective transcription CDK (CDK7 and especially CDK9) inhibitors as lead candidates.

Compounds were first tested by the MTT assay and 46 compounds with  $GI_{50}$  values below 1  $\mu$ M were further screened using a caspase-3 activation assay and a p53 stabilization assay. Candidates for transcriptional CDK9 inhibitors were selected from compounds which showed high potency in the anti-proliferative assay and induced both caspase-3 activities and p53 levels at comparative concentrations. It was reported that the reduction of CDK9 level by siRNA had no significant effect on the cell cycle distribution (Cai et al., 2006a). In this screening cascade, a mitotic index assay was performed to evaluate cell cycle effect. Compounds S3-41 and CDKI-71 are the most potent CDK9 inhibitors identified. These two compounds showed comparative potency cross the MTT, caspase-3 activity and p53 stabilization assays at

concentrations below 0.5  $\mu\text{M}$  without significant effects on mitotic index, suggesting their anti-proliferative effect would be due to CDK9 inhibition. The kinase activity assay showed that our key compounds inhibited CDK9 at low nano-molar levels and proved the efficacy of the screening cascade.

Cancer cells depend heavily on expression of anti-apoptotic proteins for survival (Koumenis and Giaccia, 1997). Some of the anti-apoptotic proteins have short half lives at both mRNA and protein level and thus they need the continuous activity of RNA polymerase II. Inhibition of transcriptional CDKs, such as CDK9, represents an attractive strategy for cancer therapy. Mcl-1 has a very short half-life and its expression is highly sensitive to transcription. Down-regulation of Mcl-1 is often sufficient to promote apoptosis in cancer cells (Derenne et al., 2002). A novel small molecular CDK9 inhibitor CDKI-71 was identified using our screening cascade and the detailed cellular mechanism was investigated and compared with a clinical CDK inhibitor, flavopiridol (Liu et al., 2011b).

Through inhibition of RNAPII phosphorylation at Ser-2, CDKI-71 and flavopiridol decreased anti-apoptotic protein Mcl-1 and induced caspase-dependent apoptosis in cancer cells. Similar results were reported for other CDK9 inhibitors, including SNS-032 (Chen et al., 2009). The majority of mRNAs that were changed in the microarray after CDKI-71 or flavopiridol treatment were down-regulated, including genes encoding transcription and transcription regulation. Since flavopiridol inhibits transcription globally in a similar way to actinomycin D and DRB (Lam et al., 2001), the microarray results suggested that CDKI-71 was also a transcription inhibitor. Importantly,

non-transformed lung fibroblast cell lines showed resistance to CDKI-71 treatment. However, flavopiridol presented little selectivity between the cancer and normal cells. The first cell-based evidence that flavopiridol induces DNA double-strand breaks was provided in this study and that may explain why flavopiridol showed little selectivity. These results suggest that CDKI-71 has a great potential to be developed as an anti-cancer agent with a better therapeutic window compared to flavopiridol.

As the only essential cell cycle CDK, CDK1 regulates cell cycle progression via phosphorylation of several substrates and facilitates G2/M phase transition (Nigg, 2001). The in vitro anti-tumour mechanism of another CDK inhibitor CDKI-83 was also investigated (Liu et al., 2011a). CDKI-83 is a nano-molar CDK1 and CDK9 inhibitor with potent anti-proliferative activity. Similar to CDKI-71, this compound reduces anti-apoptotic protein Mcl-1 and is capable of inducing apoptosis in cancer cells. Unlike CDKI-71, CDKI-83 arrests cells in G2 phase by inhibiting cellular CDK1. This study suggests that the combination of CDK9 and CDK1 inhibition results in effective induction of apoptosis and may enhance the cytotoxic effect in cancer cells.

## References

- Adams, J.M., and Cory, S. (2007). The Bcl-2 apoptotic switch in cancer development and therapy. *Oncogene* 26, 1324-1337.
- Akgul, C. (2009). Mcl-1 is a potential therapeutic target in multiple types of cancer. *Cell Mol Life Sci* 66, 1326-1336.
- Alonso, M., Tamasdan, C., Miller, D.C., and Newcomb, E.W. (2003). Flavopiridol induces apoptosis in glioma cell lines independent of retinoblastoma and p53 tumor suppressor pathway alterations by a caspase-independent pathway. *Mol Cancer Ther* 2, 139-150.
- Alvi, A.J., Austen, B., Weston, V.J., Fegan, C., MacCallum, D., Gianella-Borradori, A., Lane, D.P., Hubank, M., Powell, J.E., Wei, W., *et al.* (2005). A novel CDK inhibitor, CYC202 (R-roscovitine), overcomes the defect in p53-dependent apoptosis in B-CLL by down-regulation of genes involved in transcription regulation and survival. *Blood* 105, 4484-4491.
- Anand, P., Kunnumakkara, A.B., Sundaram, C., Harikumar, K.B., Tharakan, S.T., Lai, O.S., Sung, B., and Aggarwal, B.B. (2008). Cancer is a preventable disease that requires major lifestyle changes. *Pharm Res* 25, 2097-2116.
- Babb, M.Q.a.P. (2000). Cancer trends in England and Wales, 1950–1999 (Office for National Statistics).
- Baeriswyl, V., and Christofori, G. (2009). The angiogenic switch in carcinogenesis. *Semin Cancer Biol* 19, 329-337.
- Barriere, C., Santamaria, D., Cerqueira, A., Galan, J., Martin, A., Ortega, S., Malumbres, M., Dubus, P., and Barbacid, M. (2007). Mice thrive without Cdk4 and Cdk2. *Mol Oncol* 1, 72-83.

- Bergers, G., and Benjamin, L.E. (2003). Tumorigenesis and the angiogenic switch. *Nat Rev Cancer* 3, 401-410.
- Berthet, C., Aleem, E., Coppola, V., Tessarollo, L., and Kaldis, P. (2003). Cdk2 knockout mice are viable. *Curr Biol* 13, 1775-1785.
- Bible, K.C., Bible, R.H., Jr., Kottke, T.J., Svingen, P.A., Xu, K., Pang, Y.P., Hajdu, E., and Kaufmann, S.H. (2000). Flavopiridol binds to duplex DNA. *Cancer Res* 60, 2419-2428.
- Blagosklonny, M.V., Alvarez, M., Fojo, A., and Neckers, L.M. (1996). bcl-2 protein downregulation is not required for differentiation of multidrug resistant HL60 leukemia cells. *Leuk Res* 20, 101-107.
- Blagosklonny, M.V., Demidenko, Z.N., and Fojo, T. (2002). Inhibition of transcription results in accumulation of Wt p53 followed by delayed outburst of p53-inducible proteins: p53 as a sensor of transcriptional integrity. *Cell Cycle* 1, 67-74.
- Blasco, M.A. (2005). Telomeres and human disease: ageing, cancer and beyond. *Nat Rev Genet* 6, 611-622.
- Bryan, T.M., and Cech, T.R. (1999). Telomerase and the maintenance of chromosome ends. *Curr Opin Cell Biol* 11, 318-324.
- Buchkovich, K., Duffy, L.A., and Harlow, E. (1989). The retinoblastoma protein is phosphorylated during specific phases of the cell cycle. *Cell* 58, 1097-1105.
- Burdette-Radoux, S., Tozer, R.G., Lohmann, R.C., Quirt, I., Ernst, D.S., Walsh, W., Wainman, N., Colevas, A.D., and Eisenhauer, E.A. (2004). Phase II trial of flavopiridol, a cyclin dependent kinase inhibitor, in untreated metastatic malignant melanoma. *Invest New Drugs* 22, 315-322.

- Burkhart, D.L., and Sage, J. (2008). Cellular mechanisms of tumour suppression by the retinoblastoma gene. *Nat Rev Cancer* 8, 671-682.
- Byrd, J.C., Shinn, C., Waselenko, J.K., Fuchs, E.J., Lehman, T.A., Nguyen, P.L., Flinn, I.W., Diehl, L.F., Sausville, E., and Grever, M.R. (1998). Flavopiridol induces apoptosis in chronic lymphocytic leukemia cells via activation of caspase-3 without evidence of bcl-2 modulation or dependence on functional p53. *Blood* 92, 3804-3816.
- Cai, D., Byth, K.F., and Shapiro, G.I. (2006a). AZ703, an imidazo[1,2-a]pyridine inhibitor of cyclin-dependent kinases 1 and 2, induces E2F-1-dependent apoptosis enhanced by depletion of cyclin-dependent kinase 9. *Cancer Res* 66, 435-444.
- Cai, D., Latham, V.M., Jr., Zhang, X., and Shapiro, G.I. (2006b). Combined depletion of cell cycle and transcriptional cyclin-dependent kinase activities induces apoptosis in cancer cells. *Cancer Res* 66, 9270-9280.
- Campisi, J. (2001). Cellular senescence as a tumor-suppressor mechanism. *Trends Cell Biol* 11, S27-31.
- Castanotto, D., and Rossi, J.J. (2009). The promises and pitfalls of RNA-interference-based therapeutics. *Nature* 457, 426-433.
- Cavallaro, U., and Christofori, G. (2004). Cell adhesion and signalling by cadherins and Ig-CAMs in cancer. *Nat Rev Cancer* 4, 118-132.
- Celeste, A., Petersen, S., Romanienko, P.J., Fernandez-Capetillo, O., Chen, H.T., Sedelnikova, O.A., Reina-San-Martin, B., Coppola, V., Meffre, E., Difilippantonio, M.J., *et al.* (2002). Genomic instability in mice lacking histone H2AX. *Science* 296, 922-927.

- Chen, C.Y., and Shyu, A.B. (1995). AU-rich elements: characterization and importance in mRNA degradation. *Trends Biochem Sci* 20, 465-470.
- Chen, R., Keating, M.J., Gandhi, V., and Plunkett, W. (2005). Transcription inhibition by flavopiridol: mechanism of chronic lymphocytic leukemia cell death. *Blood* 106, 2513-2519.
- Chen, R., Wierda, W.G., Chubb, S., Hawtin, R.E., Fox, J.A., Keating, M.J., Gandhi, V., and Plunkett, W. (2009). Mechanism of action of SNS-032, a novel cyclin-dependent kinase inhibitor, in chronic lymphocytic leukemia. *Blood* 113, 4637-4645.
- Cheng, N., Chytil, A., Shyr, Y., Joly, A., and Moses, H.L. (2008). Transforming growth factor-beta signaling-deficient fibroblasts enhance hepatocyte growth factor signaling in mammary carcinoma cells to promote scattering and invasion. *Mol Cancer Res* 6, 1521-1533.
- Cheng Y, P.W. (1973). Relationship between the inhibition constant ( $K_i$ ) and the concentration of inhibitor which causes 50 per cent inhibition ( $IC_{50}$ ) of an enzymatic reaction. *Biochem Pharmacol* 22, 3099-3108.
- Chipuk, J.E., and Green, D.R. (2005). Do inducers of apoptosis trigger caspase-independent cell death? *Nat Rev Mol Cell Biol* 6, 268-275.
- Classon, M., and Harlow, E. (2002). The retinoblastoma tumour suppressor in development and cancer. *Nat Rev Cancer* 2, 910-917.
- Counter, C.M., Avilion, A.A., LeFeuvre, C.E., Stewart, N.G., Greider, C.W., Harley, C.B., and Bacchetti, S. (1992). Telomere shortening associated with chromosome instability is arrested in immortal cells which express telomerase activity. *EMBO J* 11, 1921-1929.

Coverley, D., Laman, H., and Laskey, R.A. (2002). Distinct roles for cyclins E and A during DNA replication complex assembly and activation. *Nat Cell Biol* 4, 523-528.

D'Andrea, M.R., Mei, J.M., Tuman, R.W., Galembo, R.A., and Johnson, D.L. (2005). Validation of in vivo pharmacodynamic activity of a novel PDGF receptor tyrosine kinase inhibitor using immunohistochemistry and quantitative image analysis. *Mol Cancer Ther* 4, 1198-1204.

Dai, Y., and Grant, S. (2003). Cyclin-dependent kinase inhibitors. *Curr Opin Pharmacol* 3, 362-370.

Danial, N.N. (2007). BCL-2 family proteins: critical checkpoints of apoptotic cell death. *Clin Cancer Res* 13, 7254-7263.

Danial, N.N., and Korsmeyer, S.J. (2004). Cell death: critical control points. *Cell* 116, 205-219.

David, A.R., and Zimmerman, M.R. (2010). Cancer: an old disease, a new disease or something in between? *Nat Rev Cancer* 10, 728-733.

De Falco, G., Bagella, L., Claudio, P.P., De Luca, A., Fu, Y., Calabretta, B., Sala, A., and Giordano, A. (2000). Physical interaction between CDK9 and B-Myb results in suppression of B-Myb gene autoregulation. *Oncogene* 19, 373-379.

Demidenko, Z.N., and Blagosklonny, M.V. (2004). Flavopiridol induces p53 via initial inhibition of Mdm2 and p21 and, independently of p53, sensitizes apoptosis-reluctant cells to tumor necrosis factor. *Cancer Res* 64, 3653-3660.

Derenne, S., Monia, B., Dean, N.M., Taylor, J.K., Rapp, M.J., Harousseau, J.L., Bataille, R., and Amiot, M. (2002). Antisense strategy shows that Mcl-1 rather

than Bcl-2 or Bcl-x(L) is an essential survival protein of human myeloma cells. *Blood* *100*, 194-199.

Deshpande, A., Sicinski, P., and Hinds, P.W. (2005). Cyclins and cdks in development and cancer: a perspective. *Oncogene* *24*, 2909-2915.

Dimri, G.P., Lee, X., Basile, G., Acosta, M., Scott, G., Roskelley, C., Medrano, E.E., Linskens, M., Rubelj, I., Pereira-Smith, O., *et al.* (1995). A biomarker that identifies senescent human cells in culture and in aging skin in vivo. *Proc Natl Acad Sci U S A* *92*, 9363-9367.

Dispenzieri, A., Gertz, M.A., Lacy, M.Q., Geyer, S.M., Fitch, T.R., Fenton, R.G., Fonseca, R., Isham, C.R., Ziesmer, S.C., Erlichman, C., *et al.* (2006). Flavopiridol in patients with relapsed or refractory multiple myeloma: a phase 2 trial with clinical and pharmacodynamic end-points. *Haematologica* *91*, 390-393.

Dyson, N. (1998). The regulation of E2F by pRB-family proteins. *Genes Dev* *12*, 2245-2262.

Efeyan, A., Garcia-Cao, I., Herranz, D., Velasco-Miguel, S., and Serrano, M. (2006). Tumour biology: Policing of oncogene activity by p53. *Nature* *443*, 159.

Efeyan, A., and Serrano, M. (2007). p53: guardian of the genome and policeman of the oncogenes. *Cell Cycle* *6*, 1006-1010.

Ezhevsky, S.A., Ho, A., Becker-Hapak, M., Davis, P.K., and Dowdy, S.F. (2001). Differential regulation of retinoblastoma tumor suppressor protein by G(1) cyclin-dependent kinase complexes in vivo. *Mol Cell Biol* *21*, 4773-4784.

Finlay, C.A., Hinds, P.W., and Levine, A.J. (1989). The p53 proto-oncogene can act as a suppressor of transformation. *Cell* *57*, 1083-1093.

Gojo, I., Zhang, B., and Fenton, R.G. (2002). The cyclin-dependent kinase inhibitor flavopiridol induces apoptosis in multiple myeloma cells through transcriptional repression and down-regulation of Mcl-1. *Clin Cancer Res* 8, 3527-3538.

Gomes, N.P., Bjerke, G., Llorente, B., Szostek, S.A., Emerson, B.M., and Espinosa, J.M. (2006). Gene-specific requirement for P-TEFb activity and RNA polymerase II phosphorylation within the p53 transcriptional program. *Genes Dev* 20, 601-612.

Goodrich, D.W., Wang, N.P., Qian, Y.W., Lee, E.Y., and Lee, W.H. (1991). The retinoblastoma gene product regulates progression through the G1 phase of the cell cycle. *Cell* 67, 293-302.

Grana, X., De Luca, A., Sang, N., Fu, Y., Claudio, P.P., Rosenblatt, J., Morgan, D.O., and Giordano, A. (1994). PITALRE, a nuclear CDC2-related protein kinase that phosphorylates the retinoblastoma protein in vitro. *Proc Natl Acad Sci U S A* 91, 3834-3838.

Grendys, E.C., Jr., Blessing, J.A., Burger, R., and Hoffman, J. (2005). A phase II evaluation of flavopiridol as second-line chemotherapy of endometrial carcinoma: a Gynecologic Oncology Group study. *Gynecol Oncol* 98, 249-253.

Grivennikov, S.I., Greten, F.R., and Karin, M. (2010). Immunity, inflammation, and cancer. *Cell* 140, 883-899.

Gumireddy, K., Reddy, M.V., Cosenza, S.C., Boominathan, R., Baker, S.J., Papathi, N., Jiang, J., Holland, J., and Reddy, E.P. (2005). ON01910, a non-ATP-competitive small molecule inhibitor of Plk1, is a potent anticancer agent. *Cancer Cell* 7, 275-286.

Hahn, W.C., and Weinberg, R.A. (2002). Modelling the molecular circuitry of cancer. *Nat Rev Cancer* 2, 331-341.

Hahntow, I.N., Schneller, F., Oelsner, M., Weick, K., Ringshausen, I., Fend, F., Peschel, C., and Decker, T. (2004). Cyclin-dependent kinase inhibitor Roscovitine induces apoptosis in chronic lymphocytic leukemia cells. *Leukemia* 18, 747-755.

Han, E.S., Muller, F.L., Perez, V.I., Qi, W., Liang, H., Xi, L., Fu, C., Doyle, E., Hickey, M., Cornell, J., *et al.* (2008). The in vivo gene expression signature of oxidative stress. *Physiol Genomics* 34, 112-126.

Hanahan, D., and Weinberg, R.A. (2000). The hallmarks of cancer. *Cell* 100, 57-70.

Hanahan, D., and Weinberg, R.A. (2011). Hallmarks of cancer: the next generation. *Cell* 144, 646-674.

Heath, E.I., Bible, K., Martell, R.E., Adelman, D.C., and Lorusso, P.M. (2008). A phase 1 study of SNS-032 (formerly BMS-387032), a potent inhibitor of cyclin-dependent kinases 2, 7 and 9 administered as a single oral dose and weekly infusion in patients with metastatic refractory solid tumors. *Invest New Drugs* 26, 59-65.

Henning SW, B.G. (2002). Loss-of-function strategies in drug target validation. *Curr Drug Discov*, 17-21.

Herrera, R.E., Sah, V.P., Williams, B.O., Makela, T.P., Weinberg, R.A., and Jacks, T. (1996). Altered cell cycle kinetics, gene expression, and G1 restriction point regulation in Rb-deficient fibroblasts. *Mol Cell Biol* 16, 2402-2407.

- Hosack, D.A., Dennis, G., Jr., Sherman, B.T., Lane, H.C., and Lempicki, R.A. (2003). Identifying biological themes within lists of genes with EASE. *Genome Biol* 4, R70.
- Hu, B., Mitra, J., van den Heuvel, S., and Enders, G.H. (2001). S and G2 phase roles for Cdk2 revealed by inducible expression of a dominant-negative mutant in human cells. *Mol Cell Biol* 21, 2755-2766.
- Huang, H.J., Yee, J.K., Shew, J.Y., Chen, P.L., Bookstein, R., Friedmann, T., Lee, E.Y., and Lee, W.H. (1988). Suppression of the neoplastic phenotype by replacement of the RB gene in human cancer cells. *Science* 242, 1563-1566.
- Hughes, J.P., Rees, S., Kalindjian, S.B., and Philpott, K.L. (2011). Principles of early drug discovery. *Br J Pharmacol* 162, 1239-1249.
- Iwakuma, T., and Lozano, G. (2007). Crippling p53 activities via knock-in mutations in mouse models. *Oncogene* 26, 2177-2184.
- Jacks, T., Fazeli, A., Schmitt, E.M., Bronson, R.T., Goodell, M.A., and Weinberg, R.A. (1992). Effects of an Rb mutation in the mouse. *Nature* 359, 295-300.
- Jacks, T., Remington, L., Williams, B.O., Schmitt, E.M., Halachmi, S., Bronson, R.T., and Weinberg, R.A. (1994). Tumor spectrum analysis in p53-mutant mice. *Curr Biol* 4, 1-7.
- Jacobs, J.P., Jones, C.M., and Baille, J.P. (1970). Characteristics of a human diploid cell designated MRC-5. *Nature* 227, 168-170.
- Jans, D.A., and Hubner, S. (1996). Regulation of protein transport to the nucleus: central role of phosphorylation. *Physiol Rev* 76, 651-685.
- Kepp, O., Galluzzi, L., Lipinski, M., Yuan, J., and Kroemer, G. (2011). Cell death assays for drug discovery. *Nat Rev Drug Discov* 10, 221-237.

- Knockaert, M., Greengard, P., and Meijer, L. (2002). Pharmacological inhibitors of cyclin-dependent kinases. *Trends Pharmacol Sci* 23, 417-425.
- Konstantinidou, A.E., Givalos, N., Gakiopoulou, H., Korkolopoulou, P., Kotsiakis, X., Boviatsis, E., Agrogiannis, G., Mahera, H., and Patsouris, E. (2007). Caspase-3 immunohistochemical expression is a marker of apoptosis, increased grade and early recurrence in intracranial meningiomas. *Apoptosis* 12, 695-705.
- Koumenis, C., and Giaccia, A. (1997). Transformed cells require continuous activity of RNA polymerase II to resist oncogene-induced apoptosis. *Mol Cell Biol* 17, 7306-7316.
- Kroemer, G., and Martin, S.J. (2005). Caspase-independent cell death. *Nat Med* 11, 725-730.
- Kruse, J.P., and Gu, W. (2009). Modes of p53 regulation. *Cell* 137, 609-622.
- Lam, F.F.-K. (2010). Discovery and evaluation of anti-cancer agents. In *School of Pharmacy (Nottingham, University of Nottingham)*.
- Lam, L.T., Pickeral, O.K., Peng, A.C., Rosenwald, A., Hurt, E.M., Giltncane, J.M., Averett, L.M., Zhao, H., Davis, R.E., Sathyamoorthy, M., *et al.* (2001). Genomic-scale measurement of mRNA turnover and the mechanisms of action of the anti-cancer drug flavopiridol. *Genome Biol* 2, RESEARCH0041.
- Lane, D.P., and Crawford, L.V. (1979). T antigen is bound to a host protein in SV40-transformed cells. *Nature* 278, 261-263.
- Lapenna, S., and Giordano, A. (2009). Cell cycle kinases as therapeutic targets for cancer. *Nat Rev Drug Discov* 8, 547-566.
- Lessene, G., Czabotar, P.E., and Colman, P.M. (2008). BCL-2 family antagonists for cancer therapy. *Nat Rev Drug Discov* 7, 989-1000.

Lichtenstein, P., Holm, N.V., Verkasalo, P.K., Iliadou, A., Kaprio, J., Koskenvuo, M., Pukkala, E., Skytthe, A., and Hemminki, K. (2000). Environmental and heritable factors in the causation of cancer--analyses of cohorts of twins from Sweden, Denmark, and Finland. *N Engl J Med* 343, 78-85.

Linzer, D.I., and Levine, A.J. (1979). Characterization of a 54K dalton cellular SV40 tumor antigen present in SV40-transformed cells and uninfected embryonal carcinoma cells. *Cell* 17, 43-52.

Liu, X., Lam, F., Shi, S., Fischer, P.M., and Wang, S. (2011a). In vitro antitumor mechanism of a novel cyclin-dependent kinase inhibitor CDKI-83. *Invest New Drugs*.

Liu, X., Shi, S., Lam, F., Pepper, C., Fischer, P.M., and Wang, S. CDKI-71, a novel CDK9 inhibitor, is preferentially cytotoxic to cancer cells when compared with flavopiridol. *Int J Cancer*.

Liu, X., Shi, S., Lam, F., Pepper, C., Fischer, P.M., and Wang, S. (2011b). CDKI-71, a novel CDK9 inhibitor, is preferentially cytotoxic to cancer cells compared to flavopiridol. *Int J Cancer*.

Loeb, K.R., and Loeb, L.A. (2000). Significance of multiple mutations in cancer. *Carcinogenesis* 21, 379-385.

Lu, X., Burgan, W.E., Cerra, M.A., Chuang, E.Y., Tsai, M.H., Tofilon, P.J., and Camphausen, K. (2004). Transcriptional signature of flavopiridol-induced tumor cell death. *Mol Cancer Ther* 3, 861-872.

Lukas, C., Sorensen, C.S., Kramer, E., Santoni-Rugiu, E., Lindeneg, C., Peters, J.M., Bartek, J., and Lukas, J. (1999). Accumulation of cyclin B1 requires E2F

and cyclin-A-dependent rearrangement of the anaphase-promoting complex. *Nature* *401*, 815-818.

MacCallum, D.E., Melville, J., Frame, S., Watt, K., Anderson, S., Gianella-Borradori, A., Lane, D.P., and Green, S.R. (2005). Seliciclib (CYC202, R-Roscovitin) induces cell death in multiple myeloma cells by inhibition of RNA polymerase II-dependent transcription and down-regulation of Mcl-1. *Cancer Res* *65*, 5399-5407.

Malumbres, M., and Barbacid, M. (2001). To cycle or not to cycle: a critical decision in cancer. *Nat Rev Cancer* *1*, 222-231.

Malumbres, M., and Barbacid, M. (2009). Cell cycle, CDKs and cancer: a changing paradigm. *Nat Rev Cancer* *9*, 153-166.

Malumbres, M., Pevarello, P., Barbacid, M., and Bischoff, J.R. (2008). CDK inhibitors in cancer therapy: what is next? *Trends Pharmacol Sci* *29*, 16-21.

Malumbres, M., Sotillo, R., Santamaria, D., Galan, J., Cerezo, A., Ortega, S., Dubus, P., and Barbacid, M. (2004). Mammalian cells cycle without the D-type cyclin-dependent kinases Cdk4 and Cdk6. *Cell* *118*, 493-504.

Marine, J.C., Francoz, S., Maetens, M., Wahl, G., Toledo, F., and Lozano, G. (2006). Keeping p53 in check: essential and synergistic functions of Mdm2 and Mdm4. *Cell Death Differ* *13*, 927-934.

Marine, J.C., and Lozano, G. (2010). Mdm2-mediated ubiquitylation: p53 and beyond. *Cell Death Differ* *17*, 93-102.

Marshall, R.M., and Grana, X. (2006). Mechanisms controlling CDK9 activity. *Front Biosci* *11*, 2598-2613.

McClue, S.J., Blake, D., Clarke, R., Cowan, A., Cummings, L., Fischer, P.M., MacKenzie, M., Melville, J., Stewart, K., Wang, S., *et al.* (2002). In vitro and

in vivo antitumor properties of the cyclin dependent kinase inhibitor CYC202 (R-roscovitine). *Int J Cancer* *102*, 463-468.

Michels, J., Johnson, P.W., and Packham, G. (2005). Mcl-1. *Int J Biochem Cell Biol* *37*, 267-271.

Misra, R.N., Xiao, H.Y., Kim, K.S., Lu, S., Han, W.C., Barbosa, S.A., Hunt, J.T., Rawlins, D.B., Shan, W., Ahmed, S.Z., *et al.* (2004). N-(cycloalkylamino)acyl-2-aminothiazole inhibitors of cyclin-dependent kinase 2. N-[5-[[[5-(1,1-dimethylethyl)-2-oxazolyl]methyl]thio]-2-thiazolyl]-4-piperidinecarboxamide (BMS-387032), a highly efficacious and selective antitumor agent. *J Med Chem* *47*, 1719-1728.

Montes de Oca Luna, R., Wagner, D.S., and Lozano, G. (1995). Rescue of early embryonic lethality in mdm2-deficient mice by deletion of p53. *Nature* *378*, 203-206.

Mulligan, G., and Jacks, T. (1998). The retinoblastoma gene family: cousins with overlapping interests. *Trends Genet* *14*, 223-229.

Nakano, K., and Vousden, K.H. (2001). PUMA, a novel proapoptotic gene, is induced by p53. *Mol Cell* *7*, 683-694.

Neidle, S. (2008). *Cancer drug design and discovery*.

Nigg, E.A. (2001). Mitotic kinases as regulators of cell division and its checkpoints. *Nat Rev Mol Cell Biol* *2*, 21-32.

Okada, H., and Mak, T.W. (2004). Pathways of apoptotic and non-apoptotic death in tumour cells. *Nat Rev Cancer* *4*, 592-603.

Ortega, S., Prieto, I., Odajima, J., Martin, A., Dubus, P., Sotillo, R., Barbero, J.L., Malumbres, M., and Barbacid, M. (2003). Cyclin-dependent kinase 2 is

essential for meiosis but not for mitotic cell division in mice. *Nat Genet* 35, 25-31.

Palmero, I., Pantoja, C., and Serrano, M. (1998). p19ARF links the tumour suppressor p53 to Ras. *Nature* 395, 125-126.

Parant, J., Chavez-Reyes, A., Little, N.A., Yan, W., Reinke, V., Jochemsen, A.G., and Lozano, G. (2001). Rescue of embryonic lethality in Mdm4-null mice by loss of Trp53 suggests a nonoverlapping pathway with MDM2 to regulate p53. *Nat Genet* 29, 92-95.

Paull, K.D., Shoemaker, R.H., Hodes, L., Monks, A., Scudiero, D.A., Rubinstein, L., Plowman, J., and Boyd, M.R. (1989). Display and analysis of patterns of differential activity of drugs against human tumor cell lines: development of mean graph and COMPARE algorithm. *J Natl Cancer Inst* 81, 1088-1092.

Paull, T.T., Rogakou, E.P., Yamazaki, V., Kirchgessner, C.U., Gellert, M., and Bonner, W.M. (2000). A critical role for histone H2AX in recruitment of repair factors to nuclear foci after DNA damage. *Curr Biol* 10, 886-895.

Phelps, M.A., Lin, T.S., Johnson, A.J., Hurh, E., Rozewski, D.M., Farley, K.L., Wu, D., Blum, K.A., Fischer, B., Mitchell, S.M., *et al.* (2009). Clinical response and pharmacokinetics from a phase 1 study of an active dosing schedule of flavopiridol in relapsed chronic lymphocytic leukemia. *Blood* 113, 2637-2645.

Piette, J., Neel, H., and Marechal, V. (1997). Mdm2: keeping p53 under control. *Oncogene* 15, 1001-1010.

Polier, G., Ding, J., Konkimalla, B.V., Eick, D., Ribeiro, N., Kohler, R., Giaisi, M., Efferth, T., Desaubry, L., Krammer, P.H., *et al.* (2011). Wogonin and

related natural flavones are inhibitors of CDK9 that induce apoptosis in cancer cells by transcriptional suppression of Mcl-1. *Cell Death Dis* 2, e182.

Rechsteiner, M., and Rogers, S.W. (1996). PEST sequences and regulation by proteolysis. *Trends Biochem Sci* 21, 267-271.

Reed, J.C., Tsujimoto, Y., Alpers, J.D., Croce, C.M., and Nowell, P.C. (1987). Regulation of bcl-2 proto-oncogene expression during normal human lymphocyte proliferation. *Science* 236, 1295-1299.

Rizzolio, F., Tuccinardi, T., Caligiuri, I., Lucchetti, C., and Giordano, A. (2010). CDK inhibitors: from the bench to clinical trials. *Curr Drug Targets* 11, 279-290.

Rogers, S., Wells, R., and Rechsteiner, M. (1986). Amino acid sequences common to rapidly degraded proteins: the PEST hypothesis. *Science* 234, 364-368.

Rong, Y., and Distelhorst, C.W. (2008). Bcl-2 protein family members: versatile regulators of calcium signaling in cell survival and apoptosis. *Annu Rev Physiol* 70, 73-91.

Sage, J., Miller, A.L., Perez-Mancera, P.A., Wysocki, J.M., and Jacks, T. (2003). Acute mutation of retinoblastoma gene function is sufficient for cell cycle re-entry. *Nature* 424, 223-228.

Santamaria, D., Barriere, C., Cerqueira, A., Hunt, S., Tardy, C., Newton, K., Caceres, J.F., Dubus, P., Malumbres, M., and Barbacid, M. (2007). Cdk1 is sufficient to drive the mammalian cell cycle. *Nature* 448, 811-815.

Schiavone, N., Rosini, P., Quattrone, A., Donnini, M., Lapucci, A., Citti, L., Bevilacqua, A., Nicolin, A., and Capaccioli, S. (2000). A conserved AU-rich element in the 3' untranslated region of bcl-2 mRNA is endowed with a

destabilizing function that is involved in bcl-2 down-regulation during apoptosis. *FASEB J* 14, 174-184.

Shapiro, G.I. (2006). Cyclin-dependent kinase pathways as targets for cancer treatment. *J Clin Oncol* 24, 1770-1783.

Sherr, C.J., and Roberts, J.M. (1999). CDK inhibitors: positive and negative regulators of G1-phase progression. *Genes Dev* 13, 1501-1512.

Shoemaker, R.H. (2006). The NCI60 human tumour cell line anticancer drug screen. *Nat Rev Cancer* 6, 813-823.

Smith, M.E., Cimica, V., Chinni, S., Challagulla, K., Mani, S., and Kalpana, G.V. (2008). Rhabdoid tumor growth is inhibited by flavopiridol. *Clin Cancer Res* 14, 523-532.

Sporn, M.B. (1996). The war on cancer. *Lancet* 347, 1377-1381.

Stein, G.H., Drullinger, L.F., Soulard, A., and Dulic, V. (1999). Differential roles for cyclin-dependent kinase inhibitors p21 and p16 in the mechanisms of senescence and differentiation in human fibroblasts. *Mol Cell Biol* 19, 2109-2117.

Stott, F.J., Bates, S., James, M.C., McConnell, B.B., Starborg, M., Brookes, S., Palmero, I., Ryan, K., Hara, E., Vousden, K.H., *et al.* (1998). The alternative product from the human CDKN2A locus, p14(ARF), participates in a regulatory feedback loop with p53 and MDM2. *EMBO J* 17, 5001-5014.

Stromhaug, P.E., and Klionsky, D.J. (2001). Approaching the molecular mechanism of autophagy. *Traffic* 2, 524-531.

Sumara, I., Gimenez-Abian, J.F., Gerlich, D., Hirota, T., Kraft, C., de la Torre, C., Ellenberg, J., and Peters, J.M. (2004). Roles of polo-like kinase 1 in the assembly of functional mitotic spindles. *Curr Biol* 14, 1712-1722.

Talks, A. (2008). Molecular biologist Elizabeth Blackburn.

Thurston, D.E. (2006). Chemistry and pharmacology of anticancer drugs.

Toledo, F., and Wahl, G.M. (2006). Regulating the p53 pathway: in vitro hypotheses, in vivo veritas. *Nat Rev Cancer* 6, 909-923.

Toogood, P.L., Harvey, P.J., Repine, J.T., Sheehan, D.J., VanderWel, S.N., Zhou, H., Keller, P.R., McNamara, D.J., Sherry, D., Zhu, T., *et al.* (2005). Discovery of a potent and selective inhibitor of cyclin-dependent kinase 4/6. *J Med Chem* 48, 2388-2406.

Vassilev, L.T. (2006). Cell cycle synchronization at the G2/M phase border by reversible inhibition of CDK1. *Cell Cycle* 5, 2555-2556.

Vassilev, L.T., Tovar, C., Chen, S., Knezevic, D., Zhao, X., Sun, H., Heimbrook, D.C., and Chen, L. (2006). Selective small-molecule inhibitor reveals critical mitotic functions of human CDK1. *Proc Natl Acad Sci U S A* 103, 10660-10665.

Vogelstein, B., Lane, D., and Levine, A.J. (2000). Surfing the p53 network. *Nature* 408, 307-310.

Vousden, K.H., and Lu, X. (2002). Live or let die: the cell's response to p53. *Nat Rev Cancer* 2, 594-604.

Walker, T.K.B.a.A.K. (2006). Transcription mechanisms (WormBook, ed. The *C. elegans* Research Community, WormBook).

Wang, S., and Fischer, P.M. (2008). Cyclin-dependent kinase 9: a key transcriptional regulator and potential drug target in oncology, virology and cardiology. *Trends Pharmacol Sci* 29, 302-313.

Wang, S., Griffiths, G., Midgley, C.A., Barnett, A.L., Cooper, M., Grabarek, J., Ingram, L., Jackson, W., Kontopidis, G., McClue, S.J., *et al.* (2010). Discovery

and characterization of 2-anilino-4- (thiazol-5-yl)pyrimidine transcriptional CDK inhibitors as anticancer agents. *Chem Biol* 17, 1111-1121.

Wang, S., Meades, C., Wood, G., Osnowski, A., Anderson, S., Yuill, R., Thomas, M., Mezna, M., Jackson, W., Midgley, C., *et al.* (2004). 2-Anilino-4-(thiazol-5-yl)pyrimidine CDK inhibitors: synthesis, SAR analysis, X-ray crystallography, and biological activity. *J Med Chem* 47, 1662-1675.

Weinberg, R.A. (1995). The retinoblastoma protein and cell cycle control. *Cell* 81, 323-330.

Weinberg, R.A. (2007). *The Biology of Cancer* (Garland Science).

Weintraub, S.J., Chow, K.N., Luo, R.X., Zhang, S.H., He, S., and Dean, D.C. (1995). Mechanism of active transcriptional repression by the retinoblastoma protein. *Nature* 375, 812-815.

Willis, S.N., Fletcher, J.I., Kaufmann, T., van Delft, M.F., Chen, L., Czabotar, P.E., Ierino, H., Lee, E.F., Fairlie, W.D., Bouillet, P., *et al.* (2007). Apoptosis initiated when BH3 ligands engage multiple Bcl-2 homologs, not Bax or Bak. *Science* 315, 856-859.

Zaharevitz, D.W., Holbeck, S.L., Bowerman, C., and Svetlik, P.A. (2002). COMPARE: a web accessible tool for investigating mechanisms of cell growth inhibition. *J Mol Graph Model* 20, 297-303.

Zhang, J., Yang, P.L., and Gray, N.S. (2009). Targeting cancer with small molecule kinase inhibitors. *Nat Rev Cancer* 9, 28-39.

# Appendix One

## Log2 values in the fold changes of the expression of the genes

Accession Number	log <sub>2</sub> CDKI-71	log <sub>2</sub> flavopiridol	Gene name
AB037730	-1.19	-1.46	kelch-like 13 (Drosophila)
AB037732	-1.42	-0.91	RNA binding motif protein 27
AB037780	-1.06	-1.15	mucin 20, cell surface associated
AC004889	-1.09	-0.72	olfactory receptor, family 2, subfamily AO, member 1 pseudogene
AC008737	-1.11	-0.50	C3 and PZP-like, alpha-2-macroglobulin domain containing 8
AC008934	1.16	0.30	phosphodiesterase 4D, cAMP-specific (phosphodiesterase E3 dunce homolog, Drosophila)
AC009970	-1.46	-0.84	hypothetical protein LOC100286932
AC012074	-1.26	-1.16	dystrobrevin, beta
AC018988	-1.24	-0.97	adaptor-related protein complex 3, sigma 2 subunit
AC021909	1.34	-0.07	neuregulin 1
AC022215	1.30	-0.54	ribosomal protein L31 pseudogene 21
AC024022	-1.06	-0.53	shisa homolog 3 (Xenopus laevis)
AC079127	-1.10	-0.55	kinase suppressor of ras 2
AE006639	-1.15	-0.61	mitogen-activated protein kinase 8 interacting protein 3
AF114264	-1.20	-1.01	nexilin (F actin binding protein)
AF116627	-1.17	-0.77	GTP binding protein 2
AL021155	1.16	0.29	SET binding factor 1 pseudogene
AL031118	-1.01	-0.68	zinc finger protein 391
AL031885	-1.16	-0.74	chloride channel, nucleotide-sensitive, 1B
AL078587	1.43	0.28	hypothetical LOC100134868
AL162742	-1.14	-0.42	glutathione S-transferase omega 2
AL353602	1.50	0.09	polymerase (DNA directed), eta
AL353743	-1.19	-0.55	prohibitin pseudogene
AL391839	-1.07	-0.09	coiled-coil domain containing 7
BC009350	-1.30	-0.58	eukaryotic translation initiation factor 2 alpha kinase 4
NM_000180	-1.16	-0.93	guanylate cyclase 2D, membrane (retina-specific)
NM_000216	-1.04	-0.94	Kallmann syndrome 1 sequence
NM_000261	-1.26	-0.67	myocilin, trabecular meshwork inducible glucocorticoid response
NM_000478	-1.24	-1.12	alkaline phosphatase, liver/bone/kidney
NM_000566	-1.01	-0.49	Fc fragment of IgG, high affinity 1c, receptor (CD64); Fc fragment of IgG, high affinity 1a, receptor (CD64)
NM_000751	1.22	-0.06	cholinergic receptor, nicotinic, delta
NM_000807	1.62	0.26	gamma-aminobutyric acid (GABA) A receptor, alpha 2

NM_000831	-1.32	-0.81	glutamate receptor, ionotropic, kainate 3
NM_000937	-1.63	-0.91	polymerase (RNA) II (DNA directed) polypeptide A, 220kDa
NM_000952	-1.15	-0.97	platelet-activating factor receptor
NM_001416	-1.01	-0.44	similar to eukaryotic translation initiation factor 4A; small nucleolar RNA, H/ACA box 67; eukaryotic translation initiation factor 4A, isoform 1
NM_001417	-1.04	-0.75	similar to eukaryotic translation initiation factor 4H; eukaryotic translation initiation factor 4B
NM_001634	1.70	0.36	adenosylmethionine decarboxylase 1
NM_002009	-1.35	-0.77	hypothetical LOC100132771; fibroblast growth factor 7 (keratinocyte growth factor); fibroblast growth factor 7 pseudogene 2
NM_002109	-1.57	-0.75	histidyl-tRNA synthetase
NM_002110	-1.15	-0.47	hemopoietic cell kinase
NM_002255	-1.04	-1.24	killer cell immunoglobulin-like receptor, two domains, long cytoplasmic tail, 4
NM_002410	-1.41	-0.89	mannosyl (alpha-1,6-)-glycoprotein beta-1,6-N-acetyl-glucosaminyltransferase; hypothetical LOC151162
NM_002465	-1.36	-0.71	myosin binding protein C, slow type
NM_002703	-1.45	-0.83	phosphoribosyl pyrophosphate amidotransferase
NM_002769	-1.07	-0.86	protease, serine, 1 (trypsin 1); trypsinogen C
NM_002926	-1.01	-0.02	regulator of G-protein signaling 12
NM_003222	-1.20	-1.02	transcription factor AP-2 gamma (activating enhancer binding protein 2 gamma)
NM_003292	-1.33	-1.08	translocated promoter region (to activated MET oncogene)
NM_003455	-1.21	-0.96	zinc finger protein 202
NM_003520	-1.05	-1.10	histone cluster 1, H2bn
NM_003808	-1.02	-0.56	TNFSF12-TNFSF13 readthrough transcript; tumor necrosis factor (ligand) superfamily, member 12; tumor necrosis factor (ligand) superfamily, member 13
NM_003910	-1.09	-0.64	BUD31 homolog (S. cerevisiae)
NM_004241	-1.01	-1.01	jumonji domain containing 1C
NM_004390	-1.03	-0.16	cathepsin H
NM_004436	-1.29	-1.45	endosulfine alpha
NM_004513	-1.44	-0.65	interleukin 16 (lymphocyte chemoattractant factor)
NM_004895	-1.17	-0.69	NLR family, pyrin domain containing 3
NM_004963	-1.23	0.25	guanylate cyclase 2C (heat stable enterotoxin receptor)
NM_004993	-1.10	-0.22	ataxin 3
NM_005012	-1.26	-0.41	receptor tyrosine kinase-like orphan receptor 1
NM_005108	1.42	0.40	xylulokinase homolog (H. influenzae)
NM_005319	-1.09	-0.97	histone cluster 1, H1c
NM_005321	-1.04	-0.76	histone cluster 1, H1e
NM_005322	-1.22	-0.76	histone cluster 1, H1b
NM_005488	-1.00	-0.59	hypothetical LOC100128526; target of myb1 (chicken)
NM_005537	-1.08	-0.61	inhibitor of growth family, member 1

NM_005626	-1.19	-0.94	splicing factor, arginine/serine-rich 4
NM_005674	-1.11	-0.78	zinc finger protein 239
NM_005807	-1.73	-1.59	proteoglycan 4
NM_006273	-1.01	-0.78	chemokine (C-C motif) ligand 7
NM_006608	-1.10	-1.06	putative homeodomain transcription factor 1
NM_006774	-1.00	-0.47	indolethylamine N-methyltransferase
NM_007212	-1.77	-1.29	ring finger protein 2
NM_007237	-1.22	-1.35	SP140 nuclear body protein
NM_007280	-1.10	-0.66	Opa interacting protein 5
NM_007320	-1.07	-0.62	RAN binding protein 3
NM_007328	-1.55	-0.51	killer cell lectin-like receptor subfamily C, member 1
NM_012093	-1.07	-0.81	adenylate kinase 5
NM_012352	-1.10	-0.60	olfactory receptor, family 1, subfamily A, member 2
NM_012399	-1.05	-0.05	phosphatidylinositol transfer protein, beta
NM_012446	-1.25	-0.77	single-stranded DNA binding protein 2
NM_012485	-1.04	-0.84	hyaluronan-mediated motility receptor (RHAMM)
NM_013960	-1.19	-1.16	neuregulin 1
NM_013961	-1.00	-0.89	neuregulin 1
NM_013978	-1.09	-0.90	BCL2/adenovirus E1B 19kDa interacting protein 1
NM_013980	-1.02	-0.86	BCL2/adenovirus E1B 19kDa interacting protein 1
NM_014138	-1.55	-1.42	family with sequence similarity 156, member A; family with sequence similarity 156, member B
NM_014171	-1.20	-0.36	cysteine-rich PDZ-binding protein
NM_014317	-1.29	-0.43	prenyl (decaprenyl) diphosphate synthase, subunit 1
NM_014381	-1.09	-0.94	mutL homolog 3 (E. coli)
NM_014412	-1.20	-1.16	similar to calcyclin binding protein; calcyclin binding protein
NM_014580	-1.07	-0.92	solute carrier family 2 (facilitated glucose transporter), member 8
NM_015442	1.40	0.20	CCR4-NOT transcription complex, subunit 10
NM_015485	-1.01	-1.23	RWD domain containing 3
NM_016121	-1.23	-0.51	potassium channel tetramerisation domain containing 3
NM_016299	-1.10	-0.73	heat shock 70kDa protein 14
NM_016557	-1.11	-0.73	chemokine (C-C motif) receptor-like 1
NM_016835	-1.46	-0.73	microtubule-associated protein tau
NM_017493	-1.14	-0.73	OTU domain containing 4
NM_017631	-1.08	-0.73	DEAD (Asp-Glu-Ala-Asp) box polypeptide 60
NM_017853	1.25	0.85	thioredoxin-like 4B
NM_017953	-1.00	-1.16	zinc finger, HIT type 6
NM_017972	-1.08	-0.60	chromosome 14 open reading frame 118
NM_018012	-1.22	-1.30	kinesin family member 26B
NM_018045	-1.10	-0.75	BSD domain containing 1
NM_018207	-1.20	-0.75	tripartite motif-containing 62
NM_018281	-1.11	-0.66	enoyl Coenzyme A hydratase domain containing 2
NM_018430	-1.01	-0.82	translin-associated factor X interacting protein 1

NM_018590	-1.14	-0.38	chondroitin sulfate N-acetylgalactosaminyltransferase 2; novel protein similar to chondroitin sulfate GalNAcT-2 (GALNAcT-2)
NM_018655	-1.54	-1.73	lens epithelial protein
NM_018661	-1.00	-0.86	defensin, beta 103B; defensin, beta 103A
NM_018714	-1.05	-0.57	component of oligomeric golgi complex 1
NM_018834	-1.32	-0.79	matrin 3
NM_018839	-1.31	-0.57	NSFL1 (p97) cofactor (p47)
NM_018928	-1.07	-0.70	protocadherin gamma subfamily C, 3; protocadherin gamma subfamily C, 5; protocadherin gamma subfamily C, 4; protocadherin gamma subfamily A, 12
NM_019119	-1.47	-1.08	protocadherin beta 10; protocadherin beta 9
NM_020142	1.29	-0.90	NADH dehydrogenase (ubiquinone) 1 alpha subcomplex, 4-like 2
NM_020147	-1.34	-0.39	THAP domain containing 10
NM_020533	-1.26	0.11	mucolinin 1
NM_020675	1.25	0.26	SPC25, NDC80 kinetochore complex component, homolog ( <i>S. cerevisiae</i> )
NM_020778	-1.31	-0.69	alpha-kinase 3
NM_020779	-1.07	-0.56	WD repeat domain 35
NM_020824	-1.20	-0.25	Rho GTPase activating protein 21
NM_021035	-1.64	-1.02	zinc finger, NFX1-type containing 1
NM_021186	-1.45	-1.60	zona pellucida glycoprotein 4
NM_022336	-1.71	-0.52	ectodysplasin A receptor
NM_022576	-1.56	-1.22	phosducin
NM_022781	-1.00	-0.93	ring finger protein 38
NM_022830	-1.15	-0.79	terminal uridylyl transferase 1, U6 snRNA-specific
NM_023013	-1.15	-1.04	PRAME family member 1
NM_023038	-1.02	-0.52	ADAM metallopeptidase domain 19 (meltrin beta)
NM_024071	-1.63	-0.71	zinc finger, FYVE domain containing 21
NM_024164	-1.33	-0.82	tryptase alpha/beta 1; tryptase beta 2
NM_024292	-1.07	-0.92	ubiquitin-like 5
NM_024694	-1.03	-0.79	chromosome 6 open reading frame 103
NM_024743	-1.03	-1.00	UDP glucuronosyltransferase 2 family, polypeptide A3
NM_024809	-1.09	-1.29	tectonic family member 2
NM_024814	-1.16	-1.46	Cas-Br-M (murine) ecotropic retroviral transforming sequence-like 1
NM_024908	-1.20	-0.27	WD repeat domain 76
NM_024936	-1.04	-0.88	zinc finger, CCHC domain containing 4
NM_025040	-1.31	-0.83	zinc finger protein 614
NM_025081	-1.10	-0.75	KIAA1305
NM_025170	-1.00	-0.93	phosphatidylinositol-3,4,5-trisphosphate-dependent Rac exchange factor 2
NM_025194	-1.15	-0.19	inositol 1,4,5-trisphosphate 3-kinase C
NM_032595	-1.36	0.05	protein phosphatase 1, regulatory (inhibitor) subunit 9B
NM_032946	-1.60	-1.12	nuclear RNA export factor 5

NM_033300	-1.05	-0.69	low density lipoprotein receptor-related protein 8, apolipoprotein e receptor
NM_052937	1.04	0.63	protein-L-isoaspartate (D-aspartate) O- methyltransferase domain containing 1
NM_053039	-1.16	-1.48	UDP glucuronosyltransferase 2 family, polypeptide B28
NM_080588	1.25	0.56	protein tyrosine phosphatase, non-receptor type 7
NM_145295	-1.07	-1.02	zinc finger protein 627
NM_145911	-1.69	-1.33	zinc finger protein 23 (KOX 16)
NM_173464	-1.10	-0.50	l(3)mbt-like 4 (Drosophila)
NM_175055	-1.03	-1.07	histone cluster 3, H2bb
NM_198568	-1.74	-0.95	gap junction protein, beta 7, 25kDa
NM_199144	-1.47	-0.94	ubiquitin-conjugating enzyme E2 variant 1; ubiquitin-conjugating enzyme E2 variant 1 pseudogene 2; transmembrane protein 189; TMEM189-UBE2V1 readthrough transcript
X91103	1.06	0.06	Hr44 antigen

## Appendix Two

### Awards:

- ◆ Jan/2011                      Nottingham University Endowed Postgraduate Prize
- ◆ June/2010                    University of Nottingham Pharmacy School BA Bull Postgraduate Award

### Conference presentations:

- ◆ *CDKI-71, a novel CDK9 inhibitor, is preferentially cytotoxic to cancer cells when compared with flavopiridol*  
Poster presentation: 21st Meeting of the European Association for Cancer Research  
26-29 June 2010   Oslo, Norway
- ◆ *In vitro antitumor mechanism of a novel cyclin-dependent kinase inhibitor CDKI-83*  
Poster presentation: NCRI 2010  
7-10 November 2010 Liverpool, UK
- ◆ *Pharmacokinetics, biodistribution, acute toxicity and in vivo anti-tumour efficacy of paclitaxel solid dispersion*  
Poster presentation: UK-PharmSci 2010

1-3 September 2010 Nottingham, UK

## **Publications:**

**Xiangrui Liu, Shenhua Shi, etc.** *CDKI-71, a novel CDK9 inhibitor, is preferentially cytotoxic to cancer cells when compared with flavopiridol*

**International journal of Cancer** (published online first)

**Xiangrui Liu, Frankie Lam, etc.** *In vitro antitumor mechanism of a novel cyclin-dependent kinase inhibitor CDKI-83.* **Investigational new drugs**

(published online first)

**Xiangrui Liu, Jiabei Sun, etc.** *Pharmacokinetics, biodistribution, acute toxicity and in vivo anti-tumour efficacy of paclitaxel solid dispersion* **Journal**

**of pharmacy and Pharmacology** 2010 62(10)/1234-1235

**Shenhua Shi, Xiangrui Liu, etc.** *CDK9 inhibitor design, synthesis and biological evaluation* **Journal of pharmacy and Pharmacology** 2010

62/1363/1